Contribution au pronostic de la qualité d'un produit usiné par la proposition d'un modèle basé sur l'apprentissage machine

par

Antoine PROTEAU

THÈSE PAR ARTICLES PRÉSENTÉE À L'ÉCOLE DE TECHNOLOGIE SUPÉRIEURE COMME EXIGENCE PARTIELLE À L'OBTENTION DU DOCTORAT EN GÉNIE
Ph. D.

MONTRÉAL, LE 10 JUILLET 2021

ÉCOLE DE TECHNOLOGIE SUPÉRIEURE
UNIVERSITÉ DU QUÉBEC

PRÉSENTATION DU JURY

CETTE THÈSE A ÉTÉ ÉVALUÉE

PAR UN JURY COMPOSÉ DE :

M. Antoine Tahan, directeur de thèse
Département de génie mécanique à l'École de technologie supérieure

M. Marc Thomas, codirecteur de thèse
Département de génie mécanique à l'École de technologie supérieure

M. Robert Sabourin, président du jury
Département de génie des systèmes à l'École de technologie supérieure

M. Michel Rioux, membre du jury
Département de génie des systèmes à l'École de technologie supérieure

M. Zhaoheng Liu, membre du jury
Département de génie mécanique à l'École de technologie supérieure

M. Kamal Medjaher, examinateur externe indépendant
Laboratoire génie de production, École Nationale d'Ingénieurs de Tarbes

ELLE A FAIT L'OBJET D'UNE SOUTENANCE DEVANT JURY ET PUBLIC

LE 17 JUIN 2021

À L'ÉCOLE DE TECHNOLOGIE SUPÉRIEURE

REMERCIEMENTS

Cette thèse a pu être complétée avec le soutien et l'implication de plusieurs personnes. Je tiens donc à prendre le temps de remercier et souligner l'apport de tous ceux qui ont contribué de près ou de loin au bon déroulement et au succès de ce projet de thèse.

En commençant, j'aimerais remercier mes directeurs de thèse, le professeur Antoine Tahan et le professeur Marc Thomas. Merci pour la confiance dont vous m'avez fait preuve et d'avoir accepté de vous lancer dans ce projet avec moi. Merci également pour tout le soutien, autant personnel qu'académique tout au long de cette collaboration. Vos conseils et vos contributions auront été essentiels à l'aboutissement de ce projet.

Merci également au professeur Ryad Zemouri dont la rencontre aura été un pivot dans ces travaux et avec qui la collaboration aura mené à plusieurs contributions centrales à ce projet. Merci encore pour nos discussions et tous tes précieux conseils.

Cette thèse a pu voir le jour avec la précieuse collaboration d'APN Inc. et de ses employés. Merci donc à Jean P. et Yves P. pour votre confiance et votre soutien autant personnel que financier dans ce projet. Merci aussi à Alain B. et Jonathan C. pour tout le savoir-faire partagé et vos contributions critiques ayant permis d'instrumenter l'équipement. Merci aussi à toute l'équipe de développement et de l'ingénierie pour avoir supporté des étapes essentielles à ce projet.

Je remercie aussi le Fonds de Recherche du Québec – Nature et Technologies (FRQNT) pour leur apport financier.

Je tiens également à souligner et à remercier les membres du jury pour le temps accordé à toutes les étapes d'évaluation de cette thèse, pour vos conseils et vos commentaires.

Merci à Julian F. pour tout le temps consacré à répondre à mes innombrables questions. Tes réponses, ton support et ton amitié auront été précieux tout au long de ce projet de thèse.

Je remercie aussi ma famille et mes parents, Jean et Josée, pour leur soutien et leurs encouragements tout au long de mon parcours académique. Un remerciement spécial à mon frère Charles et sa conjointe Stéphanie L. de m'avoir accueilli toutes ces années à chacun de mes passages à Québec.

Pour terminer, je tiens également à remercier ma conjointe, Agathe, de m'avoir encouragé à me lancer dans un tel projet. Merci aussi pour ta confiance, ta patience, tes sacrifices, ton soutien et tes innombrables encouragements qui auront été déterminants pour passer au travers de ces années. Il n'y a pas de mots pour quantifier l'immensité de ta contribution à l'accomplissement de cette thèse dont tu partages la réalisation.

Contribution au pronostic de la qualité d'un produit usiné par la proposition d'un modèle basé sur l'apprentissage machine

Antoine PROTEAU

RÉSUMÉ

La présente thèse est une contribution à la surveillance et au pronostic d'un produit usiné à l'aide d'une approche basée sur l'apprentissage machine utilisant une architecture de type autoencodeur variationnel. Encore aujourd'hui, les entreprises manufacturières sont toujours en proie à plusieurs pressions telles que la globalisation des marchés, les demandes constantes de réduction des coûts ou encore les requis qualité toujours plus exigeants. Pour faire suite à cette dernière, l'objectif de cette thèse est donc de démontrer la possibilité de développer un système de mesure alternatif permettant de réaliser le pronostic de la qualité d'un produit usiné, et ce, en temps réel.

Dans cette optique, notre première contribution a été de proposer un descripteur basé sur le concept d'énergie spécifique de coupe. Celui-ci est défini comme étant la quantité d'énergie nécessaire à l'enlèvement de 1 cm^3 de matériau. Il a été démontré que ce descripteur est fortement corrélé à l'usure d'un outil de coupe ($r > 90\%$). Nous avons également montré que ce descripteur a un apport considérable (14.7%) lors du processus d'apprentissage dans un contexte d'apprentissage supervisé.

Une autre contribution de ces travaux relève de notre proposition d'un modèle capable de réaliser le pronostic de la qualité d'un produit usiné. Ce modèle est basé sur un réseau de neurones de type autoencodeur variationnel. Le modèle est capable de réaliser le pronostic de la qualité avec une erreur quadratique moyenne de 5.257×10^{-4} mm. L'espace latent de deux dimensions généré par le modèle illustre également une distribution visuelle des données en fonction du niveau de la qualité. En nous basant sur cet espace latent et le concept de distance euclidienne, nous avons aussi proposé une nouvelle métrique permettant de rapidement quantifier le niveau de qualité. Cette métrique est corrélée avec les valeurs observées ($r \approx 67\%$) et avec les valeurs prédites de la qualité ($r \approx 94\%$). Cet espace latent fournit donc un outil simple et visuel pour suivre l'évolution du processus d'usinage.

Ces travaux ont été réalisés en partenariat avec un industriel : APN Inc. (Québec, Canada). Ce faisant, les résultats de cette thèse sont majoritairement fondés sur un jeu de données acquis chez celui-ci représentant plus de 600 heures de production régulière. Ceci facilite donc le potentiel de transfert technologique vers l'industrie et ainsi permettre à ces entreprises de mieux réaliser la surveillance et le pronostic de la qualité de leurs processus d'usinage. De plus, cela ouvre la porte à la possibilité d'implanter et d'utiliser un système de mesure alternatif en entreprise.

Mots-clés : autoencodeur variationnel, pronostic, qualité, tolérancement géométrique et dimensionnel, usinage, données industrielles.

A Contribution to the Quality Prognostic of a Machined Workpiece with a Model Based on Machine Learning

Antoine PROTEAU

ABSTRACT

This thesis is a contribution to the monitoring and prognostic of the quality of a machined workpiece based on a machine learning approach leveraging a variational autoencoder architecture. Still today, the manufacturing industry is prone to multiple pressures such as the globalization of markets, constant cost decrease requests or the ever-increasing quality-level requirements. Regarding the latter, this thesis' objective is to demonstrate the possibility of developing an alternative measurement system capable of realizing the prognostic of the quality measurement value of a machined workpiece in real time.

In this context, our first contribution was to propose a feature based on the concept of specific cutting energy. This feature is defined as the amount of energy required to remove 1 cm^3 of raw material. It was demonstrated that this feature is highly correlated to a cutting tool wear's level ($r > 90\%$). We also shown that this feature has a significant contribution (14.7%) during the learning process in a supervised learning context.

Another contribution of this thesis comes from our proposal of a model capable of making the prognostic of a workpiece' quality measurement value. This model is based on a variational autoencoder type of neural network. The model is able to predict the quality values with a mean square error of 5.257×10^{-4} mm. The two dimensions latent space generated by the model visually distributes the data according to the quality level. Also based on this latent space and the Euclidean distance concept, we proposed a new metric capable of quickly quantifying the quality level. This metric is correlated with the observed quality values ($r \approx 67\%$) and with the predicted quality values ($r \approx 94\%$). Consequently, this latent space is a simple and visual tool that can be used to follow the evolution of the production process.

This work was also accomplished in partnership with an industrial: APN Inc. (Quebec, Canada). Therefore, the results encompassed in this thesis are mostly based on a dataset acquired at the partner's facility and representing more than 600 hours of regular production. This increases the potential of technological transfer to the industry and will also allows companies to better realize the monitoring and prognostic of the quality of their machining process. Furthermore, this opens the door to the possibility of implementing and using an alternative measurement system in the manufacturing industry.

Keywords: variational autoencoder, prognostic, quality, geometric dimensioning and tolerancing, machining, industrial data

TABLE DES MATIÈRES

Page

LISTE DES TABLEAUX

Page

LISTE DES FIGURES

Page

LISTE DES ABRÉVIATIONS, SIGLES ET ACRONYMES

AE	AutoEncoder
ANN	Artificial Neural Network
CBM	Condition-Based Maintenance
C.I.	Confidence Interval
CMM	Coordinate Measuring Machine
CNC	Computer Numerical Control
DL	Deep Learning
EWMA	Exponentially Weighted Moving Average
FRQNT	Fonds de Recherche du Québec – Nature et Technologies
GAN	Generative Adversarial Network
GB	Gigabyte
GD&T	Geometrical and Dimensional Tolerancing
IQR	Interquartile Range
LSTM	Long Short-Term Memory
ML	Machine Learning
MLP	MultiLayer Perceptron
MSE	Mean Square Error
NN	Neural Network
PCA	Principal Component Analysis
RNN	Recurrent Neural Network
RMSE	Root Mean Square Error
RUL	Residual Useful Life

SCE	Specific Cutting Energy (Énergie Spécifique de Coupe)
SPC	Statistical Process Control
SQC	Statistical Quality Control
SVM	Support Vector Machine
Tanh	Tangente Hyperbolique
TCM	Tool Condition Monitoring
TRS	Taux de Rendement Synthétique
t-SNE	t-distributed Stochastic Neighbor Embedding
VAE	Variational AutoEncoder
VAEC	Variational AutoEncoder Classifier
VRAE	Variation Recurrent AutoEncoder
VAER	Variational AutoEncoder Regression
WO	Work Order

LISTE DES SYMBOLES ET UNITÉS DE MESURE

A	Ampère
A	Moyenne de l'énergie contenue dans un signal temporel
A_{CT}	Mesure de l'énergie à l'amplitude de la fréquence d'un outil de coupe
Acc	Précision (Accuracy)
a_e	Profondeur de coupe radiale [mm]
a_p	Profondeur de coupe axiale [mm]
A_{window}	Mesure de l'énergie à l'amplitude de la fréquence d'un outil de coupe
α	Bruit gaussien
c	Centroïde d'un groupe de points
CF	Facteur de crête
cm	Centimètre
d	Distance euclidienne entre deux points
ϵ	Variable aléatoire
f_i	Fréquence d'intérêt [Hz]
f_n	Avance par révolution [$\mathrm{mm \cdot rev^{-1}}$]
I	Courant [A]
i	Élément d'un échantillon
in	*Inch* (Pouce)
J	Joule
K	Kurtosis
k_c	*Specific Cutting Energy value* [$\mathrm{J/cm^3}$]
KL	Divergence de Kullback-Leibler

$\mathcal{L}$	Fonction de coût (*Loss function*)
λ	Niveau de défaut artificiel dans un signal temporel
m	Mètre
min	Minute
mm	Millimètre
MPa	Méga Pascal
MSE	*Mean Square Error*
μ	Moyenne
n	Nombre d'échantillons
$\mathcal{N}$	Distribution normale
ω_{ct}	Fréquence d'un outil de coupe [Hz]
P	Puissance $[W]$
P_{Basic}	Puissance requise pour conserver les systèmes d'une machine CNC en fonction $[W]$
P_{pk}	*Process performance index*
$P_{Spindle}$	Puissance requise pour conserver la vitesse de rotation de la broche $[W]$
P_{Total}	Puissance totale consommée par la machine CNC $[W]$
P_{Tool}	Puissance nécessaire pour usiner la matière brute $[W]$
P_{Idle}	Puissance requise pour garder la CNC en marche et prête à couper $[W]$
$Peak$	Valeur de crête
PTP	Valeur de crête à crête
Q	Valeur du taux d'enlèvement de matière $[\mathrm{cm}^3\mathrm{s}^{-1}]$
R ou r	Coefficient de corrélation linéaire de Pearson

ρ	Coefficient de corrélation du rang de Spearman
rev	Révolution
RMS	*Root Mean Square*
s	Seconde
σ	Écart-type
t	Temps [s]
V	Voltage
V_c	Vitesse de coupe [$\mathrm{m{\cdot}min^{-1}}$]
V_f	Avance de la table de coupe [$\mathrm{mm{\cdot}min^{-1}}$]
VB	Usure d'un outil de coupe [mm]
W	Watt
wp	Coordonnées cartésiennes d'un produit dans l'espace latent
x	Signal temporel
$\bar{x}$	Moyenne
$\boldsymbol{x}$	Vecteur d'entrée
$\hat{\boldsymbol{x}}$	Vecteur d'entrée prédit
$\mathbb{X}$	Ensemble de données d'entraînement
x_{crest}	Facteur de crête
x_d	Signal artificiel contenant un défaut
$\boldsymbol{y}$	Vecteur de sortie cible
y	Valeur cible d'un cas d'entraînement
$\hat{y}$	Valeur prédite par le modèle d'apprentissage
$\hat{\boldsymbol{y}}$	Vecteur de sortie prédit

$\mathbb{Y}$	Ensemble de données de test
z	Espace latent (*Latent Space*) [-]

INTRODUCTION

Pour survivre face à la mondialisation, aux avancées technologiques ou encore aux nouvelles formes de compétition (nouveaux procédés de fabrication), les entreprises manufacturières n'ont d'autres choix que d'évoluer. Différentes approches ont été développées et mises de l'avant pour répondre à ce besoin. La plus populaire de nos jours est connue sous le terme « Industrie 4.0 », elle se présente comme étant la 4e révolution industrielle. Simple acronyme à la mode ou véritable révolution? Il va sans dire que l'afflux de technologies numériques offre plus que jamais des opportunités de transformation. Le coût toujours plus accessible des technologies, les avancements en intelligence artificielle et la disponibilité sans cesse croissante des données se conjuguent pour offrir aux entreprises manufacturières une multitude d'opportunités d'améliorations et des pistes pour repenser leurs modèles d'affaires.

En tirant profit des éléments énumérés ci-dessus, nous explorons dans ce projet la possibilité de réduire les besoins et les ressources en contrôle de la qualité. Cette étape est devenue un goulot d'étranglement dans le processus de fabrication. En proposant un système de surveillance et de pronostic comme substitut aux opérations coûteuses de contrôle de la qualité, une entreprise pourrait profiter de plusieurs avantages comme la réduction des coûts, une plus grande flexibilité ou encore une meilleure compréhension de leur processus de fabrication. Ces avantages se traduiront inéluctablement par des avantages concurrentiels.

La thèse est structurée comme suit : le CHAPITRE 1 met en contexte notre projet et définit la problématique ainsi que les objectifs auxquels nous nous attaquons. Le CHAPITRE 2 présente une revue de la littérature afin de situer notre projet parmi l'ensemble des travaux dans le domaine et de présenter un résumé succinct de l'état de l'art. Le CHAPITRE 3 détaille la méthodologie de recherche proposée ainsi que la structure de la thèse. Étant une thèse par articles, les CHAPITRE 4 à CHAPITRE 6 présentent nos principales contributions sous la forme de trois articles de journaux avec comité de lecture. Une conclusion résume les travaux réalisés et une liste de recommandations est formulée pour des travaux futurs.

CHAPITRE 1

CONTEXTE, PROBLÉMATIQUE ET OBJECTIFS

1.1 Contexte et problématique de recherche

L'industrie manufacturière, et plus particulièrement l'industrie de l'usinage par retrait de matériau, est à la base de bien des produits que nous consommons quotidiennement. Malgré son importance pour les économies mondiales, il n'en reste pas moins que cette industrie fait constamment face à diverses pressions; que ce soit la crise financière de 2008, la globalisation des marchés de plus en plus présente, les demandes constantes de réductions de coûts, les attentes toujours plus exigeantes en terme de qualité, les contraintes environnementales et énergétiques, ainsi qu'une accélération des cadences de production (Duo, Basagoiti, Arrazola, Aperribay, & Cuesta, 2019; Ertekin, Kwon, & Tseng, 2003; Psarommatis, May, Dreyfus, & Kiritsis, 2020; Takaya, 2013).

Pour répondre à ces défis, nous avons constaté l'émergence dans les dernières années d'un mouvement d'innovations technologiques issues de ce qu'on appelle aujourd'hui la quatrième révolution industrielle : « Industrie 4.0 ». Cette nouvelle *évolution* manufacturière prône une usine du futur ultra-connectée, ultra-automatisée où la technologie côtoie l'humain en quasi-symbiose (Abellan-Nebot & Romero Subirón, 2010; Baur, Albertelli, & Monno, 2020; Cui, Kara, & Chan, 2020; Kohler & Weisz, 2016; J. Lee, Jin, & Bagheri, 2017; Martínez-Arellano, Terrazas, & Ratchev, 2019). Dans cette mouvance, et grâce à l'afflux de nouvelles innovations et technologies abordables, les entreprises manufacturières ont une opportunité inédite de revisiter des problèmes auxquels elles ont toujours fait face et qui ne sont pas encore résolus. Ces problématiques, telles que les bris d'outils de coupe, l'usure prématurée de ces derniers, les arrêts imprévus ou bien des produits non conformes, continuent aujourd'hui d'affecter ces entreprises en haussant leurs coûts de production, ce qui diminue irrémédiablement leur niveau de compétitivité sur les marchés locaux et internationaux, et affecte ainsi leur pérennité (Chadha, Rabbani, & Schwung, 2019; X. Jiang, Li, Mao, Hao, & Liu, 2018; Park & Tran, 2014; Y. Zhou & Xue, 2018).

Une métrique couramment utilisée pour mesurer la performance d'un processus manufacturier est le Taux de Rendement Synthétique (TRS). Ce taux correspond au produit de trois éléments : la disponibilité de l'équipement, la productivité (cadence) et la qualité de la production. La Figure 1.1 présente une explication visuelle de cette métrique. Le lecteur peut se référer, entre autres, à la norme NF E60-182 (AFNOR, 2002) pour plus de détail.

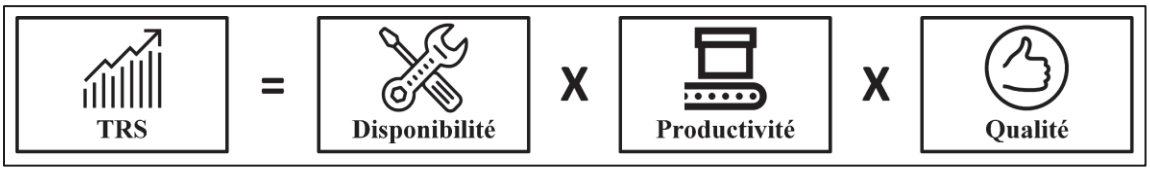

Figure 1.1 Taux de rendement synthétique

Les problèmes cités ci-dessus qui continuent d'affecter négativement l'industrie de l'usinage se retrouvent donc au cœur de cette métrique. Par exemple, un bris d'outil de coupe affectera aussi bien la productivité que la qualité du produit. Un arrêt imprévu impactera la disponibilité des équipements. Étroitement lié à la performance d'une entreprise, un TRS bas sous-entend une entreprise à risques opérationnellement et financièrement. Dans ce projet, nous ne prétendons pas pouvoir nous attaquer à tous les aspects affectant le TRS, mais nous sommes convaincus que les applications développées présentent des pistes de solutions robustes pour l'accroissement du niveau de qualité et de la productivité.

Lorsque nous nous attardons à analyser minutieusement le processus de contrôle qualité dans une entreprise d'usinage, nous constatons que celui-ci est très réactif. La Figure 1.2 fournit un exemple de ce processus. Généralement, un produit fabriqué est mesuré a posteori selon un plan d'échantillonnage prédéfini de manière empirique ou statistique (ex. : inspecter un produit sur cinq). Cette vérification se fera avec des équipements de mesure spécialisés tels qu'une CMM (*Coordinate Measuring Machine*) et ce, manuellement ou de manière automatisée par un expert spécialisé et dédié pour le contrôle de la qualité. Dans certains cas, le contrôle rudimentaire est réalisé par l'opérateur de la machine-outil CNC. En fonction de l'état de la conformité (ou non-conformité), une rétroaction est produite à l'opérateur de la machine qui tente de corriger les paramètres du procédé pour compenser l'influence des

divers phénomènes de dégradation (ex. : usure des outils de coupe) ou de variation (ex. : modifier les paramètres de coupe). Après ajustement, l'opérateur peut poursuivre sa production. Ce processus, tel que mentionné ci-dessus, est réactif. C'est-à-dire qu'une action (ex. : un ajustement) ne pourra être exécutée que lorsqu'une évaluation de la qualité est effectuée.

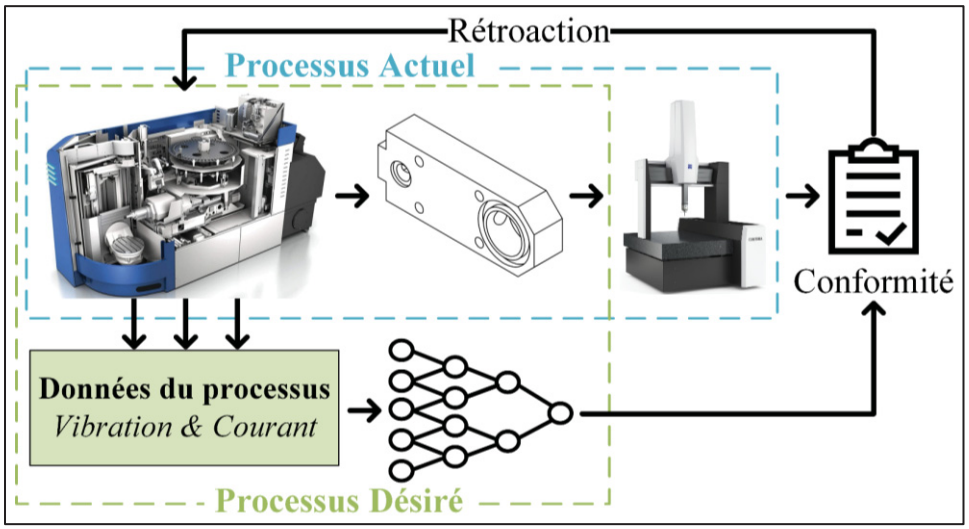

Figure 1.2 Processus de fabrication actuel versus désiré[1]

Aussi, le processus de mesure est souvent le goulot d'étranglement pour la production et est effectué à l'aide d'équipements dispendieux (~100-150$/hr). Par conséquent, ceci résulte en une diminution de la productivité, une hausse des coûts et l'augmentation du risque de compromettre la capacité de survie de l'entreprise.

En nous inspirant de la mouvance Industrie 4.0, nous nous interrogeons sur la possibilité d'assurer une meilleure surveillance (en amont) du processus de fabrication et de la qualité d'un produit usiné. Les possibilités que nous offrent aujourd'hui les technologies (disponibilité des données issues des capteurs de surveillance) et les récentes avancées du domaine de l'intelligence artificielle, nous laissent envisager qu'il serait possible de

[1] Photos: ZEISS et Grob-Werke

développer un système basé sur des données autres que seulement celles issues du contrôle de la qualité d'un produit. Le but d'un tel système serait non seulement de fournir des outils de surveillance en temps réel, mais aussi une capacité de réaliser le diagnostic (détection de l'origine d'une défaillance) et le pronostic (se projeter dans le futur avec un modèle prédictif) de la qualité pour ainsi faire une rétroaction rapide et automatisée à l'opérateur.

Les phénomènes thermomécaniques et métallurgiques à l'œuvre durant le processus de fabrication ne sont généralement pas, ou très peu, mesurés. Ce faisant, par l'utilisation de capteurs déjà disponibles à même la machine-outil et par l'ajout de nouveaux, serait-il possible de proposer un système de surveillance du procédé de fabrication? Nous désirons donc mettre en relation ces données physiques (ex. : vibration, température, etc.) avec les données opérationnelles (ex. : outil de coupe, paramètres de coupe, parcours de l'outil, etc.) du procédé de fabrication ainsi que les données de métrologie dimensionnelle reflétant la conformité d'un produit au niveau de son respect des spécifications GD&T et d'état de surface (rugosité) pour démontrer qu'il existe une relation de causalité, statistiquement significative, reliant les deux premiers éléments à la réponse dimensionnelle et géométrique du produit.

En modélisant cette relation par les méthodes appartenant au domaine de l'intelligence artificielle, nous conjecturons qu'il deviendrait envisageable de pouvoir faire la surveillance, le diagnostic et le pronostic de la conformité d'un produit tout en diminuant sensiblement le recours à des opérations coûteuses de contrôle de la qualité. La Figure 1.2 présente visuellement l'intention de notre projet (**vert**) en opposition au processus actuel (**bleu**).

De plus, nous estimons qu'un tel système implanté dans une entreprise permet à celle-ci d'être plus proactive quant au suivi et au contrôle de la fabrication de ses produits. En plus de réduire le risque de goulot d'étranglement et d'assurer une plus grande flexibilité, ce genre de système permet de se prévaloir d'un avantage concurrentiel dû à une meilleure utilisation des équipements de mesure et de ses équipements de production (Cui et al., 2020; Psarommatis et al., 2020; J. Z. Zhang & Chen, 2008).

Pour récapituler et décomposer la problématique énoncée ci-dessus, nous établissons trois questions de recherche :

1) Est-ce possible de déterminer un ou plusieurs descripteurs issus des capteurs de la machine-outil CNC et qui sont fortement reliés à la dégradation du processus de fabrication (niveau de qualité)?
2) Est-ce qu'il existe un lien causal entre les signaux des phénomènes physiques à l'œuvre durant l'usinage d'un produit et les données d'inspection (GD&T et rugosité) de celui-ci? Si oui, quels sont les meilleurs descripteurs? Et quelle est la méthode de surveillance la mieux adaptée à ce cas?
3) Est-ce possible de fournir un support permettant de suivre visuellement, d'une manière conviviale et adaptée pour un usage industriel, la dégradation (ou l'évolution) du processus de fabrication et donc, de la conformité du produit?

Ces trois questions de recherche nous fournissent le point de départ sur lequel notre projet de recherche s'articule. Être en mesure de fournir une réponse à chacune de ces questions nous permettra donc de répondre efficacement à la problématique que nous avons posée dans ce chapitre.

1.2 Objectifs de la thèse

À partir des questions de recherche, les objectifs de ce projet de recherche sont donc les suivants :

1) Proposer une méthodologie d'acquisition et de traitement des données pour le suivi et la surveillance d'un processus d'usinage sur une machine-outil CNC. Autant que possible, le formalisme doit intégrer la consolidation des variables sur des bases liées à la physique des phénomènes en cours (ex. : concept d'énergie spécifique, ergodicité des signaux, etc.), le prétraitement (ex. : filtrage) et les processus de traitement des signaux à l'aide des outils, techniques ou méthodes inspirées par l'état de l'art;
2) Déterminer et proposer un ou plusieurs descripteurs fortement corrélés à la dégradation du processus de fabrication (et par conséquent à l'état de conformité des produits usinés);

3) Proposer une méthodologie basée sur l'apprentissage machine pour démontrer qu'il est possible de réaliser le pronostic de la conformité d'un produit en se basant uniquement sur la captation des phénomènes physiques durant le processus d'usinage (captation des paramètres du procédé et non pas des mesures sur des produits);
4) Fournir pour un usage industriel un support visuel facilitant le diagnostic et le pronostic rapides de l'état du processus de fabrication.

Pour conclure, nous avons mis en contexte et énoncé notre problématique, démontré les besoins et l'urgence de développer un système permettant de faire le pronostic de la conformité d'un produit en temps réel. Nous avons segmenté et posé nos questions de recherche. Ensuite, les différents sous-objectifs de ce projet ont été énumérés. Finalement, le chapitre suivant présente une revue de la littérature pour situer notre projet dans l'ensemble de ce qui a été accompli dans les différents axes de recherche liés à notre problématique.

CHAPITRE 2

REVUE DE LA LITTÉRATURE

2.1 Introduction

Il est important de situer un projet de recherche parmi l'ensemble des travaux effectués dans le domaine. Ce chapitre présente donc une revue succincte de la littérature pertinente à notre projet. Cette revue nous permet de faire l'inventaire de ce qui a été réalisé récemment par la communauté de chercheurs, et par conséquent elle nous permet de bien cadrer ce projet et nos contributions. Nous rappelons au lecteur que cette thèse en est une *par articles* et qu'une revue de la littérature spécifique et plus ciblée est également présentée aux sections 4.3, 5.3 et 6.3.

2.2 Concept de pronostic

Rappelons-nous que l'objectif de ce travail de recherche est de développer un système capable d'établir un pronostic de la conformité d'un produit. En d'autres mots, surveiller **et** prédire la concordance entre le produit fabriqué et ses spécifications : dimensionnelles, géométriques (GD&T) et de rugosité. Développer un système capable de remplir cet objectif, et ce, en temps réel, n'est pas un nouveau concept comme tel. Dès 1995, Du, Elbestawi, et Wu (1995a, 1995b) ont proposé un cadre et une revue des méthodes et des applications reliées aux systèmes « auto ajustables ». En revanche, plus de 20 ans après, des systèmes s'ajustant automatiquement et réalisant le pronostic précis de diverses situations ne sont que rarement présents dans les entreprises manufacturières (Arinez, Chang, Gao, Xu, & Zhang, 2020; Elattar, Elminir, & Riad, 2016; Silvestri, Forcina, Introna, Santolamazza, & Cesarotti, 2020).

Pourquoi cette classe de système n'est-elle que très peu présente dans les entreprises manufacturières? Quels sont les freins actuels? Que devons-nous faire pour développer, valider et déployer un tel système? Ces questions légitimes et essentielles ont nourri le

démarrage de notre projet. Il nous semble donc évident et important de bien définir le concept de pronostic et de faire l'état de la situation.

La Figure 2.1 tente d'illustrer dans quel contexte le concept de pronostic s'intègre dans un processus décisionnel manufacturier, ainsi que sa relation avec les concepts connexes de *surveillance* et de *diagnostic*. Il faut être conscient que chaque concept (surveillance, diagnostic et pronostic), utilisé indépendamment, permet de fournir une information ou de prendre une décision. De plus, chaque concept mène une action différente (Guillén, Crespo, Gómez, & Sanz, 2016; Reis & Gins, 2017). La surveillance signifie de faire le suivi d'un ou plusieurs descripteurs représentant le comportement (état de santé) d'un procédé ou d'un phénomène dans le temps. Ce type d'analyse représente donc l'évolution d'un système dans le temps. Avec l'utilisation d'une carte de contrôle, il est donc possible de suivre un phénomène et de détecter une anomalie lorsqu'un des descripteurs dépasse une limite de contrôle (de-Felipe & Benedito, 2017; Ugaz, Sánchez, & Alonso, 2017). Ce type d'analyse se définit donc comme une analyse de type réactive.

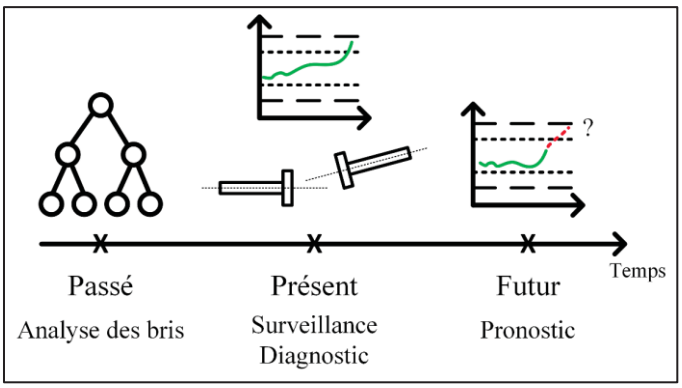

Figure 2.1 Implication du pronostic dans le processus de décision

Contrairement au concept de détection qui nous fournit une information agrégée sur l'évolution du comportement (santé) du système, le concept de diagnostic permet d'obtenir avec une plus grande précision l'état du système et la cause sous-jacente d'une anomalie (Thomas, 2011). Cette information nous aide à connaître de manière plus détaillée l'état

actuel d'un système et à mieux cibler les interventions d'entretien. Une combinaison intéressante de ces deux concepts se retrouve dans le domaine de la maintenance industrielle. Par exemple, en suivant dans le temps l'évolution de descripteurs, il est possible d'alerter un agent qui pourra ensuite faire le diagnostic de la composante défectueuse du système (Bousdekis, Magoutas, Apostolou, & Mentzas, 2015).

Le concept de pronostic désigne l'action de « connaître d'avance » (Larousse, 2015). C'est-à-dire d'être en mesure de prédire avec un certain niveau de confiance un évènement quelconque, une tendance ou une prédisposition (Kundu, Darpe, & Kulkarni, 2020; Kwon, Hodkiewicz, Fan, Shibutani, & Pecht, 2016; Lei et al., 2018; Peng, Dong, & Zuo, 2010; Vogl, Weiss, & Helu, 2016). Ce concept permet donc de passer d'un processus réactif vers un processus proactif. Les avantages de développer et d'implanter un tel système sont nombreux. Spécifiquement dans le domaine manufacturier, nous pouvons avancer la réduction des coûts grâce à une meilleure planification des activités (maintenance, contrôle de qualité, production, etc.), une réduction des bris de machine, un accroissement de la sécurité des équipements, une diminution des arrêts imprévus, une diminution des coûts liés aux rebuts, etc. (Elattar et al., 2016; Janssens, Walle, Loccufier, & Hoecke, 2017; Kundu, Chopra, & Lad, 2017; Kundu et al., 2020; Laloix, Iung, Voisin, & Romagne, 2016; R. Li, Verhagen, & Curran, 2020; Vogl et al., 2016). Toujours dans un contexte manufacturier, la forme la plus usuelle que cette prédiction peut prendre est généralement traduite par l'estimation de la durée de vie résiduelle (*Residual Useful Life* (RUL)) d'un composant ou d'un système (Elattar et al., 2016; Lei et al., 2018; R. Li et al., 2020) ou encore par la prédiction de l'état futur du système (ex : conforme ou non conforme).

À en juger par le nombre de publications recensées, le concept de pronostic est un sujet en croissance depuis plusieurs années comme le démontre la Figure 2.2. Il est également intéressant de constater à la Figure 2.3 que le sous-domaine de recherche ayant le plus de publications est celui de la « Maintenance et Fiabilité » et que notre domaine d'intérêt, « Inspection et contrôle qualité », est également parmi les sous-domaines ayant le plus de contributions. De plus, le concept de pronostic reste un sujet d'intérêt international comme le

démontre la Figure 2.4. À noter que les données pour les Figure 2.2 à Figure 2.4 ont été obtenues à partir de Elsevier (2021).

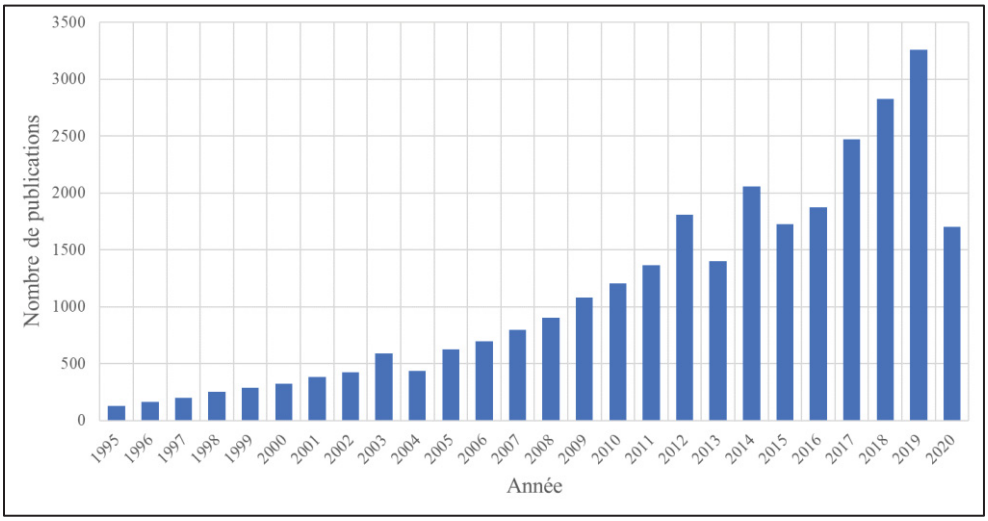

Figure 2.2 Nombre de publications par année pour le mot-clé *prognostic*

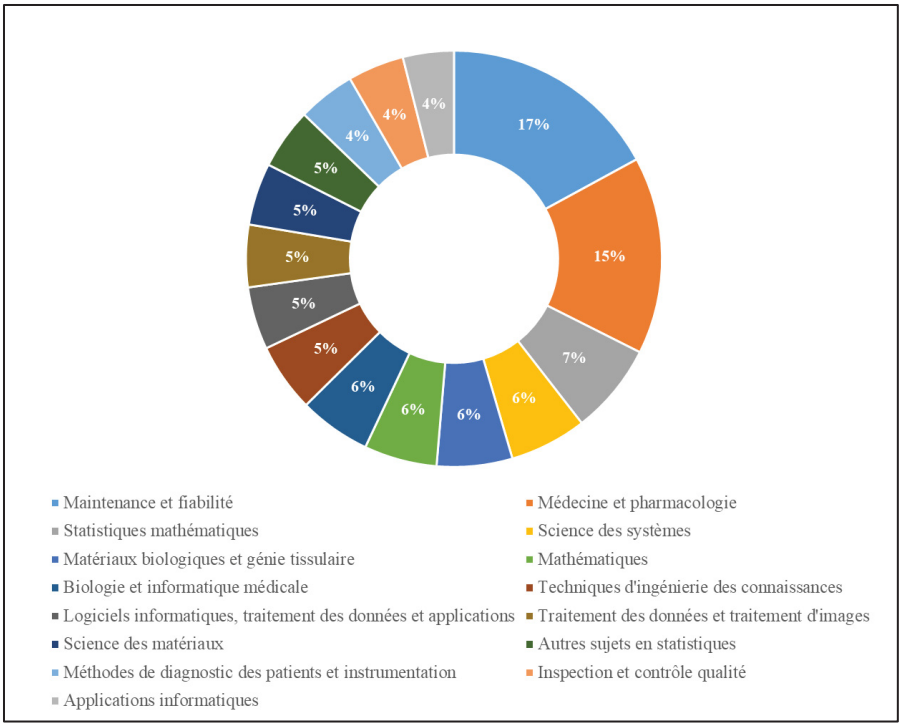

Figure 2.3 Proportion des publications depuis 1995 pour le top 15 des domaines de recherche pour le mot-clé *prognostic*

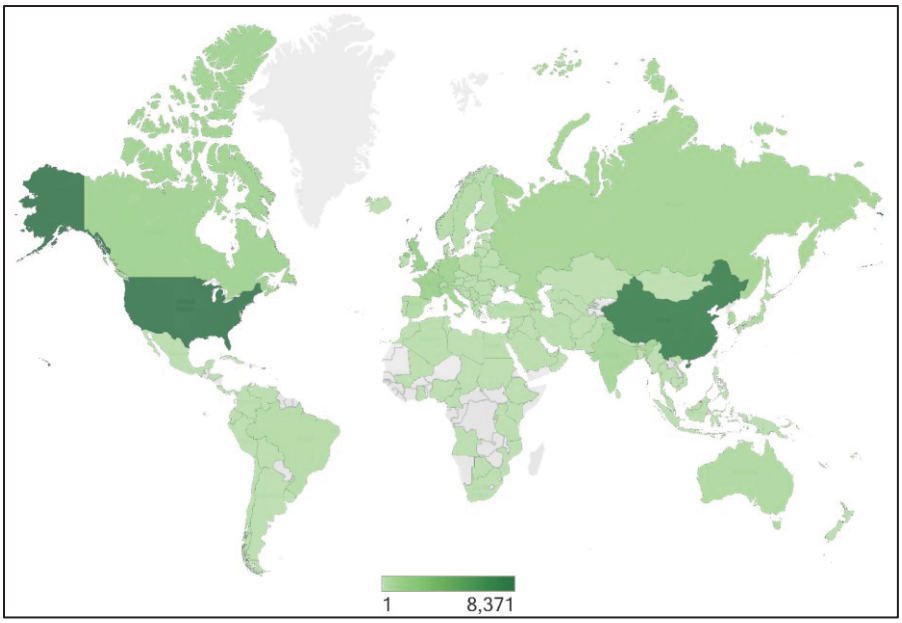

Figure 2.4 Publications par pays depuis 1995 pour le mot-clé *prognostic*

Maintenant qu'une définition générale du concept de pronostic est posée, il est normal de se demander comment, dans un contexte manufacturier, ce concept est-il traduit?

Nonobstant les sous-domaines d'application, la littérature entourant le pronostic propose principalement deux écoles de pensées quant aux méthodes de modélisation : les méthodes basées sur la physique des mécanismes de défaillances et les méthodes basées exclusivement sur les données (R. Gao et al., 2015; Gugulothu et al., 2017; Janssens et al., 2017; Kundu et al., 2017; Kundu et al., 2020; Singh, Kumar, & Dwivedi, 2017; Vogl et al., 2016; Xing-yu, Peng, Dong-dong, & Chengcheng, 2017). La première repose sur une modélisation paramétrique, produite par nos connaissances des lois de la physique, et une approche empirique pour identifier et ajuster les paramètres du modèle. La deuxième se base sur la disponibilité exhaustive des données historiques. Un algorithme d'apprentissage modélise alors la relation entre une ou plusieurs variables entrantes et la réponse étiquetée (i.e. apprentissage supervisé).

Comme démontré à la Figure 2.3, le domaine de la maintenance et de la fiabilité occupe une place importante dans les contributions. On dénombre effectivement plusieurs travaux appliquant les méthodes précédemment définies. Par exemple, J. Lee, Ni, Djurdjanovic, Qiu, et Liao (2006) introduisent dans leur article le concept d'« e-Maintenance » où ils appliquent une méthode physique basée sur une version modifiée de l'approche *Proportional Hazards* à un banc de test expérimental simulant la dégradation rapide d'un roulement à billes. Pour un même type de composant, mais appliqué dans le domaine des éoliennes, Cambron, Tahan, Masson, et Pelletier (2017) ont développé un modèle inspiré par la modélisation physique (bilan des flux thermique) pour établir un suivi de l'état de dégradation d'un roulement. Leur modèle est combiné à une carte de contrôle de type *Exponentially Weighted Moving Average* (EWMA), il permet de détecter les bris de roulement à billes avec une précision suffisante pour permettre d'être proactif dans la planification des activités de maintenance.

À l'inverse d'une méthode basée sur la connaissance des lois physique des mécanismes de défaillances, Aydin et Guldamlasioglu (2017) ont utilisé une approche basée exclusivement sur les données. Ils ont utilisé un réseau d'apprentissage profond (*Deep Learning*) pour prédire le RUL d'un turboréacteur. Bien qu'intéressant, leurs résultats sont basés sur les données d'une simulation fournie par la NASA (*C-MAPSS Aircraft Engine Simulator Data*) et non sur des données industrielles. Gugulothu et al. (2017) et Zheng, Ristovski, Farahat, et Gupta (2017) ont également proposé des méthodes de pronostic en se basant sur l'apprentissage machine à partir des données de simulation. Dans le même esprit qu'Aydin et Guldamlasioglu (2017), Zheng et al. (2017) ont utilisé un réseau d'apprentissage profond, mais ils y ont intégré une variante en adoptant une architecture de type *Long Short-Term Memory* (LSTM). Ils soutiennent donc pouvoir prédire le RUL avec une erreur minimale grâce à ce type de structure. B. Wang, Lei, Yan, Li, et Guo (2020) ont proposé un réseau à convolution récurent issu d'une combinaison entre une architecture à convolution et une architecture récurrente.

La particularité des travaux cités précédemment est que les auteurs n'ont pas extrait de descripteurs, mais plutôt utilisé les données brutes issues de leurs sources (capteurs). Il est

connu que les méthodes se basant sur l'apprentissage machine aboutissent à une modélisation beaucoup plus abstraite, de type *black box*, rendant l'interprétation du réseau et l'extrapolation de la connaissance difficiles pour un humain (Janssens et al., 2017; F. Jia, Lei, Guo, Lin, & Xing, 2017).

Néanmoins, malgré cet inconvénient, les récents succès reliés au *Deep Learning* n'ont pas empêché la communauté scientifique de tirer profit de ces techniques (Khan & Yairi, 2018; R. Liu, Yang, Zio, & Chen, 2018; Rezaeianjouybari & Shang, 2020; S. Zhang, Zhang, Wang, & Habetler, 2019; R. Zhao et al., 2019). En effet, plusieurs auteurs tel que Janssens et al. (2017), W. Zhang, Li, Peng, Chen, et Zhang (2018), X. Li, Ding, et Sun (2018), Haidong, Hongkai, Xingqiu, et Shuaipeng (2018), Michau, Palmé, et Fink (2017), Verstraete, Droguett, et Modarres (2020) ou encore S. Wang, Xiang, Zhong, et Zhou (2017) ont tenté d'appliquer ce concept au contexte de la maintenance industrielle prédictive. De plus, la particularité de ces travaux réside dans le fait que ceux-ci tirent profit de la capacité des modèles à générer de manière autonome les descripteurs. Y. Fu et al. (2017) ont même tenté d'utiliser directement l'image du spectrogramme d'un signal temporel vibratoire à l'aide d'une architecture de type réseau de neurones à convolution (CNN) pour prédire l'état d'une machine-outil CNC. Dans le même ordre d'idée, Janssens et al. (2017) ont utilisé des images d'une caméra thermographique pour prédire l'état et le niveau d'huile de roulements à billes. Il est important de noter que les résultats de ces auteurs sont tous basés sur des données issues d'expérimentations en laboratoire. En effet, un laboratoire procure la liberté d'expérimenter différents cas de figures permettant ainsi un apprentissage qui couvre l'étendue des éventualités des modes d'opérations.

Il nous serait possible d'énumérer d'autres cas d'application du concept de pronostic dans le domaine de la maintenance industrielle, mais nous constatons, qu'en règle générale, les travaux présentent des cheminements similaires. Effectivement, des auteurs comme Meziani, Zarour, et Thomas (2017), P. Hou, Wen, et Dong (2017), Kundu et al. (2017), Xing-yu et al. (2017), M. Liang, Cao, et Tang (2021), Zemouri, Al Masry, Remadna, Terrissa, et Zerhouni (2020) ont tous proposé des modèles basés soit sur une approche par les données ou bien sur

la physique des mécanismes de défaillances. De plus, leurs résultats sont majoritairement basés sur des données expérimentales obtenues en laboratoire et non pas issues d'applications en industrie. Ces auteurs ont également proposé différentes combinaisons de capteurs (ex. : accéléromètre, émission acoustique, etc.) et de descripteurs. Ce faisant, bien que chacun apporte une nouveauté et une contribution originale, les éléments et les objectifs fondamentaux de ces recherches restent semblables.

Plus près de notre contexte de recherche, l'usinage et le pronostic de l'état d'un outil de coupe sont des créneaux de recherche bien établis. Prédire lorsqu'un outil devra être remplacé apporte de nombreux avantages pour une entreprise. Des réductions de coûts suite à la diminution de la consommation d'outils de coupe, une diminution des coûts par rapport aux produits endommagés par des outils de coupe brisés en cours d'usinage et une meilleure planification des changements d'outils sont quelques-uns de ces bénéfices (Balan & Epureanu, 2008a; J. Z. Zhang & Chen, 2008; Y. Zhou & Xue, 2018).

Nous retrouvons d'ailleurs plusieurs cas d'applications. Des auteurs comme M Lamraoui, Thomas, et El Badaoui (2014) et Girardin, Rémond, et Rigal (2010) ont préconisé des méthodes axées sur la physique des mécanismes de défaillances avec, dans leurs cas, une modélisation basée sur les outils de l'analyse de la cyclostationnarité. Albertelli, Goletti, Torta, Salehi, et Monno (2016), quant à eux, ont tenté de suivre l'état de l'outil de coupe en se basant sur une modélisation physique de l'outil à l'aide de capteurs de vibration, de déplacement et de tests d'impact. Uekita et Takaya (2017) ont proposé une approche par la fusion des données d'émission acoustique et de consommation de courant du moteur de la broche. Il est intéressant de mentionner que les auteurs ont proposé d'inclure les concepts d'ébauche, de semi-finition et de finition dans leur modélisation avec la notion de seuil adaptatif.

Nous retrouvons également plusieurs travaux qui se basent sur le concept de l'énergie pour surveiller et prédire l'usure d'un outil de coupe. Par exemple, Agrawal, Khanna, Pruncu, Singla, et Gupta (2020) s'intéressent à la progression de l'usure des pastilles de coupe dans

diverses conditions de coupe en se basant sur la consommation énergétique. S. Gao et al. (2017) s'intéressent à l'optimisation des paramètres de coupe en se basant sur une approximation de l'énergie spécifique de coupe basée sur l'acquisition, à l'aide d'une table dynamométrique, du signal de l'effort de coupe. Dans Z. Zhu et al. (2019) et Shen, Cao, Li, Zhu, et Zhao (2018) les auteurs tentent de modéliser une signature du procédé d'usinage en se basant sur la consommation énergétique de l'équipement. Dans les deux cas, les auteurs soutiennent que leurs approches respectives permettent de modéliser et de suivre le processus de coupe. Dans le même ordre d'idées, d'autres auteurs tels que S. Jia, Yuan, Cai, Lv, et Hu (2019), Qiu (2018), L. Wang, Meng, Ji, et Liu (2019), J. Zhao, Li, Wang, et Sutherland (2019) et Z. Jiang, Gao, Lu, Kong, et Shang (2019) placent la notion d'énergie au centre de leur modélisation. Le concept d'énergie devient donc une avenue intéressante à investiguer dans notre contexte et en relation avec notre objectif de définir un ou plusieurs descripteurs physiques liés à la dégradation du processus d'usinage.

Comme pour le domaine de la maintenance industrielle, nous dénombrons également plusieurs travaux utilisant des méthodes basées sur les données pour le domaine du pronostic de l'état d'un outil de coupe. Par exemple, l'étude de Kong, Chen, Li, et Tan (2017) propose une méthode de suivi et de pronostic de l'état de l'outil de coupe qui se base sur le signal de l'effort de coupe et sur l'algorithme du *Support Vector Machine* (SVM) appelée *v*-SVR. Aghazadeh, Tahan, et Thomas (2018b) proposent une méthode de pronostic basée sur une architecture CNN. Les auteurs offrent également une étude comparative où ils supportent que le réseau CNN permet d'atteindre la meilleure performance (précision de 87.2%). Les auteurs avaient déjà offert une autre étude comparative dans Aghazadeh, Tahan, et Thomas (2018a). X. Zhang, Lu, Li, et Wang (2021) proposent également une architecture CNN, mais celle-ci est combinée à une architecture LSTM. Les auteurs soutiennent que cette approche permet d'atteindre une précision de pronostic de 87.3%. Nous retrouvons, comme pour le domaine de la maintenance industrielle, une approche similaire dans les travaux explorés. Effectivement, Chen, Jin, et Jiri (2018), Terrazas, Martínez-Arellano, Benardos, et Ratchev (2018), J.-T. Zhou, Zhao, et Gao (2019), M.-K. Liu, Tseng, et Tran (2019), Y. Liu, Hu, et Jin (2019), Marani, Zeinali, Kouam, Songmene, et Mechefske (2020) ou encore Cai, Zhang, Hu,

et Liu (2020) ont tous proposé des concepts visant à faire le suivi et le pronostic de l'état d'un outil de coupe avec une approche de modélisation par les données. De même que pour la maintenance industrielle, nous retrouvons aussi des auteurs tel que Martínez-Arellano et al. (2019) ou K. Zhu, Li, et Zhang (2020) qui misent sur l'utilisation de l'image des séries temporelles du signal comme données d'entrées de leur modèle de pronostic. Malgré tout, même dans le domaine du pronostic de l'usure et de l'état d'un outil de coupe, la principale différentiation entre les travaux se trouve au niveau du choix du capteur (ex. : accéléromètre, sonde thermique, etc.) ou des descripteurs utilisés pour représenter le phénomène, et ce, avec différents algorithmes d'apprentissage machine (classificateurs ou modèle de régression) tels que CNN, SVM, etc.

De plus, les conclusions des différents auteurs sont généralement et également fondées sur des données obtenues en laboratoire, donc en quantité et de variété restreintes. Il serait donc intéressant de voir comment tous ces modèles pourraient se comporter face à une application industrielle où nous retrouvons des conditions de coupe très variées et une multitude de types d'outils de coupe.

Précédemment, nous avons mentionné qu'il y a principalement deux écoles de pensée : une modélisation basée sur la physique ou basée sur les données. Malgré tout, nous avons constaté que plusieurs travaux tentent de combiner les deux écoles dans une approche hybride. Par exemple, Hanachi, Yu, Kim, Liu, et Mechefske (2019) proposent la combinaison d'une modélisation de l'usure d'un outil de coupe basée sur un modèle physique (l'usure en fonction du temps et des paramètres de coupe) avec un modèle d'apprentissage machine (*Adaptative Neuro-Fuzzy*) et soutiennent que leur approche procure de meilleurs résultats que chaque modèle utilisé indépendamment : un *Root Mean Square Error* (RMSE) de 0.22 versus 0.42 et 0.56. Hassan, Sadek, Attia, et Thompson (2018) proposent un processus de surveillance et de pronostic ainsi que la classification de l'état de l'outil de coupe, basé sur une série de descripteurs statistiques et physiques combiné à une approche d'apprentissage non supervisée. Leurs travaux proposent également d'utiliser la prédiction de leur modèle pour adapter les paramètres de coupe ou arrêter la machine-outil

(dans le cas d'un bris) en temps réel. D'autres travaux comme ceux de Afshari Behzad, Abedi, et Shahryari (2017) et Janssens et al. (2017) présentent aussi des conclusions positives par l'application d'une approche hybride dans leur modélisation. Ces applications réussies d'une approche hybride nous confortent donc dans notre intention de combiner des descripteurs physiques avec une approche de modélisation basée sur l'apprentissage machine.

Pour résumer, nous avons constaté que de nombreuses recherches ont été effectuées. Qu'en est-il pour notre domaine spécifique de recherche : le pronostic de la qualité d'un produit usiné? Lorsque nous observons ce domaine, nous pouvons avancer qu'il existe des applications visant à prédire la qualité d'un produit. Par exemple, Voisin, Laloix, Iung, et Romagne (2018) proposent un indicateur de santé basé sur l'analyse d'un signal vibratoire dans l'optique de faire le suivi de requis qualité : la localisation d'une surface et le parallélisme. Également, Papananias, McLeay, Mahfouf, et Kadirkamanathan (2019) prédisent la valeur de deux types de GD&T : la circularité et le positionnement grâce à un modèle basé sur l'apprentissage machine et alimenté par l'effort de coupe. Par contre, nous percevons qu'il ne semble pas y avoir un consensus quant à la définition du terme « qualité » dans un contexte d'usinage. En guise d'exemple, Laloix et al. (2016) supportent que la notion de qualité soit reliée au contrôle statistique de procédé. Il y a déjà 30 ans, Irgens (1991) définissait cette notion comme étant la qualité fonctionnelle du produit. Park et Tran (2014) affirment que la qualité est reliée à l'usure de l'outil de coupe et à la rugosité de la surface. García, Sánchez, Rodríguez-Picón, Méndez-González, et Ochoa-Domínguez (2018) sous-entendent que la qualité est reliée aux caractéristiques de performance du produit et du processus de fabrication. Nous pouvons donc discerner qu'il y a un manque de consensus au niveau de cette définition. Comme préalablement explicité, nous définissons la qualité comme étant la conformité d'un produit par rapport au respect de ses requis (spécifications GD&T et rugosité). Nous nous positionnons donc proche des travaux de Voisin et al. (2018) et de Papananias et al. (2019).

Cette revue de la littérature, inévitablement limitée et partielle, nous permet tout de même de faire un premier constat : il existe définitivement un engouement, une volonté et des bénéfices à appliquer ce concept dans le domaine de l'usinage. Un deuxième constat nous laisse envisager que les résultats, validations et conclusions des études explorées sont majoritairement basés sur des données obtenues en laboratoire avec des expérimentations planifiées. Les aléas industriels n'ont pas été pris en compte.

Ce faisant, l'accès à un jeu de données industrielles, ainsi qu'un transfert technologique en industrie semble toujours se faire attendre. Aussi, nous considérons qu'il est important de valider un modèle ou une conclusion sur des données industrielles; les données expérimentales ne représentent pas toujours la totalité de la complexité d'un phénomène (Lei et al., 2018).

À ce stade de notre étude, nous conjecturons que pour modéliser et prédire le phénomène complexe qu'est la qualité d'un produit usiné par rapport à ses requis, des données variées représentant la totalité d'un processus d'usinage, d'un niveau de qualité adéquat, dans une quantité suffisante et disponibles en temps réel sont nécessaires. Acquérir un tel jeu de données peut s'avérer complexe ou bien trop coûteux autant pour un industriel que pour un laboratoire de recherche. C'est une conclusion qui semble être également soutenue par Rezaeianjouybari et Shang (2020). Malgré tout, nous sommes convaincus qu'avec la disponibilité croissante des technologies et l'influence pressante de la mouvance Industrie 4.0, les entreprises peuvent tirer de la valeur et des bénéfices au travers de l'acquisition et de l'utilisation de telles données. Un troisième constat de cette revue nous conforte dans notre désir de miser sur une approche de modélisation hybride basée sur des descripteurs et autant que possible sur une interprétation physique des phénomènes d'usinage, combinée à une modélisation par les algorithmes d'apprentissage machine.

De plus, nous ne prétendons pas avoir fait une revue exhaustive et complète de tous les travaux. Néanmoins, un quatrième constat se dégage et nous porte à croire que l'activité dans le domaine du pronostic de la qualité d'un produit usiné s'avère moindre que dans ceux du

pronostic de l'état d'un procédé (ex. : outil de coupe). Malgré tout, plusieurs auteurs s'entendent sur les bienfaits d'un système de pronostic de la qualité d'un produit usiné : Laloix et al. (2016) supporte qu'un tel système de pronostic serait en mesure de réduire les besoins en contrôle de la qualité après l'usinage. J. Lee, Lapira, Bagheri, et Kao (2013) proposent de mettre en relation les données d'un équipement de production avec les données d'inspection afin de faire la distinction entre la dégradation de l'équipement et celle du procédé. K.-S. Wang (2013) propose la surveillance constante et continue du procédé de fabrication dans une optique de fabrication avec zéro défaut. Ces auteurs sont tous en accord sur le fait que le développement d'un système qui, en surveillant le procédé de fabrication en temps réel, pourrait théoriquement réaliser le pronostic de sa condition et s'ajuster de manière autonome afin d'éviter les défauts de qualité. Un système capable de réaliser ceci procurerait des avantages non négligeables pour les entreprises (Ertekin et al., 2003).

2.3 Conclusion

Bien qu'il semble y avoir une volonté de la part de la communauté scientifique et un besoin des industriels, notre revue, bien que non exhaustive, ne nous permet pas, à ce stade-ci de nos travaux, d'être en mesure de trouver une réponse satisfaisante et unanimement acceptée à nos questions de recherche. Nonobstant le fait que plusieurs auteurs veulent se diriger dans cette direction, nous avons également constaté qu'il y a encore peu ou pas d'applications dans l'industrie manufacturière et, de manière plus précise, dans le domaine de l'usinage. Cette absence de consensus vient donc, selon nous, renforcer le besoin inhérent de réaliser ce projet de recherche.

CHAPITRE 3

MÉTHODOLOGIE ET ORGANISATION DE LA THÈSE

3.1 Introduction

Ce chapitre présente notre démarche pour atteindre les objectifs fixés à la section 1.2 et par conséquent, la méthodologie adoptée pour tenter de répondre à notre problématique. Le chapitre est structuré de la manière suivante : nous présentons notre environnement de recherche puis, nous déterminons le cadre et les frontières entourant ces travaux, nous proposons une méthodologie de recherche et finalement, nous décrivons l'organisation et la structure de la thèse en relation avec nos contributions publiées.

3.2 Environnement de recherche

Dans le cadre de ce projet, nous avons l'opportunité de travailler en partenariat avec un partenaire industriel. APN Inc. est un leader dans la fabrication de produits usinés destinés à des entreprises provenant d'industries de pointe telles que l'aéronautique, la défense, ainsi que la haute-technologie (communication, science de la vie, etc.). APN Inc. est également membre du groupe APN Global qui est un leader en usinage de produits de hautes précisions, ainsi qu'en conception, fabrication, assemblage et réparation de valves chromatographiques.

Plus précisément, ce projet est entrepris avec la division localisée à la ville de Québec (Qc, Canada). Cette division est spécialisée dans l'usinage de très haute précision de produits à base de matériaux exotiques (ex. : alliage de titane, alliage de nickel, carbure de tungstène, etc.). De plus, elle est également une des entreprises au Québec qui se situe à l'avant-plan du mouvement Industrie 4.0 au Canada. Récemment, cette division est devenue la première

vitrine 4.0 du Québec[2] selon le standard BNQ 6545-200 (Bureau de Normalisation du Québec, 2018).

Une des raisons pour lesquelles APN Inc. a mérité cette certification est que l'entreprise est en pleine transformation numérique, ce qui implique également une numérisation avancée de ses procédés de fabrication. En d'autres mots, elle est en train de s'assurer de capter un maximum de données représentant chacune des étapes ou phénomènes en action lors de son processus de fabrication dans le but de les exploiter à des fins de surveillance, de diagnostic et de pronostic. La même chose se déroule également avec ses processus connexes (ingénierie, qualité, etc.). Par conséquent, une multitude de données est accessible à notre équipe de recherche.

Des équipements à la fine pointe de la technologie, une volonté d'innover et d'intégrer les technologies de l'information au cœur de ses processus d'affaires, ainsi que des experts dans le domaine sont quelques-unes des raisons qui font d'APN Inc. un partenaire idéal pour ce projet de recherche. Finalement, cet environnement nous procure un avantage considérable dans la réalisation de nos travaux en comparaison des autres études explorées qui se basent davantage sur des données issues de simulations ou obtenues en laboratoire.

3.3 Cadre de recherche

Vu l'ampleur du projet, nous avons dressé une liste d'éléments dans le but d'encadrer la portée de ce dernier et de fixer ses frontières. Certaines de ses balises sont inspirées des travaux réalisés précédemment par Proteau (2016).

1) Seule la famille de procédés du partenaire industriel est considérée dans ce projet. Fondamentalement, il s'agit d'un atelier d'usinage de haute précision;

---

[2] https://www.criq.qc.ca/fr/vitrine-4-0.html

2) Nous considérons que les modèles 3D sont une source parfaitement fidèle à la définition nominale du produit;
3) L'interprétation des requis et spécifications GD&T des produits est selon le formalisme ASME Y14.5 (ASME, 2009, 2018a) et ASME Y14.36 (ASME, 2018b);
4) L'avis des experts industriels est considéré comme cohérent et représentatif;
5) Nous considérons que les programmes de fabrication ou de mesure sont cohérents et représentatifs du processus de fabrication ou de mesure;
6) Nous considérons que les mesures métrologiques (i.e. vérification de la qualité du produit) sont réalisées dans le respect des procédures, des bonnes pratiques et des normes de qualité;
7) Dû à des contraintes temporelles et logistiques, nous avons décidé de nous concentrer sur un type de procédé : l'usinage sur un centre d'usinage. Ce faisant, nous excluons tout autre type d'opération d'usinage (tournage, meulage, etc.);
8) Nous considérons que la géométrie et la précision de la machine-outil CNC sélectionnée pour ce projet sont selon les spécifications du fabricant et que, si des variations existent, elles n'affectent pas sensiblement la qualité du produit;
9) Nous considérons que la principale source de variation de la qualité d'un produit usiné est l'usure des outils de coupe utilisés pour produire celui-ci.

3.4 Méthodologie de recherche

Cette section fournit les fondements de notre méthodologie et la structure sur laquelle s'articuleront nos résultats. Nous présentons, tout d'abord, le banc de test spécifique sur lequel nous collecterons les données (procédé et qualité). Ce processus est ensuite détaillé. Nous présentons par la suite les détails de l'architecture du réseau de neurones utilisée. Une méthodologie détaillée est également décrite aux sections 4.4, 5.5, 6.4, 6.5, ainsi qu'à l'ANNEXE I. La Figure 3.1 présente un résumé de la méthodologie de recherche en relation avec les objectifs de cette thèse.

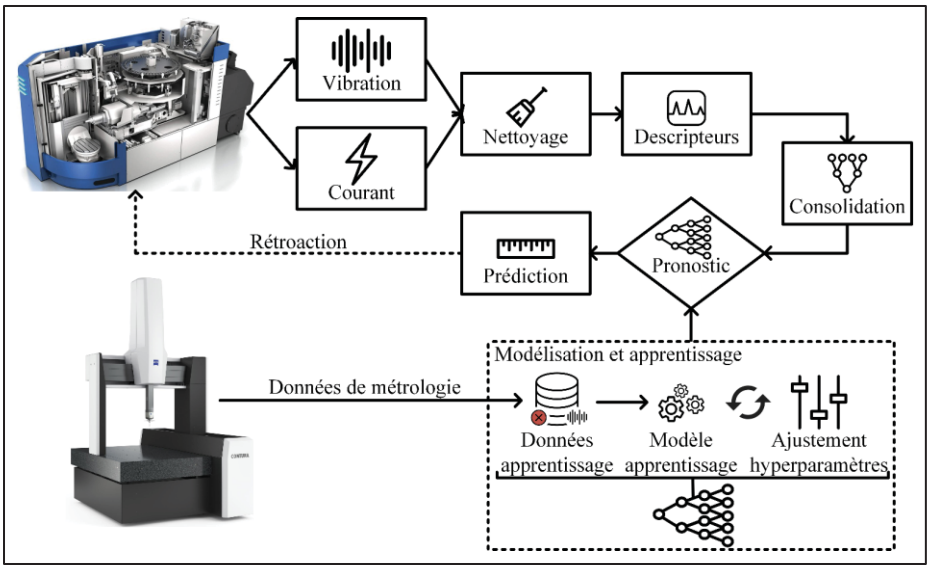

Figure 3.1 Résumé de la méthodologie de recherche

Nous pouvons constater que des données représentant les phénomènes d'usinage sont acquises à partir de capteurs et d'un système d'acquisition (section 3.4.2) installés sur un équipement de fabrication (section 3.4.1). Ces signaux contextualisés sont ensuite traités et consolidés pour extraire des descripteurs statistiques temporels, fréquentiels et cyclostationnaires (sections 4.4.1, 5.5.2 et 6.4.3). Ces descripteurs sont finalement employés comme données d'entrées pour un modèle de régression basé sur une approche par apprentissage machine (sections 3.4.3, 5.5.3 et 6.5) permettant d'estimer la mesure de la qualité du produit. Nous pourrions également entrevoir que ce système puisse, basé sur la prédiction et un niveau de confiance, faire la rétroaction à l'équipement de fabrication pour que celui-ci s'ajuste.

3.4.1 Banc de test spécifique

Ce projet s'articule autour d'un équipement de fabrication appartenant au partenaire industriel et qui joue le rôle de banc de test spécifique. L'équipement sélectionné est une machine-outil CNC 5 axes modèle G353 (G350 2e génération) provenant du fabriquant Grob-Werke. La Figure 3.2 présente un aperçu de cet équipement. Voici également quelques spécifications de l'équipement :

- Vitesse maximale de la broche : 16 000 RPM
- Puissance de la broche (100% / 40%) : 25/32 kW

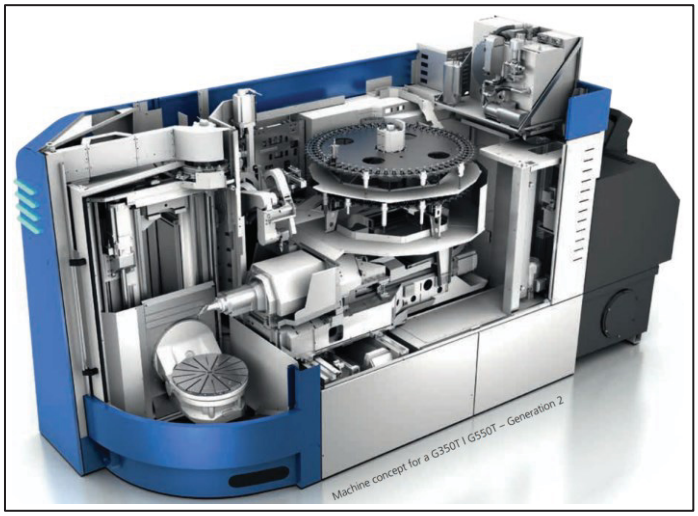

Figure 3.2 Machine-outil CNC 5 axes Grob G352[3]

L'équipement étant relativement récent, cela permet d'avoir accès à des données issues de capteurs déjà installés et qui reflètent son état.

3.4.2 Système et processus d'acquisition

Cette section vise à mettre en lumière les différents éléments composant le système et le processus d'acquisition des données sur l'équipement de production. Nous présentons tout d'abord les différents composants du système, puis le processus d'acquisition et finalement, nous décrivons le jeu de données collecté.

Le système d'acquisition est composé d'un module d'acquisition et de trois types de capteurs. Le Tableau 3.1 présente les détails des différents capteurs, ainsi que la fréquence d'échantillonnage (f_s) utilisée pour chacun. Le Tableau 3.2 spécifie les détails des équipements utilisés pour l'acquisition des données.

[3] Photo: Grob-Werke

Tableau 3.1 Spécifications des capteurs

Type de capteur	Fournisseur	Modèle	Portée	Quantité
Accéléromètre uniaxial	IFM	VSA004	1-10 000 Hz	1
Accéléromètre triaxial	PCB	356A33	2-10 000 Hz (y et z) 2-7000 Hz (x)	1
Courant	LEM	LF210-S	200 A	4

Tableau 3.2 Spécification des équipements d'acquisition

Type d'équipement	Fournisseur	Modèle	Max f_s	Quantité
Boîtier d'acquisition	National Instruments	cDAQ-9174	N/A	1
Module vibration	National Instruments	NI-9232	102.4 kHZ	2
Module voltage	National Instruments	NI-9239	50 kHZ	1

La Figure 3.3 présente la position relative des capteurs sur la machine-outil CNC tels que décrits dans Proteau, Zemouri, Tahan, et Thomas (2020). Plus précisément, nous avons utilisé le capteur IFM VSA004 déjà présent dans la broche de la machine-outil (voir Figure-A I-2) en subtilisant le signal brut du capteur à l'aide d'un conditionneur de signal (Phoenix Contact modèle MACX MCR-UI-IU) tel qu'illustré à la Figure 3.4.

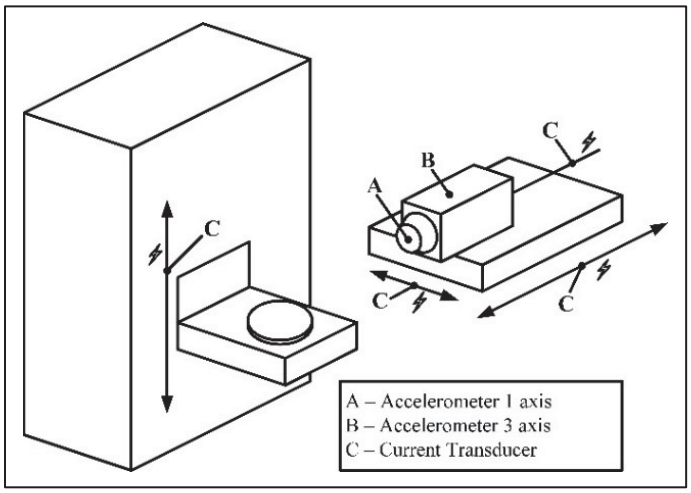

Figure 3.3 Position relative des capteurs
Tirée de Proteau et al. (2020)

Figure 3.4 Installation du conditionneur de signal

Ensuite, la Figure 3.5 présente la position où est installé l'accéléromètre triaxial (PCB) sur le châssis de la broche. Ce choix de positionnement résulte d'une problématique liée à l'accès à la zone de coupe, à un accès restreint à la broche, ainsi qu'à l'obligation de ne pas obstruer ou limiter la capacité de production de la machine-outil par la présence du capteur ou des câbles.

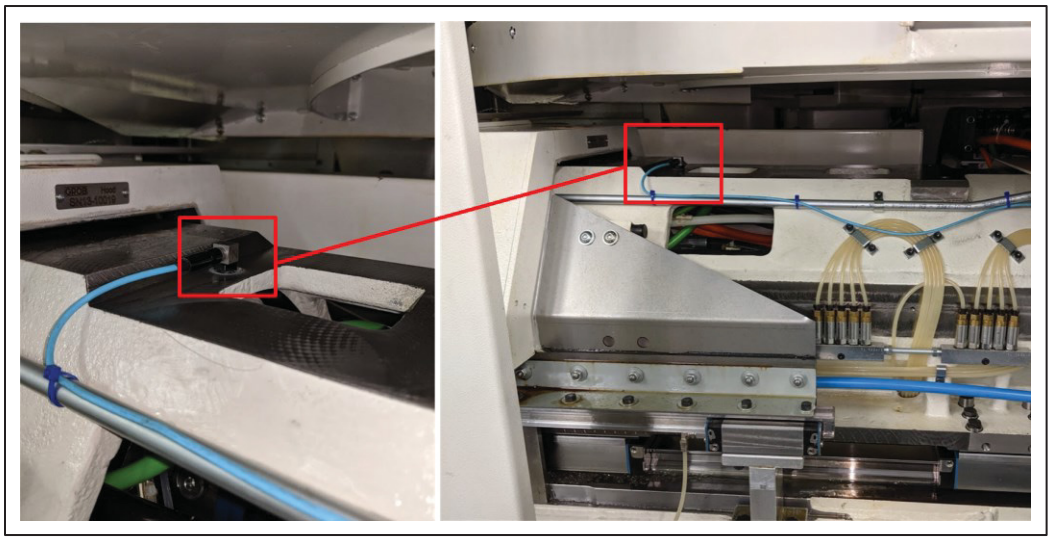

Figure 3.5 Position de l'accéléromètre sur le châssis de la broche

Puis, la Figure 3.6 présente la position des capteurs de courant installés sur une phase des moteurs des axes principaux (X, Y et Z), ainsi que sur une phase du moteur de la broche. En (b), la Figure 3.6 présente aussi le boîtier de conversion que nous avons développé pour convertir le signal du capteur en signal lisible par le module d'acquisition.

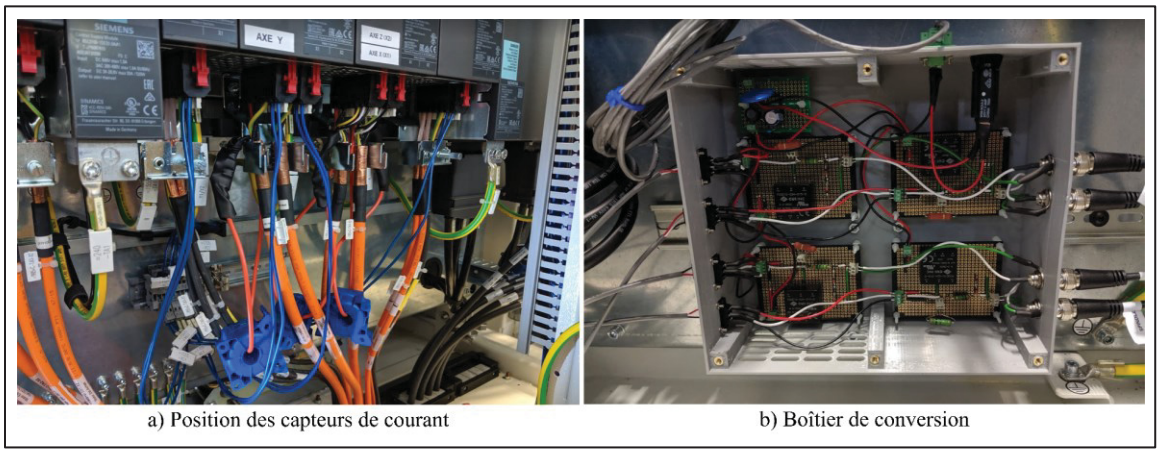

Figure 3.6 Position des capteurs de courant (a) et boîtier de conversion (b)

La Figure 3.7 présente un aperçu de l'architecture et du processus d'acquisition. Le système d'acquisition est cadencé par l'état de la machine-outil CNC, c'est-à-dire que le système

n'acquière des données que lorsque la machine-outil est opérationnelle et en processus de coupe. Les phases transitoires (changement d'outil, retour à l'origine, etc.) sont exclues des fichiers de données. Chacun de ceux-ci est également attaché avec les données opérationnelles (opération de coupes, paramètres de coupe, type d'outil, etc.) ainsi qu'avec les données de métrologie du produit usiné (en **rouge**). Chaque fichier représente, au plus, 5 secondes d'acquisition avec une fréquence d'échantillonnage de 20 kHz, ce qui représente une résolution dans le domaine fréquentiel de 0.2 Hz ($f_s/N = 0.2$ Hz). L'acquisition est également réalisée en mode continue tant que l'état de la machine-outil est en mode de coupe.

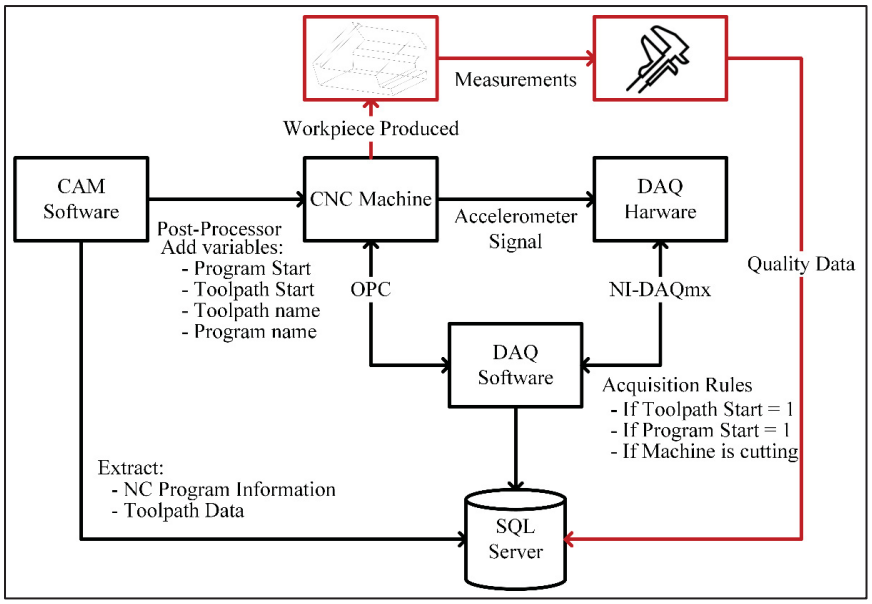

Figure 3.7 Architecture et processus du système d'acquisition
Tirée de A. Proteau, A. S. Tahan, et M. Thomas (2019b)

Le jeu de données acquis représente plus de 342 500 fichiers de signaux bruts équivalents à plus de 2 TB de données. Ces données couvrent six ordres de travail du partenaire totalisant plus de 600 heures de production régulière et des dizaines d'outils, d'opérations et de conditions de coupe différentes. C'est un jeu de données qui représente adéquatement la diversité des phénomènes physiques à l'œuvre, ainsi que les variations (ex. : usure des outils de coupe) et les aléas présents dans un contexte industriel.

Le lecteur est invité à se référer à l'ANNEXE I et aux sections 5.5.1 et 6.4.1 pour plus de détails sur le processus d'acquisition et le jeu de données.

3.4.3 Architecture du réseau de neurones

L'objectif de cette thèse est de proposer une méthodologie pour estimer le niveau de qualité d'un produit usiné par une approche basée sur l'apprentissage machine et en se basant exclusivement sur les données de surveillance du procédé. Cette section présente de manière générale cette approche et ses implications.

Aujourd'hui, il est presque admis qu'une approche par apprentissage machine est une bonne approche pour un contexte industriel et manufacturier (Chadha et al., 2019; S. Lee, Kwak, Tsui, & Kim, 2019). Malgré les avantages qu'elles peuvent procurer, ces approches présentent tout de même des désavantages : la nécessité d'avoir des données de qualité et en quantité couvrant toute l'étendue du domaine d'étude, des problématiques liées à la dimensionnalité du problème (San Martin, López Droguett, Meruane, & das Chagas Moura, 2019) et leur nature « boîte noire » inhérente à cette approche (S. Yu & Príncipe, 2019) n'en sont que quelques un.

Pour contrevenir à ces problématiques, nous optons pour une approche basée sur une architecture de type *Variational AutoEncoder* (VAE). Cette dernière fournit de bonnes capacités de visualisation et de réduction de dimensionnalité (San Martin et al., 2019). Ce type de réseau proposé par Kingma et Welling (2013) est une variante de l'*AutoEncoder* (AE) qui est fondamentalement un réseau de neurones entraîné à reproduire son vecteur d'entré. Un VAE est composé de trois parties : un encodeur, un espace latent et un décodeur. La Figure 3.8 illustre la structure générale qui lie ces trois éléments.

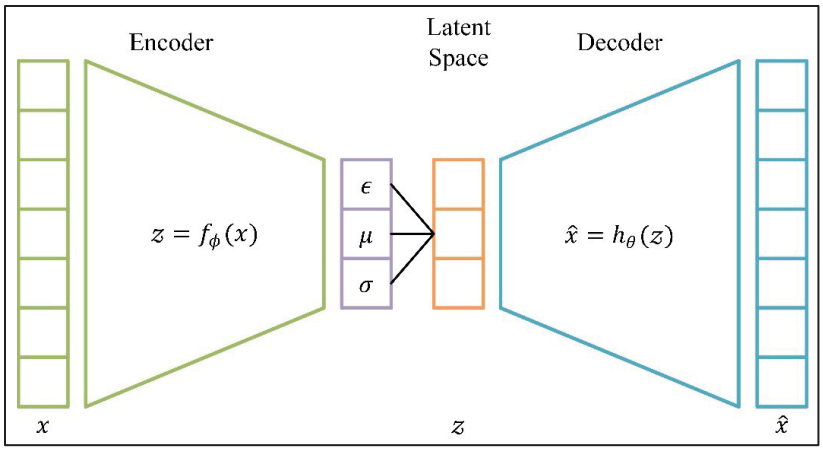

Figure 3.8 Structure d'un VAE
Tirée de Proteau et al. (2020)

Cette structure sera ensuite combinée à une couche de classification ou une couche de régression afin de mener à bien les objectifs de notre modélisation. Nous optons également pour un espace bidimensionnel ($\mathbb{R}^2$) qui permet une visualisation accessible et commode pour un usage industriel.

Pour conclure cette section, plus de précisions sur l'architecture spécifique de nos implantations, les choix quant aux hyper paramètres et la méthodologie d'apprentissage pour ce projet sont détaillés aux sections 5.5.3 et 6.5. Finalement, le lecteur est invité à se référer à Doersch (2016) pour une introduction à la théorie derrière le concept de VAE.

3.5 Organisation de la thèse

La présente thèse est abordée sous la forme d'une thèse par articles. L'objectif de cette section est donc d'exposer l'organisation de nos contributions en relation avec nos objectifs de recherche. Au CHAPITRE 1, nous avons mis sur la table notre contexte de recherche et la problématique sous-jacente. Le CHAPITRE 2 a présenté une revue de la littérature pertinente à notre contexte qui a permis de consigner l'importance et l'originalité du projet.

L'ANNEXE I propose une première version de l'architecture et du processus d'acquisition des données nécessaires à répondre à notre premier objectif. Cette publication (Conférence Survishno, Lyon, France, 2019) fournit une première exploration des résultats obtenus.

Le CHAPITRE 4 propose une réponse à notre deuxième objectif visant l'identification d'un descripteur fortement corrélé à l'évolution du processus de fabrication (dans notre cas : l'usure d'un outil de coupe). Cette contribution a été publiée dans un article au *The International Journal of Advanced Manufacturing Technology*. La contribution met en avant le concept d'énergie spécifique de coupe. Les signaux de consommation de courant sont convertis sous la forme d'un descripteur décrivant l'énergie nécessaire à l'enlèvement d'1 cm^3 de matériau. Nos conclusions démontrent que ce descripteur est fortement corrélé à l'usure d'un outil de coupe et donc, à l'évolution du processus de fabrication. Plus précisément, nos contributions sont les suivantes :

1) La description et la proposition du concept d'énergie spécifique de coupe tel que défini par nos travaux et la démonstration que celui-ci est fortement corrélé à l'usure d'un outil de coupe;
2) Le support à notre hypothèse qu'il est pertinent d'utiliser une approche par apprentissage machine pour modéliser et prédire des phénomènes dans le contexte d'usinage par l'utilisation d'un modèle de type LSTM pour prédire l'usure des outils de coupe;
3) La proposition d'une méthodologie de suivi visuel de l'évolution de l'outil basé sur une approche par carte de contrôle de type EWMA.

Au CHAPITRE 5, nous répondons à notre premier objectif de recherche. Le système d'acquisition est amélioré et finalisé. Aussi, nous répondons partiellement à notre troisième objectif (obtenir un modèle de pronostic basé sur une approche d'apprentissage machine). Cette contribution a été publiée dans *The International Journal of Advanced Manufacturing Technology*. Nous y proposons un modèle de pronostic des types d'opérations de coupe par l'utilisation d'une architecture basée sur le VAE. Les principales contributions de cet article sont les suivantes :

1) La proposition d'une méthodologie basée sur un apprentissage non supervisé puis sur un apprentissage supervisé;
2) La démonstration qu'il est possible de faire la classification des opérations de coupe basée simplement sur les signaux de capteurs émis par ces dites opérations;
3) Le renforcement de notre conclusion précédente à savoir que l'énergie spécifique de coupe est un descripteur qui permet de représenter adéquatement l'évolution du processus de fabrication (usure) et de notre hypothèse qu'une consolidation sous une base physique permet une meilleure modélisation. Ceci est supporté par le fait que ces deux éléments sont ceux qui apportent le plus au modèle.

Le CHAPITRE 6 vient finalement lier tous les éléments décrit précédemment et répond aux troisième et quatrième objectifs, et donc, à notre problématique. Cette dernière publication a été soumise au *Journal of Intelligent Manufacturing*. Elle présente la capacité de notre modèle à faire le pronostic (estimation) de la qualité d'un produit usiné. Cette modélisation est rendue possible avec le concept de VAE présenté au CHAPITRE 5 ainsi que notre proposition liée à l'énergie spécifique de coupe décrite au CHAPITRE 4. Plus précisément, les contributions de cette publication sont les suivantes :

1) La proposition d'un modèle de pronostic de la qualité d'un produit usiné basé sur une approche dérivée du concept de VAE;
2) Que notre proposition permet d'utiliser l'espace latent comme outil de visualisation et que celui-ci est fortement distribué selon l'évolution de la qualité;
3) La proposition d'une métrique basée sur le concept de distance euclidienne et de l'espace latent permet de rapidement et visuellement estimer le niveau de qualité d'un produit usiné.

Pour conclure, la Figure 3.9 résume l'organisation de cette thèse de manière visuelle. Cette section a également mis en lumière les interrelations de nos publications puisque les résultats de chacune permettent à la publication suivante de se concrétiser.

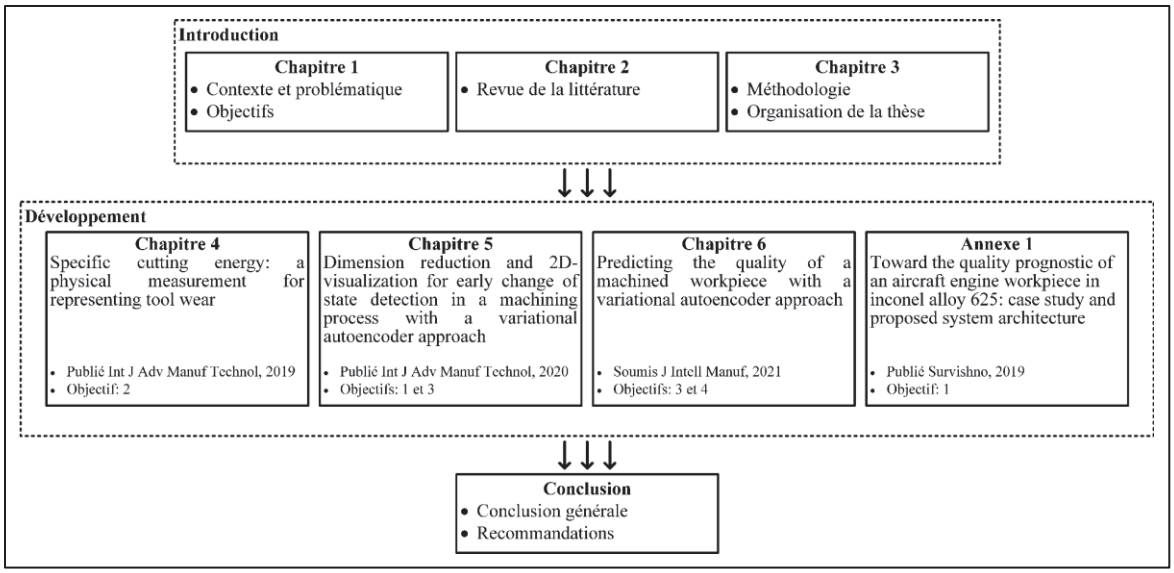

Figure 3.9 Résumé de l'organisation de la thèse par articles

CHAPITRE 4

SPECIFIC CUTTING ENERGY: A PHYSICAL MEASUREMENT FOR REPRESENTING TOOL WEAR

Antoine Proteau[a], Antoine Tahan[a], Marc Thomas[a]

[a]Département de génie mécanique, École de technologie supérieure, Montréal, Qc, H3C 1K3, Canada

Article publié dans « The International Journal of Advanced Manufacturing Technology », mars 2019

Publication originale disponible à: https://doi.org/10.1007/s00170-019-03533-4

4.1 Résumé

Dans un contexte d'usinage, les bris soudains d'outils de coupe sont toujours une des principales causes de l'augmentation des coûts de production et des arrêts machines. Ce faisant, pour augmenter la productivité et assurer la survie financière des entreprises, une méthode de surveillance des outils de coupe est essentielle. Par conséquent, cet article propose de démontrer qu'il est possible de faire le pronostic de l'usure d'un outil de coupe, avec une faible erreur, en utilisant une architecture de réseau de neurones de type récurrent (*Long Short-Term Memory*). Par contre, pour atteindre un modèle général, une proposition ne requérant aucun apprentissage est aussi nécessaire. Pour répondre à ce besoin, cet article introduit le concept d'Énergie Spécifique de Coupe basé sur les travaux de Debongnie (2006) qui est défini comme étant la quantité d'énergie nécessaire à l'enlèvement de 1 cm^3 de matériau. Nous démontrons que ce descripteur est fortement corrélé ($R > 90\%$) à l'usure d'un outil de coupe. Ce concept obtient également un R^2 ajusté élevé ($R^2 > 90\%$) avec un modèle de régression linéaire. Ces résultats sont basés sur un jeu de données expérimental rendu disponible par Agogino et Goebel (2007). Nonobstant l'atteinte de nos objectifs, les travaux futurs devraient inclure une méthodologie pour mesurer la durée de vie résiduelle d'un outil de coupe basée sur l'énergie spécifique de coupe, ainsi qu'une application industrielle de notre méthodologie afin de vérifier si les résultats supportent nos conclusions. Malgré tout,

notre proposition pourrait déjà aider les entreprises d'usinage à surveiller de manière précise la condition de leurs outils de coupe avec un seul descripteur.

4.2 Abstract

In a machining context, unexpected tool breakage is still one of the primary causes of increase costs and machine downtimes. Hence, to increase productivity and ensure a company's financial survival, a way to monitor cutting tool is essential. Thus, this paper proposes to show that it is possible to predict tool wear, with a low error, by using a recurrent neural network with a long short-term memory architecture. However, to achieve a general tool condition monitoring model, a proposition requiring no training is needed. Therefore, this paper introduces the concept of Specific Cutting Energy based on the work of Debongnie (2006), which is defined as the amount of energy required to remove 1 cm^3 of material. Based on our work, we show that this feature is highly correlated ($R > 90\%$) to the tool wear value. This concept also achieve a high adjusted R^2 ($R^2 > 90\%$) with a linear regression model. These results are based on an experimental dataset provided by Agogino et Goebel (2007). We succeed in achieving our objectives, however future work should include a methodology to measure the residual useful life of a cutting tool based on the Specific Cutting Energy and an industrial application of our methodology to see if the results support our conclusions. Still, our proposition could help machining companies accurately monitor their cutting tool wear condition with a single feature.

4.3 Introduction

In today's economy, a machining process by material removal is still widely accepted as the best method to obtain a complex workpiece. However, in the current context of globalization, digital transformation and the arrival of new disruptive technologies (artificial intelligence, additive manufacturing, etc.), it is increasingly difficult for companies to stay ahead of the competition. This global context combined with an ever-growing demand for a rise in both productivity and quality at a lower cost forces companies to look for every possible improvement. To help them, they can now rely on new concepts such as Industry 4.0 to

provide them with a new vector to invigorate the manufacturing industry and stimulate innovation through new technologies (Kohler & Weisz, 2016). In the specific context of machining, it is known that Industry 4.0 can have a positive impact on productivity and profitability by providing new technologies. Nevertheless, unexpected tool breakages or machine downtimes are all problems still affecting machining companies today. It is generally known that cutting tool defect is still one of the primary causes of poor quality, increase in production costs and machine downtime (Gebremariam, Xiang Yuan, Azhari, & Lemma, 2017; X. Jiang et al., 2018; J. Yu, Liang, Tang, & Liu, 2016; J. Z. Zhang & Chen, 2008; Y. Zhou & Xue, 2018). Therefore, monitoring its state and being able to predict either its Remaining Useful Life (RUL) or the amount of wear is a key toward an optimal usage of this resource. Ultimately, to achieve the Industry 4.0 dream of a fully automated production process, a more optimal cutting tool usage through Tool Condition Monitoring (TCM) is essential.

Still today, TCM is a very active research field that has concentrated its effort on two aspects: direct and indirect monitoring (X. Jiang et al., 2018). Direct methods will use technologies to make an actual and precise measurement of the tool condition. Indirect methods will try to determine the tool condition through the measurement and analysis of signals acquired from sensors such as accelerometers or current sensors (Aghazadeh et al., 2018a; Y. Zhou & Xue, 2018). Indirect measurement has been widely used both in research and in an industrial context since they require less investment and are less invasive in the production unit (Y. Zhou & Xue, 2018).

One of the main challenges of TCM is coming up with a general TCM model. In fact, most of the published work still proposes “tool specific” models (e.g. J. Yu et al. (2016), X. Jiang et al. (2018) or M Lamraoui et al. (2014)). To achieve a general model, we believe it is primordial to have access to a feature accurately representing the tool wear behavior. This feature should also be obtainable through indirect monitoring. What we saw from the literature is that most papers are based on the same statistical features to describe tool wear. For instance, Gebremariam et al. (2017) used features such as the mean and the kurtosis of a

signal. In J. Yu et al. (2016), they decided to only use the Root Mean Square of the vibration signal to predict the tool wear. Another example is P. Fu, Hope, et King (1998) where they used all the above and added the standard deviation and mean power in the frequency domain. However, most of them do not represent the physics behavior happening in the CNC machine. For a more exhaustive review of the commonly used features in TCM, the reader can refer himself to the work of Y. Zhou et Xue (2018), Abellan-Nebot et Romero Subirón (2010) or Elattar et al. (2016).

Since cutting parameters may vary during production, the ability of the model to represent non-linear phenomenon is needed (Aghazadeh et al., 2018a). Data-driven methods such as those from machine learning (support vector machine, artificial neural networks, deep learning, etc.) have been widely seen in the literature to perform such tasks. For instance, in Chen et al. (2018) they used machine learning algorithms to predict the tool wear. They also included a comparative study between three types of models: a deep belief network, an artificial neural network and a least square support vector regression. However, one drawback of such methods is the need for a high numbers of training examples to achieve generalization to other types of tools, which makes it harder to reach a general TCM model. Plus, these data-driven methods are as good as the quality of the features used in their training. Consequently, we believe that a feature representing more accurately the behavior of a cutting tool health state through time is a key to the development of a more general TCM model. Consequently, the aim of this paper is to demonstrate that a physics approach to feature engineering could better represent tools wear than traditional statistical feature engineering seen in the literature. Recently, authors such as Z. Jiang et al. (2019) and S. Jia et al. (2019) have used the physical concept of power to either monitor and model a CNC machine or make predictions with good results. Hence, strengthening our hypothesis that a physical approach could deliver better outcomes.

This paper develops two propositions: first, to demonstrate that it is possible to accurately predict the tool wear amount using data-driven methods such as those provided by the field of machine learning. Second, to establish the performance of a feature called Specific Cutting

Energy (SCE) based on the work of Debongnie (2006). To accomplish this aim, our proposal is based on the NASA Milling Dataset (Agogino & Goebel, 2007). We first show that it is possible to predict the tool wear value with a model based on an artificial neural network. To build this network, we first performed a correlation analysis and a Principal Component Analysis to construct an input vector and then we built and trained the neural network. At that point, we introduced our proposed feature: the Specific Cutting Energy. To validate its performance and support our claim that it can better represent tool wear than commonly used features, we detailed the results of correlation analysis and a linear regression analysis. We finally applied our data to a control chart. Thus, this paper is structured as follows: section 4.4 will present the methodology we used in this paper as well as some concept definitions. Section 4.5 will describe the experimental dataset used. Section 4.6 will then exhibit the neural network we built and its results. Finally, section 4.7 and 4.8 will respectively detail our proposed feature and our conclusion.

4.4 Methodology

In this section, we defined our proposed methodology to establish that the SCE concept can accurately represent the behavior of a cutting tool degradation process. To do so, we first present the concepts used in our neural network model. Then, a principal component analysis will be performed to illustrate correlation phenomena between features and to help us in selecting the features for our neural network's input vector. After that, we present the used neural network. A Recurrent Neural Network (RNN) based on a Long Short-Term Memory (LSTM) architecture is used in our study. These types of neural networks are well suited to model time series such as the dataset we used in this paper (Goodfellow, Bengio, & Courville, 2016). Then the results of this step are detailed and will show that it is possible to accurately predict the tool wear value with a low Mean Square Error (MSE). At that point, we introduce our proposed feature, which, in our opinion, is a step toward a general TCM model. Then we present the results of multiple statistical analysis showing its ability to accurately describe the degradation behavior of a cutting tool.

At this point, we also like to introduce a condition for which we believe could affect our work or its implementation. It is well known that to extract meaningful information from a signal, the ratio signal-to-noise (S/N) must be greater than 1 ($S/N > 1$). If this condition is not respected, in our context, we believe it will cause the tool wear signal to vanish in the spindle default noise. Although we have not empirically tested this condition or the limits of our proposed methodology, we believe anyone interested in reproducing or implementing our work should be aware of the limit in which this work has been developed.

Next, we detail the features used in our LSTM network. The list is drawn from the work of Abellan-Nebot et Romero Subirón (2010) and Elattar et al. (2016). After that, we describe the dataset on which this paper is based.

4.4.1 Extracted features

Feature #1: Root Means Square

The first feature we calculated is the Root Mean Square (RMS) computed from the mean value. It is a well know feature that represents the signal in terms of its energy content. It is given by Eq. (4.1).

$$RMS = \sqrt{\frac{1}{N}\sum_{i=1}^{N}(x_i - \overline{x})^2} \tag{4.1}$$

where N is the number of samples acquired, x_i is the value of each sample and $\overline{x}$ is the average of the signal values.

Feature #2: Kurtosis

The second feature is the kurtosis (K). It represents the ratio between the fourth-order moment and the square of the second moment. The kurtosis is a statistical signal highly sensitive to the spikiness (shocks) in the data (Thomas, 2011). It is given by the Eq. (4.2).

$$K = \frac{\sum_{i=1}^{N}(x_i - \bar{x})^4}{\frac{1}{N}[\sum_{i=1}^{N}(x_i - \bar{x})^2]^2} \tag{4.2}$$

Feature #3 and #4: Peak and Peak to peak

The third and fourth features are respectively the peak ($Peak$) and peak-to-peak (PTP) value, which are defined as the maximum amplitude and the range between the maximum and minimum amplitude. They are given by Eq. (4.3) and Eq. (4.4).

$$Peak = \max(x) \tag{4.3}$$

$$PTP = \max(x) - \min(x) \tag{4.4}$$

Feature #5: Crest Factor

From Thomas (2011), we defined the fifth feature, the crest factor (x_{crest}), as being the ratio between the $Peak$ and the RMS. For a harmonic vibration, its value will be equal to 1.41 and will increase over 3 for a random signal. It is given by Eq. (4.5).

$$x_{crest} = \frac{Peak}{RMS} \tag{4.5}$$

Feature #6: Frequency Window

The last and final feature used, A_{Window}, is the measure of the energy amplitude of a signal in the frequency domain between two specified frequency values. In our case, the cutting speed (RPM) is 826 RPM for all experimentations. This gives us an equivalent value of 13.8 Hz. Hence, the frequency of the tool is 82.6 Hz (13.8×6 (inserts)). The value of the window's amplitude is given by Eq. (4.6).

$$A_{window} = \sqrt{\sum_{i=a}^{b} A_i^2} \tag{4.6}$$

Where A_i is the amplitude of the signal at the ith frequency and a and b are the two corners of the window. In our case, we assigned $a = 75$ Hz and $b = 85$ Hz; around the frequency of interest.

4.5 Experimental Dataset

To determine the validity and capability to adequately represent a cutting tool's wear behavior, we based all our experiments on the Milling Dataset developed and provided by NASA AMES and UC Berkeley (Agogino & Goebel, 2007). This dataset record various signals (vibration, acoustic emission and current) as well as several other information contextualizing the signals. This dataset encompasses 16 experiments where the cutting parameters were varied between each experiment. Each experiment is comprised of several machining runs where the flank wear (VB) was recorded at the end. VB is a well-known metric to measure a cutting tool wear and is defined as the distance from the cutting edge to the end of the abrasive wear on the flank face of the tool (Agogino & Goebel, 2007).

To conduct these experiments, the authors used a Matsuura machining center model MC-510V with a 70 mm face mill mounted with 6 KC710 (Kennametal) inserts. The cutting parameters for each experiment are displayed in Tableau 4.1. In this paper, we used the dataset's current and vibration signals that were acquired from a current sensor: OMRON model K3TB-A1015 (1 phase of the spindle motor) and a vibration sensor mounted on the spindle: ENDEVCO model 7201-50 (0-13 kHz range). For complete and detailed description of this dataset, the reader can refer himself to Agogino et Goebel (2007).

Tableau 4.1 Cutting parameters
Adapted from Agogino et Goebel (2007)

Experiment	Depth of cut [mm]	Width of cut [mm]	Feed [mm·rev^{-1}]	Speed [m·min^{-1}]
1	1.5	5.842	0.5	200
2	0.75	5.842	0.5	200
3	0.75	5.842	0.25	200
4	1.5	5.842	0.25	200
5	1.5	5.842	0.5	200
7	0.75	5.842	0.25	200
8	0.75	5.842	0.5	200
9	1.5	5.842	0.5	200
10	1.5	5.842	0.25	200
11	0.75	5.842	0.25	200
12	0.75	5.842	0.5	200
13	0.75	5.842	0.25	200
14	0.75	5.842	0.5	200
15	1.5	5.842	0.25	200
16	1.5	5.842	0.5	200

Even though this dataset is of quality, some data preparation was required. Below, we defined our work hypothesis regarding the dataset:

1) Since voltage (V) is not measured at each run, we estimated it to 400 V. It is a common value found in most recent CNC machines (e.g. Kessler spindles)
2) Since we do not have access to the exact current (I) value, we estimated it by doing the RMS of the current sensor signal at each run
3) Since width of cut is missing across all runs, we estimated it as being the radius of the smallest circle encompassing the insert. The estimated value is 5.842 mm.

In the next section, we present the results of the statistical analysis and the LSTM performance.

4.6 Neural networks

As of today, RNN, including the LSTM architecture (Figure 4.1), are one of the most effective sequences ($\boldsymbol{x}^{(1)}, \dots, \boldsymbol{x}^{(t)}$), also known as time series, model used in practical application (Goodfellow et al., 2016). For instance, in Aydin and Guldamlasioglu (Aydin &

Guldamlasioglu, 2017), they used an LSTM network to predict the RUL of an engine with success.

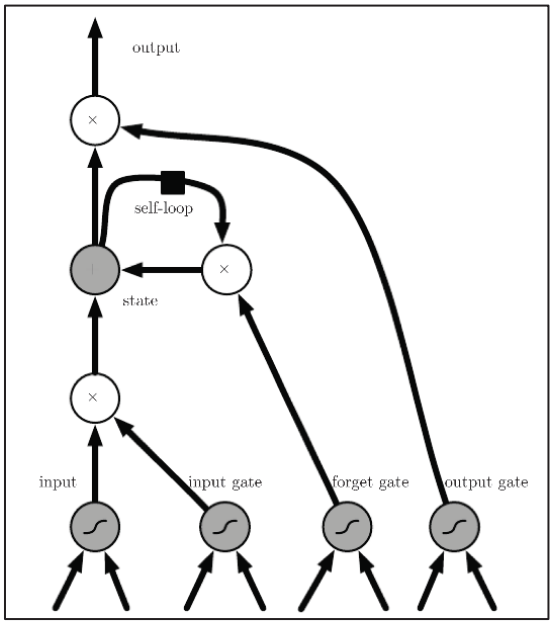

Figure 4.1 LSTM computational graph
From Goodfellow et al. (2016)

Their capability to accurately model time series is particularly useful in our situation since we are exactly looking at that: understanding and modelling the evolution (degradation in our case) of the tool wear phenomenon through time. For a more exhaustive description of the internal mechanics of a RNN and the LSTM architecture, the reader can refer himself to the work of Goodfellow et al. (2016). In this paper, we made use of the Keras library (Chollet, 2017) to build our LSTM network. This library is useful to quickly prototype neural networks with good performance since it is built on top of the renowned Tensorflow Library (Google).

The LSTM network we built is composed of four components: an input vector composed of three features (see section 4.6.1), two LSTM layers of 50 neurons each, a flattening layer and a dense layer with one output neuron with a sigmoid activation function. The chosen loss function is the Mean Square Error (MSE) (see Eq. (4.7)). This type of measure is typically

well suited for regression problems since it compares the error between the observed value (y) and the predicted value ($\hat{y}$). In our case, a lower value is better and means higher prediction accuracy.

$$MSE = \frac{1}{n}\sum_{i=1}^{n}(y_i - \hat{y}_i)^2 \tag{4.7}$$

Since neural networks are a stochastic process by nature, we must perform multiple iterations of each configuration. By doing so, we can obtain the average error which is nearer to the "true" error of the network. In this case, the reported MSE value is the average obtained after 30 training cycles. In other words, we trained each configuration of our LSTM network 30 times and calculated the average of all the MSE values. The configuration presenting the best results is conveyed in this paper.

Finally, to train our network, we separated our dataset in three distinct groups: training, validation and test with the following proportion: 60%-20%-20% (9-3-3 samples). The training and validation groups are going to be used for the training part of the LSTM development where the network is trained on the training group. Performance measurement is then going to be made on the test group. This is where we measure the generalization capability of our LSTM network. Next, we present our results.

4.6.1 Results and discussion

As stated in our methodology, we performed a linear Pearson's correlation analysis between all listed features and the tool wear value as defined in Agogino et Goebel (2007). Results of this process for each experiment are shown in Tableau 4.2.

Tableau 4.2 Linear correlation between each feature and the tool wear per experiment

Exp. Number	RMS		K		PTP		$Peak$		x_{Crest}		A_{Window}	
	R	P-Value	R	P-Value	R	P-Value	R	P-Value	R	P-Value	R	P-Value
1	-0.82	0.00	0.08	0.77	-0.79	0.00	-0.73	0.00	0.59	0.01	-0.89	0.00
2	-0.56	0.05	0.29	0.34	-0.76	0.00	-0.61	0.03	-0.07	0.81	-0.62	0.02
3	-0.30	0.30	0.08	0.79	-0.12	0.68	0.08	0.79	0.10	0.73	-0.36	0.20
4	-0.81	0.03	-0.04	0.94	-0.57	0.18	-0.47	0.29	-0.02	0.97	-0.81	0.03
5	-0.54	0.27	-0.15	0.77	-0.45	0.37	-0.27	0.60	-0.16	0.76	-0.55	0.26
7	-0.45	0.31	0.16	0.72	0.16	0.74	0.18	0.70	0.26	0.58	-0.46	0.30
8	0.02	0.97	0.11	0.84	0.08	0.88	0.10	0.84	0.11	0.84	-0.43	0.40
9	-0.21	0.59	0.73	0.03	0.01	0.98	0.37	0.33	0.64	0.06	-0.60	0.09
10	-0.31	0.38	-0.43	0.22	-0.38	0.28	-0.38	0.28	-0.31	0.39	-0.48	0.16
11	-0.45	0.03	0.44	0.03	-0.24	0.27	0.08	0.72	0.53	0.01	-0.65	0.00
12	0.07	0.81	0.09	0.76	0.05	0.87	0.06	0.83	-0.36	0.21	0.08	0.78
13	-0.45	0.09	-0.01	0.98	-0.07	0.81	-0.06	0.82	0.14	0.62	-0.17	0.54
14	-0.08	0.84	0.55	0.12	0.37	0.33	0.39	0.30	0.37	0.32	-0.19	0.62
15	-0.55	0.20	-0.55	0.20	-0.52	0.23	-0.52	0.23	-0.41	0.36	0.38	0.40
16	-0.98	0.00	-0.88	0.02	-0.97	0.00	-0.96	0.00	0.26	0.62	-0.48	0.34

A first observation we can make from the results of Tableau 4.2 is that there is not a clear pattern that seems to draw out. However, we can see that most features have multiple negative R coefficient, especially with the frequency domain feature (A_{Window}). This could be due to the fact that, because of tool wear, there is less shock or impact between the workpiece and the tool, hence resulting in a decreasing signal amplitude through time. In the end, no feature seems to express a clear pattern of linear correlation.

Then, we performed a Principal Component Analysis (PCA) based on the correlation matrix over all the features values. Results are presented as follows: Figure 4.2 shows the loading plot and Tableau 4.3 detailed the results of the PCA.

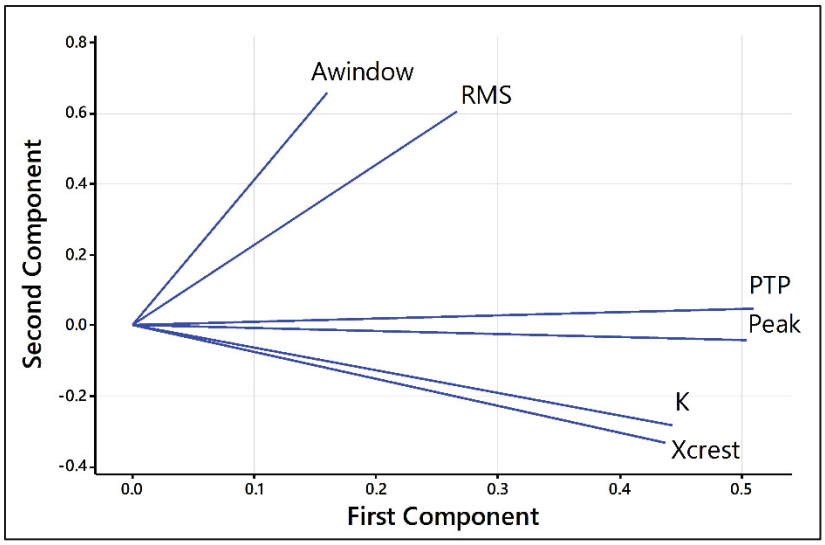

Figure 4.2 PCA loading plot

Tableau 4.3 PCA results

	PC1	PC2	PC3	PC4	PC5	PC6
Eigenvalue	3.6942	1.9425	0.2264	0.1013	0.0341	0.0015
Proportion	0.6160	0.3240	0.0380	0.0170	0.0060	0.0000
Cumulative	0.6160	0.9390	0.9770	0.9940	1.0000	1.0000

From Figure 4.2, we can see that three directions seem to exist, but each is comprised of two features. When we look at the correlation between both features, for each direction, we see that each pair is highly correlated (linear Pearson's correlation) together: 91.4% between RMS and A_{Window}, 98.8% between PTP and $Peak$ and 89.0% between K and x_{Crest}. Therefore, to build and train our LSTM network, we discarded the following features: A_{Window}, PTP and x_{Crest} and kept the three other features due to their physics significances. Also, by using three features in our input vector, we explain 97.7% of the dataset variance (Tableau 4.3). By including the features explaining most of the variance, it will surely help the performance of our LSTM network as well as reducing computing time due to a lower network complexity. The results regarding the performance of the LSTM network presented below are based on this input vector.

We trained an LSTM neural network to predict the tool wear. Results of the test phase are recorded in Tableau 4.4. This table presents the MSE value for the test phase (all three samples) and in detail for each test sample (experiment number).

Tableau 4.4 LSTM neural network MSE results

	Test	**14**	**15**	**16**
MSE	0.0239	0.0368	0.0150	0.0200

From Tableau 4.4, we can see that our proposed LSTM neural network produces good results. In fact, a low MSE value for each test sample indicates a good generalization capability in our context. Therefore, by choosing features with a physic meaning we can accurately predict the tool wear amount. Our results also support the work of Aghazadeh et al. (2018a) where a machine learning approach was also used to predict tool wear using the same dataset as us.

As we can see, by using a LSTM network, we are able to achieve very good prediction capability. However, in a general TCM model mindset, the drawback of this prediction capability is the amount of data required in order to generalize these results to multiple different types of cutting tools. In other words, since the neural network must be trained on data, it makes the task of bringing this concept to an industrial application very complex in terms of data collection since it exists thousands of cutting tools' types, sizes, coatings, etc. Thus, we believe that a feature accurately describing cutting tool wear and easily obtainable in an industrial context is essential and would certainly reduce the gap toward a general TCM model. To answer this need, we propose a single feature to accurately represent the behavior of a cutting tool wear process: the Specific Cutting Energy.

4.7 Specific Cutting Energy

This proposition is based on the concept of Specific Cutting Energy (k_c) developed by Debongnie (2006). It is defined as the amount of energy required to remove 1 cm^3 of material and has $\mathrm{J/cm^3}$ as its unit. In other words, we consider that a cutting tool (drill, end mill, tap, cutting insert, etc.), in a certain state, will consume a certain amount of energy to keep a constant material removal rate (Q) $[\mathrm{cm^3 s^{-1}}]$ in a defined material (assuming that the raw material's proprieties are constant). The fundamental hypothesis behind this concept is: because of tool wear, the energy required to keep this material removal rate in the same raw material will increase due to an increase in friction by cause of the cutting effort rising. This logic is also indirectly supported by Balan et Epureanu (2008a) since they affirmed that tool wear will lead to an increase in the cutting forces and P. Fu et al. (1998) that stated that motor current varies nearly linearly according to the tool wear. Eq. (4.8) gives us the SCE.

$$k_c = \frac{P[\mathrm{W}]}{Q[\mathrm{cm^3 s^{-1}}]} = \frac{[\mathrm{J s^{-1}}]}{[\mathrm{cm^3 s^{-1}}]} = [\mathrm{J cm^{-3}}] \tag{4.8}$$

where P [W] is the power ($P = I \cdot V$) and Q $[\mathrm{cm^3 s^{-1}}]$ is the material removal rate given by equation (4.9).

$$Q = \begin{cases} \propto a_e\, a_p\, V_f, & \text{for milling} \\ \propto V_c\, a_p\, f_n, & \text{for turning} \end{cases} \tag{4.9}$$

where a_e is the radial depth of cut [mm], a_p is the axial depth of cut [mm], V_f is the table feed $[\mathrm{mm{\cdot}min^{-1}}]$, V_c is the cutting speed $[\mathrm{m{\cdot}min^{-1}}]$ and f_n is the feed per revolution $[\mathrm{mm{\cdot}rev^{-1}}]$.

Based on Z. Jiang et al. (2019), we could consider a CNC machine as a closed system and draw its boundaries. This definition is represented by Figure 4.3. Because it is a closed system, all the energy submitted to the machine is used and transformed in either work (e.g. cutting, movement, pumps rotation, etc.) or heat (e.g. electrical cabinet heat emission,

friction, etc.). Based on Z. Jiang et al. (2019), we defined a simplified model on which we developed our work with equation (4.10).

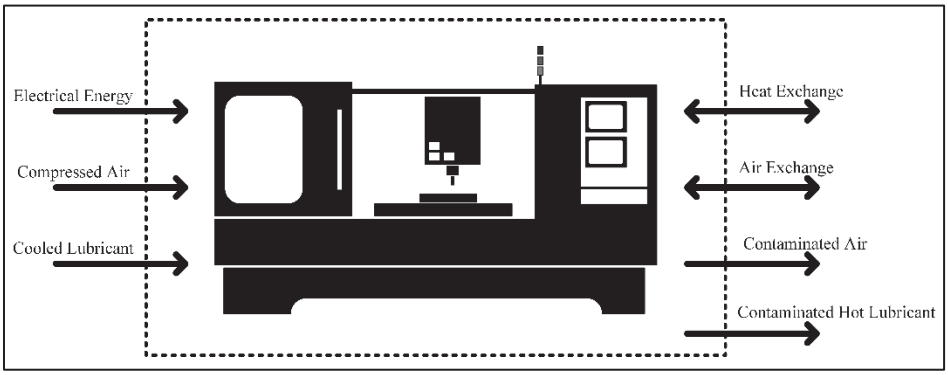

Figure 4.3 System boundaries for a CNC machine
Inspired by Z. Jiang et al. (2019)

$$P_{Total} = P_{Tool} + P_{Idle} \tag{4.10}$$

Where P_{Total} [W] is the total power consumed by the machine, P_{Tool} [W] is the power needed to cut the workpiece (the actual metal removing process) and P_{Idle} [W] is related to all the power consumption to keep the machine on and ready to cut. P_{Idle} is given by equation (4.11).

$$P_{Idle} = P_{Spindle} + P_{Basic} \tag{4.11}$$

Where $P_{Spindle}$ [W] is the power required to keep the spindle rotating and P_{Basic} [W] is related to the power required to keep all the machine's basic systems alive (e.g. computer, pumps, electrical cabinet, light system, etc.).

From these definitions, we conjuncture that the value P_{Idle} varies little throughout the machining process and that the variation in the power consumption comes from the actual work being executed. Therefore, we could rewrite equation (4.8) and get equation (4.12).

$$k_c = \frac{P_{Tool}[\mathrm{W}]}{Q[\mathrm{cm}^3\mathrm{s}^{-1}]} = \frac{[\mathrm{Js}^{-1}]}{[\mathrm{cm}^3\mathrm{s}^{-1}]} = [\mathrm{Jcm}^{-3}] \tag{4.12}$$

By returning to the fundamental physics understanding of a CNC machine system and the behavior between a cutting tool and the raw material, we consider this concept can better represent the evolution of the degradation of the tool health and thus, provide a way to model tool wear in a TCM model. Also, the clarity of its mathematical development makes it easier to be implemented in an industrial context.

4.7.1 Results and discussion

As we did previously, we also performed a linear Pearson's Correlation analysis between the tool wear and the SCE. Results for this analysis are presented in Tableau 4.5.

Tableau 4.5 Correlation between k_c and the tool wear per experiment

Exp. Number	1	2	3	4	5	7	8	9	10	11	12	13	14	15	16
R	0.98	0.98	0.95	0.97	0.97	0.97	0.99	0.96	0.97	0.95	0.97	0.99	0.98	0.99	0.92
P-Value	0.00	0.00	0.00	0.00	0.00	0.00	0.00	0.00	0.00	0.00	0.00	0.00	0.00	0.00	0.01

A first observation we can make from the results of Tableau 4.5 is that our proposed feature seems to be highly correlated to the tool wear measurement as defined in Agogino et Goebel (2007). Pearson's R coefficient is over 0.90 (90%) for all experiments and most P-Value are near zero, which is very good. In other words, our feature, derived from a physics understanding of the relation between the cutting tool and the workpiece, provides good linear correlation results across all experiments.

Also, it seems that our feature expresses a clear pattern of linear relationship. When we compare these results with the ones in Tableau 4.2, we see that k_c is clearly superior in terms of linear relationship. In other words, even though there is less impact due to tool wear, the energy required to keep the same material removal rate is increasing. Therefore, it appears

that our data support our claim that the SCE can better represents the behavior of a tool wear degradation process than typical features found in the literature.

Also, if we plot (see Figure 4.4) our proposed concept versus the tool wear measured as VB, we can clearly see this linear relationship. Moreover, this figure shows the existence of two "phases" in the cutting tool degradation process: a stability phase where the tool is working properly and no wear is occurring and a degradation phase where tool wear is happening. It then supposes the existence of some kind of moment where the state is changing from one phase to the other.

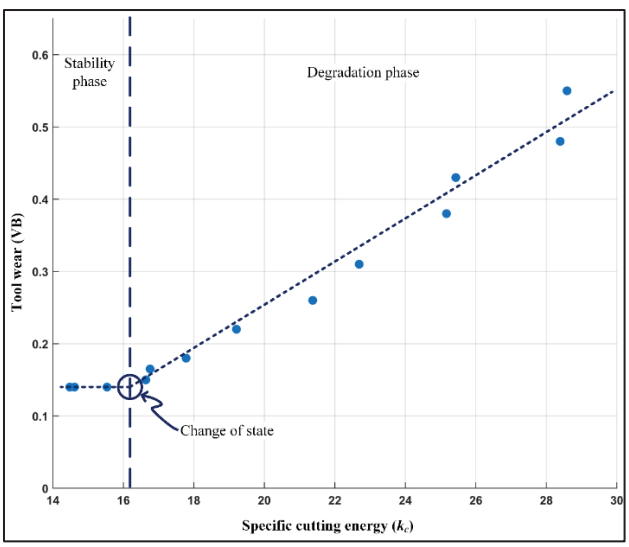

Figure 4.4 Scatter plot of k_c vs VB
data from experiment #2

To demonstrate that the SCE can explain the tool wear behavior we performed a linear regression analysis over each experiment with a statistical software. Results of this process are shown in Tableau 4.6.

Tableau 4.6 Linear regression results

Exp. Number	1	2	3	4	5	7	8	9	10	11	12	13	14	15	16
R^2	0.96	0.96	0.90	0.92	0.94	0.93	0.96	0.92	0.94	0.91	0.94	0.97	0.95	0.98	0.98

From Tableau 4.6, we see that most adjusted R^2 are over >90 %, which is very good and a good indicator that this concept can accurately explain a tool wear degradation process. At this point in our study, we can conclude with a certain amount of confidence that, in fact, the SCE can represent tools wear more efficiently than most features used in the literature. But what about its practical use and its relation to a general TCM model? In our opinion, a general TCM would need to require little to no training (i.e. not based on machine learning).

By looking at Figure 4.4, we thought we could exploit this notion of stability phase, degradation phase and moment of state change. Hence, we decided to apply an Exponentially Weighted Moving Average (EWMA) control chart to each experiment. This kind of chart is used to detect small shifts in a process. To perform this task, we calculated the limits of the chart on the stability phase data and then performed the EWMA analysis. For such control chart to work in our context, limits must be calculated against the stability phase data since this is the section of the data that reflects a process under control. Otherwise, if estimated from the whole data, the limits will be too high and will not provide the desired outcome. For instance, we applied this methodology to experiment #2 and its results are shown in Figure 4.5. From this figure, we clearly see that something has changed between the third and fourth run; that is that the degradation process has begun. Then, as soon as the data exceed the upper limit, the degradation process increase.

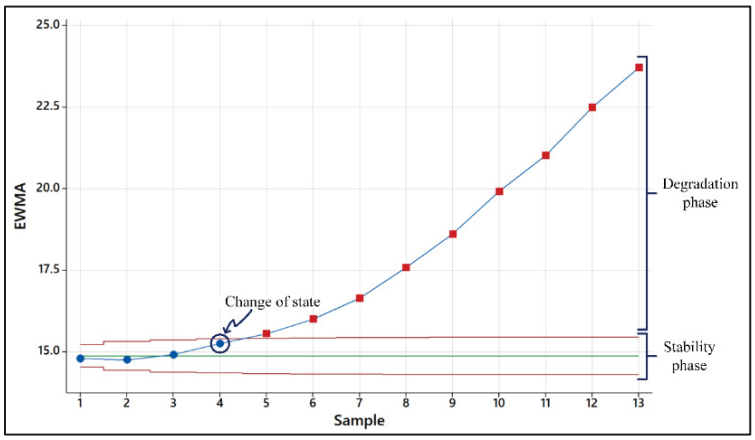

Figure 4.5 EWMA chart results, data from experiment #2

Data outside the control limits do mean that cutting tool degradation is happening. However, it does not imply that a cutting tool change must be performed. To do so, a threshold value based on a criteria, such as the workpiece quality, could be implemented so that as soon as SCE crosses it, a tool change is requested. It could also be interesting to try to estimate the RUL to know the amount of "time" between the current tool wear value and the threshold value to better plan a cutting tool change and avoid unexpected breakages.

Still, without any sort of specific training we were able to identify when the tool wear started. This methodology could, in our opinion, be easily implemented in an industrial context and be used to monitor a cutting tool's condition. Even though our work is also tool specific due to the nature of the dataset we used, we believe that this methodology could stay true with other types and variances of cutting tools since we based this concept on a physic understanding of the process.

4.8 Conclusion

To conclude, let's first remind ourselves the objectives of this paper. Our goals were to be able to predict tool wear while also establishing that the SCE concept can better represent the evolution of a tool wear value through time compared to typically used features in the literature. To do so, we first shown that it is possible to accurately predict tool wear using a LSTM neural network and achieved an overall MSE of 0.0239. To build this network, we used multiple features commonly used in the literature. They were selected after performing a linear correlation analysis and a PCA. These analysis showed no clear pattern for linear relationship and also that some features were negatively correlated. These results allowed us to conclude that it is possible to predict tool wear using data-driven method. However, the requirements to achieve such precision makes it difficult for an industry-wide application, hence problematic to achieve a general TCM model.

To lessen the gap toward a general TCM, we presented the concept of SCE which is based on a physic approach to tool wear. Results from a linear correlation analysis has shown that our

concept is linearly correlated (over 90%) with the tool wear as measured in the experimental dataset. Additionally, a linear regression analysis showed an adjusted R^2 of, again, more than 90%. Finally, we proposed a methodology based on a EWMA control chart to monitor when tool wear starts since Figure 4.5 showed that there is two phases in a cutting tool life: a stability phase and a degradation phase. By using this type of control chart, it was possible to show when a shift occurred in the process, thus, allowing us to closely monitor the degradation evolution.

Even though we were able to propose some kind of general methodology; using a EWMA chart would not give us the capability to measure the RUL of the cutting tool. Also, while we believe that our approach is more general than a data-driven one, we cannot state that we achieved a general TCM model since all our work is based on a tool specific dataset. Hence, future work should include first, the investigation of a way to measure a cutting tool RUL based on the concept of SCE while still minimizing the need for any kind of training. Second, future work should also include the implementation of the concept of SCE and our methodology at an industrial partner's facility. By doing so, we will have access to much more data about more types, sizes and variances of cutting tools used in multiple types of material thus, paving the way for a general TCM model. Nonetheless, our methodology, in its current state, could surely help machining companies to better monitor their cutting tools, hence reducing the cost due to unexpected breakages.

4.9 Acknowledgement

The authors would like to thank UC Berkely and NASA Ames Prognostic Data Repository for providing the Milling Dataset. We would also like to acknowledge the financial support of the *Fonds de Recherche du Québec – Nature et Technologies* (FRQNT) to this project through grant #257668.

CHAPITRE 5

DIMENSION REDUCTION AND 2D-VISUALIZATION FOR EARLY CHANGE OF STATE DETECTION IN A MACHINING PROCESS WITH A VARIATIONAL AUTOENCODER APPROACH

Antoine Proteau[a], Ryad Zemouri[a,b], Antoine Tahan[a], Marc Thomas[a]

[a]Département de génie mécanique, École de technologie supérieure, Montréal, Qc, H3C 1K3, Canada
[b]Laboratoire CÉDRIC du Conservatoire National des Arts et Métiers (CNAM), HESAM Université, 750141, Paris Cedex 03, France

Article publié dans « The International Journal of Advanced Manufacturing Technology », Novembre 2020

Publication originale disponible à: https://doi.org/10.1007/s00170-020-06338-y

5.1 Résumé

Dans cet article, nous avons appliqué une approche basée sur un autoencodeur variationnel à une problématique industrielle en usinage. Nous proposons un modèle basé sur un processus d'apprentissage en deux étapes et sur un espace latent de deux dimensions. Cet espace latent à deux dimensions procure une meilleure réduction de la dimensionnalité comparativement à une analyse en composantes principales qui requiert 24 composants pour exprimer 90.0% de la variation. De surcroît, le modèle proposé est en mesure de réaliser la classification des opérations de coupe en se basant seulement sur les données obtenues à partir de capteurs installés sur une machine-outil CNC et ce, avec une précision de 99.24%. Le modèle suggéré se veut aussi un outil visuel efficace capable de détecter les premiers changements d'état d'un processus d'usinage. Nous démontrons que cette approche peut visuellement identifier les défauts causés par un accroissement de moins de 1% de l'énergie dans le signal, ce qui est plus rapide que les méthodes de surveillance conventionnelle. De plus, nos travaux sont basés sur un jeu de données industrielles acquis durant la production régulière. Ceci augmente le potentiel de transfert technologique en ce qui concerne une meilleure

compréhension et une meilleure surveillance des premiers changements dans un processus d'usinage.

5.2 Abstract

In this paper, we applied a variational autoencoder approach to an industrial machining problematic. We proposed a model based on a two-steps training process and a two-dimensional latent space. This two-dimensional latent space has better dimension reduction capability compared to a principal component analysis, which would require 24 components to express 90.0% of the variation. Moreover, the proposed model is shown capable of classifying a cutting operation based solely on data obtained from sensors mounted on a CNC machine, with an accuracy of 99.24%. The suggested model is also shown capable to be an efficient visual process monitoring tool capable of detecting early changes of state in a machining process. We show that this approach can visually identify defect caused by an increase of less than 1% of the energy in the signal, which is earlier than conventional monitoring methods. Additionally, our work is based on an industrial dataset acquired during regular production. This increases the opportunity for technological transfer when it comes to better understanding and better monitoring early changes in a machining process.

5.3 Introduction

The manufacturing industry continues to face constant pressure to decrease costs, improve quality, and increase production rates. Over the past few years, the industry has been leveraging new concepts, such as Industry 4.0 or smart manufacturing, to introduce new affordable technologies and models promising new ways to improve production (Baur et al., 2020; Huang, Chen, & Huang, 2019; Kohler & Weisz, 2016). In the specific context of machining, it is widely known that the kinds of technologies (connectivity, augmented reality, artificial intelligence, etc.) brought forward by Industry 4.0 can have highly positive impacts on a company (Han, Liu, Yang, & Jiang, 2019; Martínez-Arellano et al., 2019). Nonetheless, even in this new environment, production throughput and quality levels continue to be affected by unpredictable machine maintenance schedules and faster cutting

tool wear, which results in cutting tool breakage, and which ultimately drives up costs and lowers financial performance (Chadha et al., 2019; Y. Zhou & Xue, 2018). The ability to monitor and predict the remaining useful life of a cutting tool or of a CNC machine, or to predict the quality level of a workpiece in real time, could thus lend a real competitive advantage to a machining company (Baur et al., 2020; Hanachi et al., 2019).

In Proteau et al. (2019b), we reached a milestone toward achieving a system capable of predicting the quality level of a machined workpiece in real time. We presented the first version of a data acquisition system capable of contextualizing the operational data with physical data synchronized by the real-time state of a CNC machine and of a cutting operation. In this paper, we intend to present a new milestone in our journey to predict the quality level of a workpiece by displaying our ability to use a machine learning approach to classify cutting operations. We also show that our approach can be used to provide an accurate visualization of our dataset, in addition to being a capable tool to monitor a cutting operation process.

There are mainly two possibilities to develop our model: a data-driven approach or a physic based one (Elattar et al., 2016; R. Gao et al., 2015; Vogl et al., 2016). A physic-based approach provides a mathematical modeling of a system in order to make accurate prediction. However, this required more knowledge and a complete understanding of the mechanical system (R. Gao et al., 2015). Nonetheless, we have seen several applications in the literature such as M Lamraoui, Thomas, El Badaoui, Zaghbani, et Songmene (2011) for cyclostationarity analysis of the vibration signal to model the machining chatter effect, Azimi, Mirjavadi, Asli, et Hamouda (2017) with finite element modeling for fracture analysis or Mirjavadi, Mohasel Afshari, Shafiei, Rabby, et Kazemi (2018) and Mirjavadi, Afshari, Barati, et Hamouda (2019) for the geometrical modeling based on vibration analysis.

An interesting approach is a hybrid method where physical information is fed to a data-driven method such as a machine learning one. Successful applications of this can be found in the literature. For instance, Afshari Behzad et al. (2017) combined a genetic algorithm and

a physic-based model to optimize the mass and pressure drop of a satellite component. Furthermore, Janssens et al. (2017) successfully used thermal imagining combined to a deep learning model (convolutional neural network) for machine health monitoring or Hanachi et al. (2019) for a hybrid methodology for tool wear prediction.

We proceed by using a hybrid method where physic-based features are fed to a data-driven - a machine learning - approach. We have seen over the last few years an extensive usage of data-driven model such as artificial neural networks (ANN) or deep learning (DL) (Khan & Yairi, 2018; R. Liu et al., 2018; R. Zhao et al., 2019). In fact, they are particularly suited for the monitoring and diagnosis of mechanical systems (R. Zemouri et al., 2020) or production processes (Chadha et al., 2019; S. Lee et al., 2019) and operate well in non-linear contexts (S. Lee et al., 2019). For instance, in the specific domain of tool condition monitoring, data-driven methods are widely used: in Duo et al. (2019), the authors used multiple machine learning approaches to predict the wear of two types of drill bits and to determine which signals were the most sensitive to tool wear. Also, in Martínez-Arellano et al. (2019), the authors used raw signal's images and a deep learning approach to accurately classify tool wear.

However, even with their advantages and wide usages, these methodologies are plagued by three drawbacks: first, the non-availability of good data in sufficient quantity; second, there is the curse of dimensionality, especially in an industrial context where operational data is often of high dimensionality and noisy (San Martin et al., 2019); and third, the "black-box" nature of the methodologies (S. Yu & Príncipe, 2019) still makes it difficult to realize a production deployment in an industrial context due to the lack of any explainable capability. To overcome this black-box constraint, some researchers have started to work on methodologies to try to explain the prediction of neural networks. For instance, Ribeiro, Singh, et Guestrin (2016) have come up with a method to understand the prediction of classifier models.

In R. Zemouri et al. (2020), the authors propose a methodology based on a Variational AutoEncoder (VAE) that addresses both the black-box nature of a neural network and the problem of high dimensionality. They propose using the two-dimensional latent space obtained from the VAE as a visualization space to understand how data is distributed in order to get a sense of how the network is interpreting the data. The reduction from a space of n dimensions ($\mathbb{R}^n$) to a space of two dimensions ($\mathbb{R}^2$) is then used for unsupervised classification, with good performance. This is supported by Goodfellow et al. (2016), who argue that being able to map a lower-dimensional space can help the generalization capabilities of a model. The authors also conjecture that a reduced representation could lead to a better performing model, for instance, in terms of classification.

A VAE approach is a promising methodology for reducing the effect of dimensionality and the black-box problem; as well, it is also well suited for applications in an industrial context (San Martin et al., 2019). In Cheng, He, et Zhao (2019), the authors propose a Variational Recurrent AutoEncoder (VRAE) as a process monitoring tool, which according to their results, could better detect faults than traditional statistical methods or other neural network approaches. This is also supported by R. Zemouri et al. (2020), who posit that a VAE approach can lead to better reproducibility than other statistical methods such as the t-distributed Stochastic Neighbor Embedding (t-SNE) projection (Maaten & Hinton, 2008). Similar to Cheng et al. (2019), Chadha et al. (2019) propose a comparative analysis for different autoencoder architectures and find that the VAE architecture provides the best anomaly detection capability in an industrial process monitoring context.

In Huang et al. (2019), the authors also use a VAE approach in an industrial context where they try to detect a motor's faults. Like Cheng et al. (2019), they combine a VAE approach with a Recurrent Neural Network (RNN) structure. In their situation, the authors use this method as a dimensionality reduction tool to reduce the dimension of their dataset to 25. They then use this reduced space as an input for a classification model. The authors also hold that a combination of the VAE and a two-layer neural network achieves a 99.8% classification accuracy. In Hemmer, Klausen, Khang, Robbersmyr, et Waag (2020), the

authors also use a VAE approach for fault detection in axial bearings, but additionally, also employ the VAE to calculate health index by using the latent representation.

These successful applications of VAE in an industrial context for the monitoring of industrial processes and for the detection of faults suggests that VAEs represent a good approach, and strengthen our decision to apply this method to our industrial research context. It is also based on the above and the visual opportunity of the VAE that we decided to apply this approach instead of a more conventional methodology like an autocorrelation method as used in the work of L. Li, Tang, Wen, et Shao (2019) or Iglesias-Martínez, Córdoba, Antonino-Daviu, et Conejero (2019). Therefore, this paper aims at three objectives: first, we want to demonstrate that combining a VAE approach with a classifier and using a two-step training methodology can improve the dimensionality reduction capability, provide a better latent space distribution, and increase the overall visualization and interpretation capability of the high-dimensional dataset used in this article. The ability to diminish the black-box effect of a machine learning approach is an important factor for a successful industrial deployment. Second, we show that this same methodology can be used for a highly accurate classification of cutting operations based on signals acquired from sensors of a CNC machine. Finally, we show that based on the same proposed model, the resulting 2D latent space can be used as a process monitoring tool to monitor a cutting operation state, and that this tool can detect defects earlier. We previously saw that multiple applications of VAE have been realized in an industrial context. However, to the best of our knowledge, there is no application in the specific context of the machining industry, with an industrial dataset and application. Furthermore, even though some authors, such as Huang et al. (2019), have combined a classifier with a VAE approach, no one seems to have implemented a two-step training such as the one we propose herein.

The rest of this article is structured as follows: in section 5.4, we present background information on the VAE concepts. Section 5.5 presents the methodology we used, as well as an updated version of the industrial dataset used in this article. Then, in section 5.6, we present and discuss our results. Finally, we conclude the paper in section 5.7.

5.4 VAE background

Introduced by Kingma et Welling (2013), a VAE is a variant of a classical AutoEncoder (AE). An AE is basically a neural network trained to reproduce its input (Cheng et al., 2019; R. Zemouri et al., 2020), and is composed of three elements: an encoder, a latent space, and a decoder. Underlying the function of the AE is the encoder, which encodes the input data into a latent space z with the function $z = f_\phi(x)$, and the decoder, which decodes the encoded data from the latent space with the function $\hat{x} = h_\theta(z)$. Figure 5.1 provides a visual representation of this structure. During this process, the input data is encoded into a smaller dimension, forcing the model to prioritize the most important part of the input data, and thus learning some useful properties (Goodfellow et al., 2016).

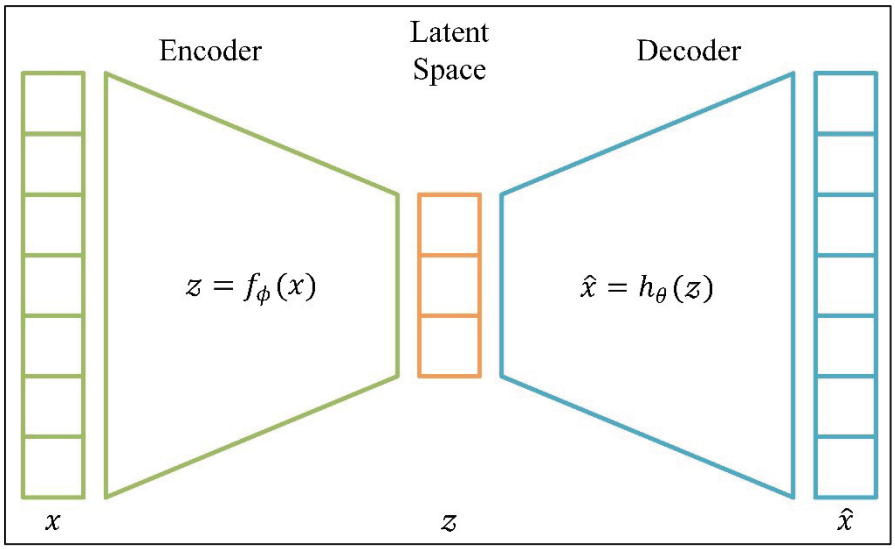

Figure 5.1 AE structure

A VAE has a similar architecture as a classical AE, but traditionally has been used for its generative capabilities (e.g., image generation) (Goodfellow et al., 2016; X. Hou, Sun, Shen, & Qiu, 2019; S. Lee et al., 2019; R. Zemouri et al., 2020). Figure 5.2 provides an overview of the structure of a VAE. To be able to perform the generative task with good results, a traditional AE lack a well-regularized latent space. To deal with this constraint, a VAE uses a re-parameterization trick that allows the latent space to be regularized (Doersch, 2016; S. Lee

et al., 2019; R. Zemouri et al., 2020). Thus, each element z_i sampled from the latent space can be obtained with equation (5.1).

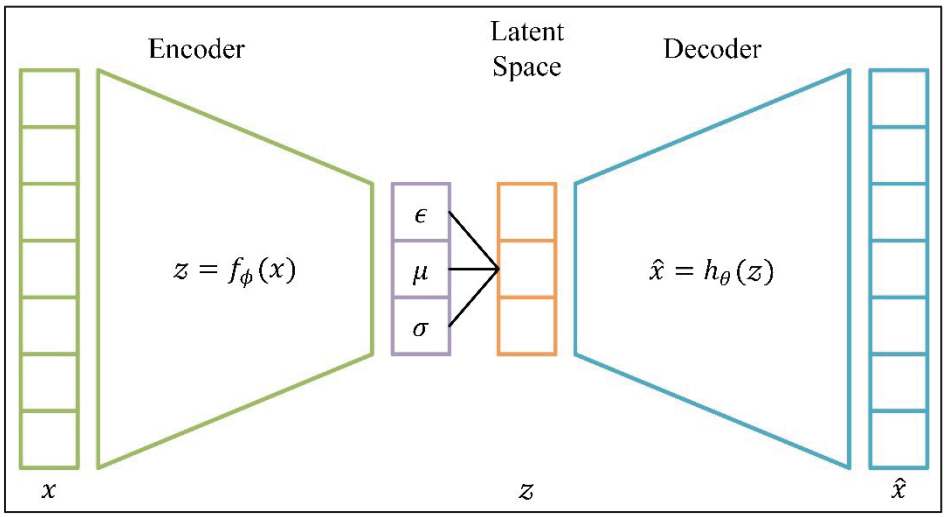

Figure 5.2 VAE structure

$$z_i = \mu_i + \sigma_i \cdot \epsilon \tag{5.1}$$

where μ_i is the mean, σ_i is the standard deviation, i is a component of the vector, and ϵ is a random variable following a normal distribution such as $\epsilon \sim \mathcal{N}(0,1)$.

The second difference between AE and VAE lies within their loss functions. For a classical AE, one can use a simple Mean Square Error (MSE) loss function, which ensures the minimization of the reconstruction error with the decoder. For the latter, the centerpiece of the model lies within its loss function ($\mathcal{L}$), which is given by equation (5.2).

$$\mathcal{L} = E_{q\phi(z|x)} \log[P_\theta(x|z)] - KL[q_\phi(z|x) \parallel P(z)] \tag{5.2}$$

The left side of the equation is the reconstruction cross-entropy loss function where we want to maximize the probability of $P(x)$. It should be noted that since this left term is the reconstruction error, the MSE could also be used (R. Zemouri et al., 2020). While we are

maximizing the left-hand side term, we are also minimizing the right-hand side term, which is the Kullback-Leibler divergence (Doersch, 2016). This term forces the model to generate a latent space with the specified normal distribution (R. Zemouri et al., 2020).

After being trained, the VAE's components can be used independently for specific tasks. For instance, the encoder can be used for dimensionality reduction, and the decoder, to generate new examples. The reader is referred to the work of Doersch (2016) for a more extensive review of the underlying behaviors of the VAE method.

5.5 Methodology

This section develops three elements on which our methodology is based to achieve our objectives: first, we present the industrial dataset we used throughout this article, as well as the elements added since its first publication in Proteau et al. (2019b). Second, we elaborate on the different features that compose the input vector of our model, along with our signal processing methodology. Third, we present the architecture of the VAE models, together with the version combined with a classifier (VAEC).

With these elements in mind, the methodology we apply to achieve our objectives is as follow: for our first objective, we will compare the visual distribution of the latent space representation of our proposed VAE model (see section 5.5.3) based on classical one-step training versus our two-step proposal. Then, to reach our second objective, we will apply this two-step approach to a classification problem where we will display the capacity of our model to accurately classify each cutting operation to its respective label based solely on an input vector obtained from the trained latent space. Finally, regarding our third objective, we will use a subset of our dataset (see section 5.5.3 for details), with the same approach, to illustrate that it is possible to use the latent space as a process monitoring tool to monitor the change of state (from normal to abnormal) or faulty states of a cutting operation. Figure 5.3 below summarizes the three phases of our methodology.

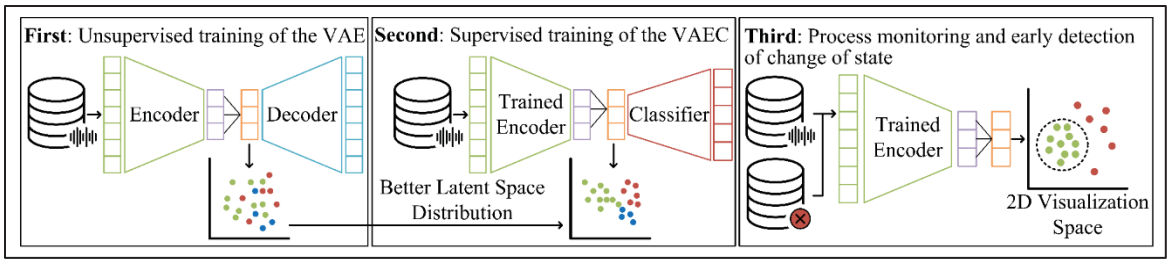

Figure 5.3 Methodology summary

5.5.1 Industrial dataset

As stated above, in this article, we use an updated version of our previously published dataset. In Proteau et al. (2019b), we proposed a system architecture to contextualize, in real time, the physical data (vibration) acquired from a data acquisition system with operational data (e.g., type of cutting operation and cutting parameters). This was done at the premises of an industrial partner, APN Inc. (Quebec, Canada), a national leader in Industry 4.0, specialized in the manufacturing of complex aerospace products made from exotic alloys (e.g., titanium and Inconel). Since its first publication, we have added another type of physical data, namely, motor current consumption. More precisely, we installed a current sensor (LEM model LF 210-S[4]) to one phase of each motor powering each of the three main axes of the CNC machine (X, Y and Z) and one phase of the motor powering the CNC machine spindle. Additionally, we added a triaxial accelerometer (PCB model 356A33[5]) on the housing of the spindle. In Figure 5.4, we show the position of each sensor installed on the CNC machine.

[4] Specification can be found at: https://www.lem.com/sites/default/files/products_datasheets/lf_210-s.pdf
[5] Specification can be found at: https://www.pcb.com/products?model=356a33

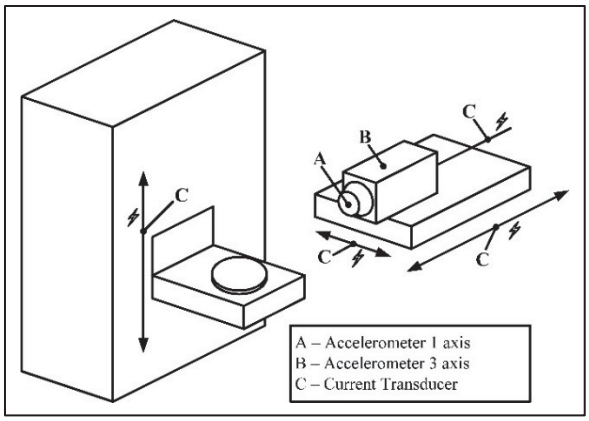

Figure 5.4 Sensors layout

In the specific context of this article, we used the data collected from three work orders (WO) related to the same product. These WO cover a total of 166 produced parts, which is close to a dataset of 2.2 GB of acquired signals data. The product is a component used in the aerospace industry, and was manufactured from Inconel 625 (AMS-5666) as raw material. We provide more information about the cutting operations in Tableau 5.1, and in Tableau 5.2, we list the details of the two cutting tools used to perform these cutting operations. The depth of cut values obtained from the industrial partner systems is the average values of the cutting operation.

Tableau 5.1 Cutting operations details

Name	**Spindle speed [RPM]**	**Feed [mm/s]**	**Depth of cut [mm]**	**Est. cutting time [sec]**	**Volume removed [cm^3]**	**Cutting tool Id**	**Class label**
OP140	1047	265.94	0.127	15.424	0.4440	2	0
OP150	1047	265.94	0.127	15.422	0.1520	2	0
OP160	1047	265.94	0.000	15.422	0.0003	2	N/A
OP280	6035	858.52	0.152	123.770	0.0427	1	1
OP290	6035	858.52	0.064	77.470	0.0248	1	2
OP430	6035	858.52	0.165	36.641	0.0258	1	3
OP440	6035	858.52	0.165	39.727	0.0103	1	4

Tableau 5.2 Cutting tool details

Id	Type	Diameter [mm]	Number of flutes
1	Ball Nose	6.35	4
2	End Mill	12.70	5

While the data collected in this dataset is of high quality, after some preliminary analysis and explorations, some adjustments, however, had to be made. Some work hypotheses that are used throughout this paper are presented below. By looking at the cutting operation details for operations OP140, OP150, and OP160, we can, at first sight, see that the cutting parameters are similar for all three of them. After an analysis of the inherent information about each cutting operation, the CNC machine program, and their related simulations, we can assume the following:

1) Operations OP140 and OP150 are the exact same cutting operation, hence in the case of our classification problem, both operations will bear the same label (0);
2) In the process of our industrial partner, operation OP160 is a “free” operation. This type of cutting operation is used to repeat a previous cutting operation (OP140 and OP150 in this context) to make sure that there is no burr after their execution or in order to minimize the cutting tool’s flex behavior. Therefore, since no real cutting is being made, no material is removed, and the collected signal data represents a different state of the previous cutting operation, we decided to remove OP160 from the training process.

When we look at the details for the OP280, OP290, OP430 and OP440, even though they bear similar cutting strategy and they have similar cutting parameters, each of them is used to machine different sections of a specific geometrical feature of the workpiece. Also, none of them is considered to be a “free” operation. It must also be noted that OP430 and OP440 are even executed during a second setup. Therefore, the aforementioned hypothesis cannot be applied in the context of these four cutting operations and each of them should be treated as different.

The hypothesis regarding the OP160 is still interesting in the context of our third objective, i.e., to demonstrate that the trained latent space can be used for process monitoring. Since

OP160 data represent another cutting state of OP140 and OP150, we can use its data to determine if our model, after its training, is indeed capable of creating another cluster representing this different cutting state.

Additionally, for a second verification of this claim, we artificially created faulty signals in the acquired signals on three samples related to OP140. The faulty signal x_d was obtained from equation (5.3) by applying it to each of the first, second and third harmonics of each signal. Generally, tool wear impacts the amplitude at the cutting tool frequency and its second and third harmonics due to higher friction between the tool and the workpiece (Haber, Jiménez, Peres, & Alique, 2004; Nath, 2020). For the second and third harmonics, the right-hand side of equation (5.3) was reduced to 80% and 60%, respectively, of its value to ensure a decreasing value of the amplitude from the first to the third harmonic.

$$x_d = x + \lambda A \cos(2\pi t \omega_{ct}) + \alpha \tag{5.3}$$

where x is the original signal, A is the average energy contained in the signal, t is the time vector, ω_{ct} is the cutting tool frequency in Hz, and α is a Gaussian noise ($\alpha \sim \mathcal{N}(0,1)$).

We introduced a defect equal to a λ value of the average energy contained in a signal plus a random noise following a normal distribution on the acquired vibration signals of each sample. This defect ranged from 0.05 to 3 times the average energy (3 times the average energy is usually used as an alarm in mechanical systems maintenance, by considering a normal distribution (Thomas, 2011). This resulted in a dataset of 20 test cases. To provide an example, we display, in Figure 5.5, the signal in the time domain for the original signal (a), with a defect level of 0.1 (b), with a defect level of 2.0 (c) and a defect level of 3.0 (d). The displayed signals are all for the same channel of the triaxial accelerometer.

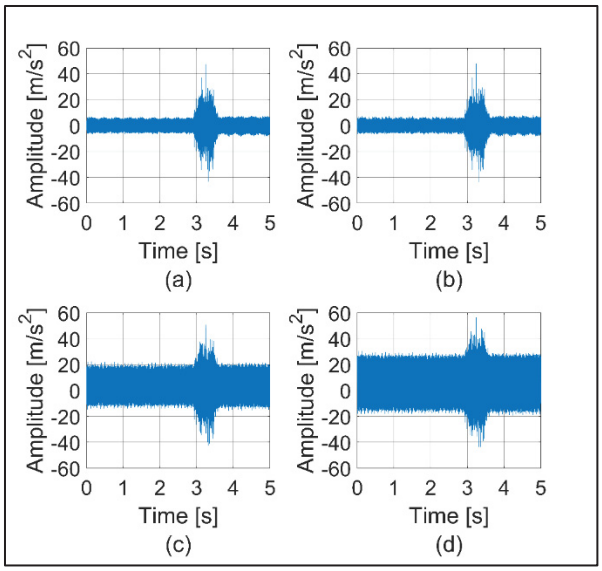

Figure 5.5 Time domain plot for the original signal and three faulty signals

5.5.2 Signal processing

In this subsection, we discuss the signal processing methodology we used and the diverse features we extracted from the signal to construct our input vector. In order to minimize the black-box effect of our model and increase its interpretability, we focused mainly on features that give a physical meaning to our signal. To minimize possible sources of signal error, all transition phases (e.g. spindle start and workpiece approach) were removed through the data acquisition process shown in section 5.5.1. We therefore used seven features to describe each signal (x): the Root Mean Square (RMS) given by equation (5.4), the kurtosis (K) given by equation (5.5), the peak ($Peak$) given by equation (5.6), the peak-to-peak (PTP) given by equation (5.7), the crest factor (x_{crest}) given by equation (5.8), the cutting tool frequency amplitude (A_{ct}) given by equation (5.9), and the specific cutting energy (k_c) given by equation (5.10). These choices were made following the work of Abellan-Nebot et Romero Subirón (2010), Elattar et al. (2016), Ahmad et al. (2020) and Duo et al. (2019). For more information on equation (5.9), the reader is referred to the work of Thomas (2011). Equation (5.10) is included in this list since k_c is a good feature to represent the state of the cutting

tool. For more details and a complete description of k_c, see A. Proteau, A. Tahan, et M. Thomas (2019a).

$$RMS = \sqrt{\frac{1}{N}\sum_{i=1}^{N}(x_i - \overline{x})^2} \tag{5.4}$$

Here, N is the number of samples acquired, x_i is the value of each sample and $\overline{x}$ is the average value of the signal.

$$K = \frac{\sum_{i=1}^{N}(x_i - \bar{x})^4}{\frac{1}{N}[\sum_{i=1}^{N}(x_i - \bar{x})^2]^2} \tag{5.5}$$

$$Peak = \max(x_i) \tag{5.6}$$

$$PTP = \max(x_i) - \min(x_i) \tag{5.7}$$

$$x_{crest} = \frac{Peak}{RMS} \tag{5.8}$$

$$A_{ct} = \sqrt{\sum_{i=a}^{b} A_i^2} \tag{5.9}$$

A_i is the amplitude of the signal at the ith frequency and a and b are the two corners of the window. In our case, the corners of the window are ±5Hz of the cutting tool frequency.

$$k_c = \frac{P[\text{W}]}{Q[\text{cm}^3\text{s}^{-1}]} = \frac{[\text{Js}^{-1}]}{[\text{cm}^3\text{s}^{-1}]} = [\text{Jcm}^{-3}] \tag{5.10}$$

where P [W] is the power consumed and Q [$\mathrm{cm^3 s^{-1}}$] is the material removal rate.

For the vibration signals, we applied equations (5.4) to (5.9) to three domains: the time domain, the frequency domain and the first and second order of the cyclostationarity domain. For the frequency domain, we applied equation (5.9) to each of the first five harmonics. For more information on the cyclostationarity domain, the reader is referred to the work of Antoni (2009) for an introduction to the subject. For the current consumption signals, we applied equations (5.4) and (5.10) to the time domain signal. Tableau 5.3 presents a summary of the features used per signal type per domain. For consistency, when a feature is not used for a specific signal, the input vector for the model is padded with zeros.

Tableau 5.3 Features per type of signal

Signal	RMS	K	$Peak$	PTP	x_{crest}	A_{ct}	k_c
Vibration	T, C	T, C	T, C	T, C	T, C	F	-
Current	T	-	-	-	-	-	T

T: Time domain, F: Frequency domain, C: Cyclostationarity domain (first and second order)

Because errors can be recorded in the signal during the acquisition process, we included another step of data processing after the signal processing and before building the input vectors. At this step, we removed any corrupted features or outliers values. Furthermore, the advantage of using a neural network-based machine learning approach is that small errors or noise that could have remained in our data are discarded during the training process (Abellan-Nebot & Romero Subirón, 2010; Elattar et al., 2016).

With a total of 8 channels (4 for the vibration signals and 4 for the current consumption signals), we can define the input vector of our machine learning model with equation (5.11).

$$\boldsymbol{x} = [RMS^i, K^i, Peak^i, PTP^i, {x^i}_{crest}, {A^i}_{ct}, {k^i}_c] \tag{5.11}$$

where i is an index representing the channel number. In our case, i goes from 1 to 8. With 7 features calculated over 3 domains and applied to 4 channels for every 2 sensors, the length of $\boldsymbol{x}$ is 168 ($2 \cdot 4 \cdot 7 \cdot 3 = 168$).

5.5.3 VAE and VAEC architecture and training methodology

In this subsection, we present the detailed architecture of both the VAE and VAEC we used to achieve our results. To quickly prototype our network and obtain our results, we employed the Keras library, which uses the TensorFlow library developed by Google as the back-end (Chollet, 2017). Based on section 5.3, we built a typical VAE with an encoder/decoder and a latent space of dimension 2. Contrary to the work of Cheng et al. (2019) and Huang et al. (2019), we did not need to use an RNN architecture to achieve our results, as a simple multilayer perceptron (MLP) structure was sufficient. Below, Figure 5.6 presents the overall architecture and detailed structure of the VAE.

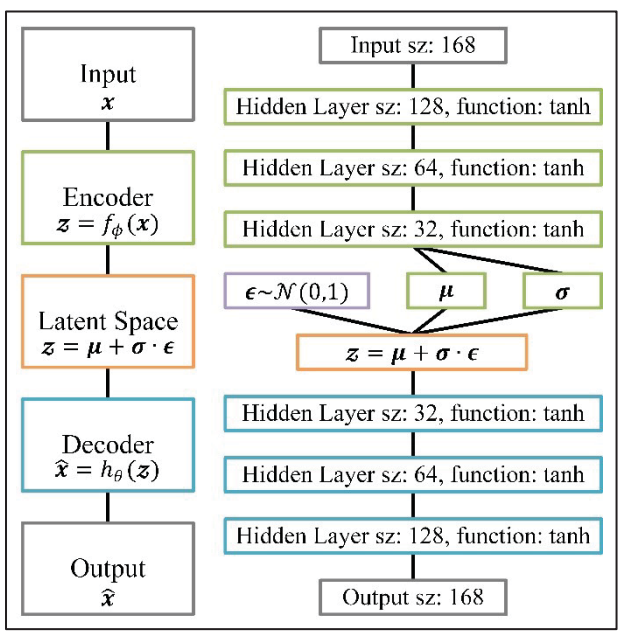

Figure 5.6 VAE architecture;
inspired by Hemmer et al. (2020)

To build our classifier, we attached a SoftMax classifier to the encoder part of the trained VAE. The overall architecture and detailed structure of the VAEC are shown in Figure 5.7.

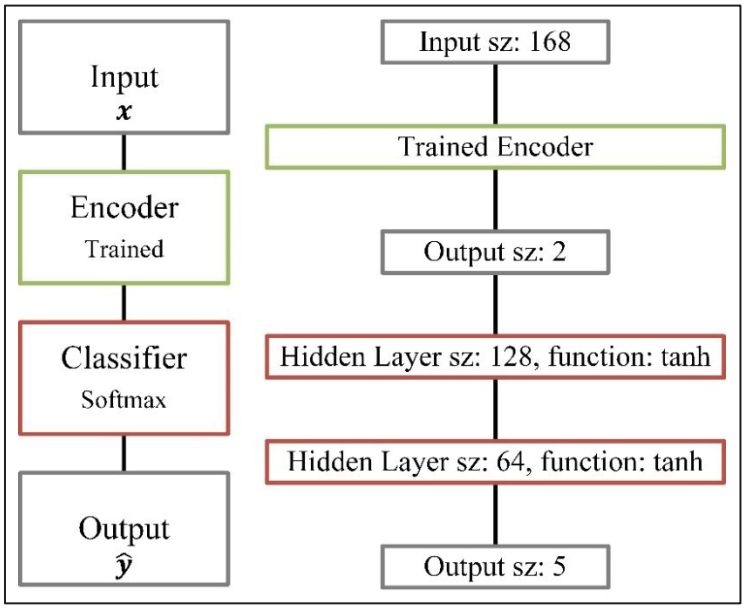

Figure 5.7 VAEC architecture;
inspired by Hemmer et al. (2020)

The data preparation process for the three WO resulted in a dataset of 15,530 examples. We used a typical $1/3$ - $2/3$ segmentation to create the training dataset ($\mathbb{X}$) and the test dataset ($\mathbb{Y}$). That being said, two WO are used for the training dataset and the third WO is used for the test dataset in order to do the evaluation of the performance of the model.

As stated in our introduction, the training process is a two-step process. First, the VAE is trained with the objective of minimizing its reconstruction error with the MSE loss function ($\mathcal{L}_1$) as per equation (5.12).

$$\mathcal{L}_1 = MSE = \frac{1}{n}\sum_{i=1}^{n}(x_i - \hat{x}_i)^2 \tag{5.12}$$

Where x_i is the true input vector values, $\hat{x}_i$ is the reconstructed input vector and n is the number of sample i in the training dataset.

Following the completion of this first training, we take the trained VAE encoder and its encoded latent space as the input for the classifier. We then perform another training step where the objective of the model is to minimize the binary cross-entropy loss function ($\mathcal{L}_2$) as per equation (5.13).

$$\mathcal{L}_2 = \frac{1}{n}\sum_{i=1}^{n} y_i \cdot \log\big(P(\hat{y}_i)\big) + (1 - y_i) \cdot \log\big(1 - P(\hat{y}_i)\big) \tag{5.13}$$

Where y_i is the true label and $\hat{y}_i$ is the predicted label.

To evaluate the performance of our VAEC classification model, the performance metric used is the accuracy (Acc), which is the ratio of accurate prediction to the total number of predictions, and is defined by equation (5.14).

$$Acc(y, \hat{y}) = \frac{1}{n}\sum_{i=1}^{n} \left| \frac{\hat{y}_i \cap y_i}{\hat{y}_i \cup y_i} \right| \tag{5.14}$$

Here, n is the number of sample i in the test dataset.

In the next section, we present and discuss our results.

5.6 Results and Discussion

As stated in our methodology, our first step was to train the VAE and VAEC to see how accurately the latent space can represent the underlying logic of the data. Figure 5.8 displays the resulting VAE latent space distribution. On the one hand, we can see that the VAE alone does not seem to be able to cluster our dataset according to a well-defined reasoning. For

instance, the clusters OP-280, OP-290 and OP-440 appear to be stacked on each other, whereas they are different cutting operations. On the other hand, as we can see in Figure 5.9, as soon as we apply our two-step training with the VAEC, where we retrain the encoder while training the encoder and classifier as a whole model, the latent space is more accurately distributed and seems to follow a better logic. We can then assume that this two-step training allows the encoder to be guided by the classifier cost function in the selection of the most important elements during the dimensionality reduction, which allows the VAEC to distribute and cluster more effectively. We can then more easily see the underlying structure of the data and how the model is interpreting it in the context of the classification problem. This is therefore in agreement with the work of R. Zemouri et al. (2020), when the authors state that the VAE approach can help understand the network behavior and reduce the black-box effect of a machine learning approach. In both Figure 5.8 and Figure 5.9, the colors represent the true label y.

It is also interesting to see the difference between the approximate covered areas of Figure 5.8 and Figure 5.9. We can see that the purely unsupervised training resulted in a more compacted distribution with the horizontal axis spanning from approximately 0 to -5. In Figure 5.9, however, the distribution seems to cover more area with the horizontal axis spanning from -8 to 5. While we do not have control on how the latent space is going to be distributed during the training process, we can notice that the supervised part of the training seems to have provided a latent space distribution that is more structured and seems more expanded.

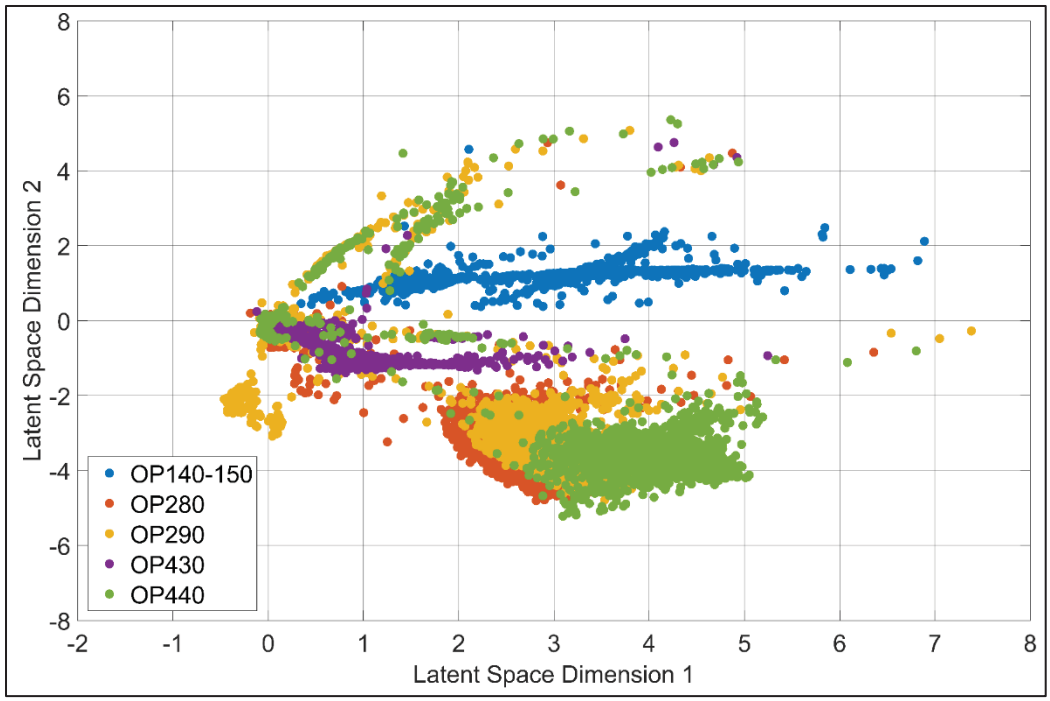

Figure 5.8 Latent space visualization of training and test datasets after VAE training

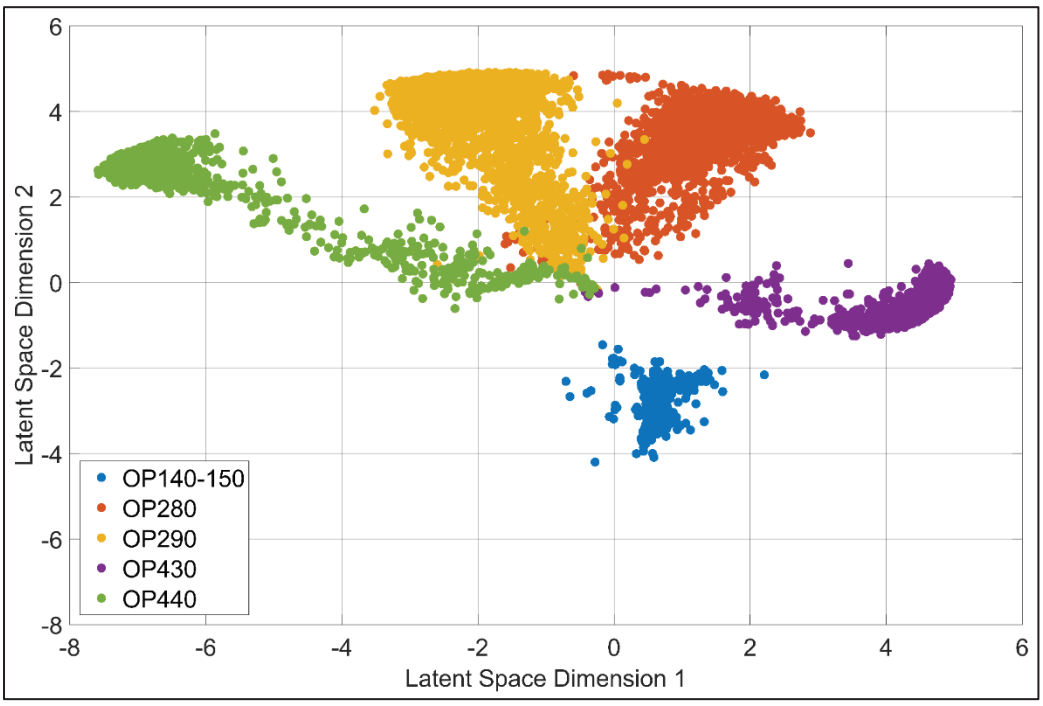

Figure 5.9 VAEC (VAE Classifier) resulting latent space for training and test datasets

Our next step was to demonstrate the ability of our model to accurately classify cutting operations based on our input vector entirely composed of signal information (section 5.5.2). In Figure 5.10, we display the latent space distribution based on the test dataset. We see that there is a good structure and well-defined cluster (colors represent the predicted label $\hat{y}$). This last statement is supported by the results of the confusion matrix presented in Figure 5.11. This confusion matrix was obtained on the test dataset, and was used to validate the performance and generalization capability of our VAEC model. We can see that our model achieves very good performance across all labels and an overall good accuracy of 99.24%. We see in Figure 5.12 that very few data points were poorly classified, and that the latter are concentrated around the same areas. We could assume that this concentrated area represents some sort of conflict zone where the model is not able to accurately discriminate the cutting operations. This could be due to the fact that some aspects of the conflicted operations resemble one another in terms of physical process signature. These positive results show that the VAEC approach can, in fact, successfully classify cutting operations.

Figure 5.10 Latent space visualization of test dataset after VAEC training

True Class \ Predicted Class	OP140-150	OP280	OP290	OP430	OP440
OP140-150	810 (99.8%)	0 (0.0%)	0 (0.0%)	0 (0.0%)	0 (0.0%)
OP280	0 (0.0%)	2254 (99.7%)	27 (1.3%)	0 (0.0%)	5 (0.5%)
OP290	0 (0.0%)	7 (0.3%)	2123 (98.7%)	0 (0.0%)	11 (1.0%)
OP430	2 (0.2%)	0 (0.0%)	0 (0.0%)	779 (100.0%)	0 (0.0%)
OP440	0 (0.0%)	0 (0.0%)	2 (0.1%)	0 (0.0%)	1082 (98.5%)

Figure 5.11 Confusion matrix of the test dataset

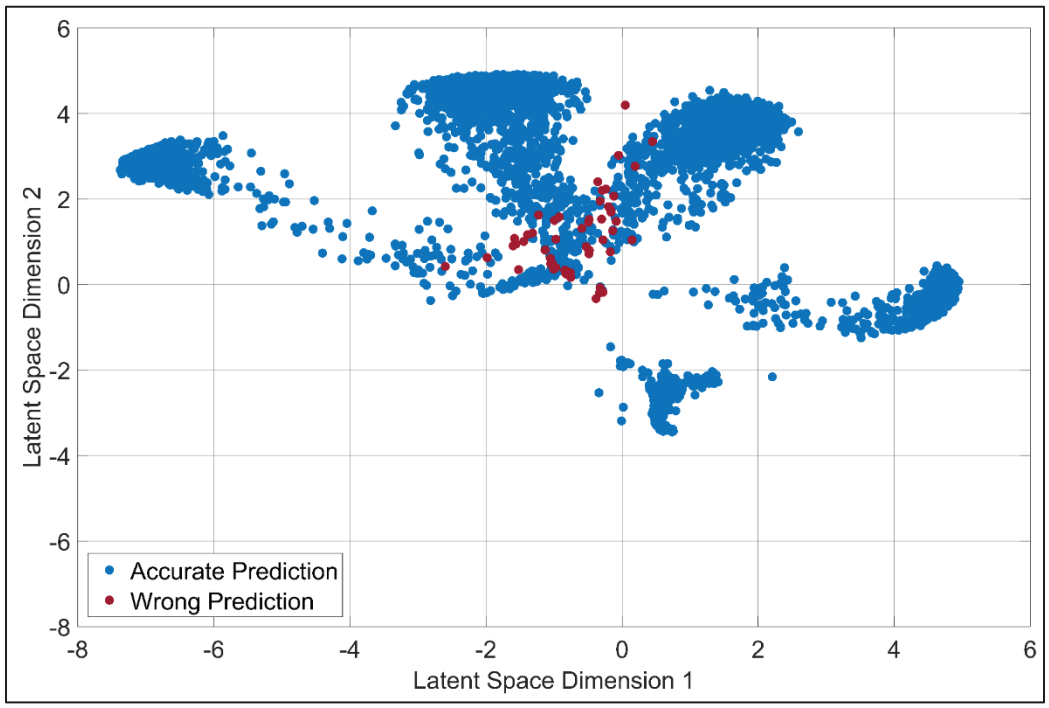

Figure 5.12 Visualization of training and test datasets' conflict zones between accurate and wrong predictions

What is also interesting in our result is that we were able to achieve an overall classification accuracy of 99.24% on our test datasets, with only two features encoded from our trained

encoder. Thus, we were able to achieve a good dimensionality reduction while still keeping the essential information required to solve our classification problem. As a comparison, we decided to do a Principal Component Analysis (PCA) based on the correlation matrix of our dataset to determine the number of components needed to achieve a representation of 99% of the variance. Based on our PCA results, it would require 24 components to achieve 90.0% of cumulative variance and 50 components to achieve 99.0%. These results show that a PCA approach would result in a significantly higher dimension representation than what we achieved with our VAEC and two-step training method.

Furthermore, as discussed in the introduction, one of the drawbacks of a machine learning approach is its resulting black-box effect. To diminish this effect, in section 5.5.2, we proposed a feature vector with physical meaning. To validate our hypothesis that using features with a physical meaning can also reduce the black-box effect of a machine learning approach, we trained the same VAEC model, but with each training iteration, we removed a category of features to determine the category providing the most information to the model. In Tableau 5.4, we can see that the feature providing the most information is k_c, followed by the cutting tool frequency amplitude, which seems to provide slightly more information than the cyclostationarity or the time domains. We believe that this supports our hypothesis that a feature with a physical meaning can provide more information to a model than only traditional statistical features. This is mainly because k_c and the cutting tool frequency amplitude are two categories of features directly aligned with the cutting tool and its physical response during the machining of a workpiece. This observation seems to be in adequacy with the current literature state. In fact, we can observe several recent publications such as Z. Jiang et al. (2019), Shen et al. (2018), or Z. Zhu et al. (2019) where the authors used the concept of energy to describe some aspect of the machining process.

Tableau 5.4 VAEC performance based on the removal of categories of features

Without	**VAEC Test Accuracy**	**Loss (vs. 99.24%)**
k_c	84.57%	-14.67%
A_{ct}	98.38%	-0.86%
k_c and A_{ct}	84.19%	-15.05%
First-order cyclostationarity	98.56%	-0.68%
Second-order cyclostationarity	98.86%	-0.38%
Time domain	98.87%	-0.37%

The next step in our methodology was to highlight that this latent space could also be used as a visual process monitoring tool to quickly and visually detect faults or changes of state during a machining process. Based on our work hypothesis, we used the subset related to the operation OP160 from our dataset. We fed this subset to the already trained VAEC model in order to see if the model would correctly and visually cluster it in another cluster than the one belonging to the OP140-150. From Figure 5.13, we can see that the model was able to successfully create two separate clusters. What is also interesting is that some data points seem to transition from one cluster to the other, which could lead us to believe that, in a real-time application, an operator or a decision maker could visualize the transition from one state to another. Nevertheless, since we cannot confirm this yet, these transitory points might also be due to the inherent nature of the machine learning training process. While we achieved great classification results, there is still some residual error left which could likewise explain these scattered points between the two groups. This is something we can also notice in other studies such as R. Zemouri et al. (2020) where their clusters are not perfectly exhaustive.

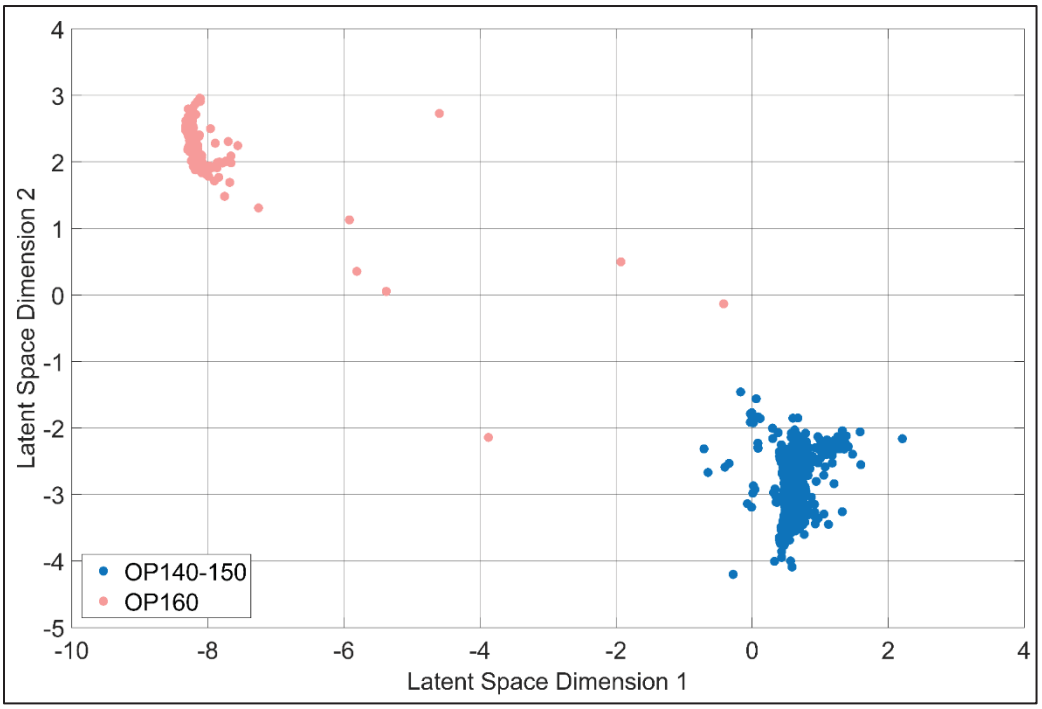

Figure 5.13 Visualization of the data points of OP140-150 and OP160

While these results support our hypothesis, as we stated, the subset related to the OP160 represents another state of the operations OP140-150, and is not a defect or faulty cutting operation. Consequently, as stated in our methodology, our last experiment was to feed the artificially faulty subset to our trained VAEC model to see if it could again visually cluster these points in another cluster. From Figure 5.14, we can see that the model was indeed capable of clustering this subset in another cluster from the one belonging to OP140-150. While not all the subset points are clustered in the same region, they are all in the periphery of the OP140-150 cluster. However, our belief was that we could visually see a transition from one state to the other as the defect increased. By looking at the distribution in the latent space, the subset does not seem to be distributed like that. This led us to believe that the latent space distribution is aligned with the training objective, and consequently, the model clustered the faulty subset together. Therefore, we could assume that the model, in terms of this training objective, is not able to correctly measure the level of a defect, and thus be able to distribute the subset according to its defect level. Even though the model does not seem able to achieve such results, the results can still be used to support our claim that a well-

trained VAEC and its related two-dimensional latent space can be used as a process monitoring space for visual machining process monitoring.

In comparison, a traditional process or mechanical system monitoring proceeds by following the RMS value through time. In Figure 5.15, we plot the evolution of the RMS value against the evolution of the defect level. On the one hand, in Figure 5.15, we display the difference in percentage between some defect levels and the original signal for the second accelerometer (X axis). With this, we can see, for instance, that between the original signal and the one with a defect of 0.1×, there is only 0.62% difference in the RMS value. It is both visually and quantitatively difficult to detect a meaningful change at that level. Additionally, we also used the first four data points of each distribution to calculate the mean and standard deviation in order to estimate an alarm value based on three times the standard deviation ($\overline{x} + 3\sigma$) (Thomas, 2011). In each case, this alarm would be triggered between defect values of 0.2×-0.3×. Moreover, we can visually detect that an increase in the RMS value is beginning around a defect level of 0.3×-0.4×, where as at a defect level 0.5× it is visually clearer and we can highlight a difference of 11.91% from the original signal. On the other hand, we can denote that while there is not a quantitative relationship between the latent space position of a value and the respective defect level, we can still visually detect the defect from the earliest level compared to the visual inspection and the 3σ alarm. Consequently, we believe our proposal is indeed an efficient visual tool for detecting small defects in a process earlier than in a classical approach. We could therefore define some sort of threshold border that limits the area between a subset without defect and one with defects. As a visual example, in Figure 5.14, we define the OP140-150 cluster center based on the k-means clustering algorithm and arbitrarily define a circle encompassing all the normal subset. Anything outside this border is directly considered faulty as compared to the normal cluster. Further work could be done to properly define this threshold border position in the latent space.

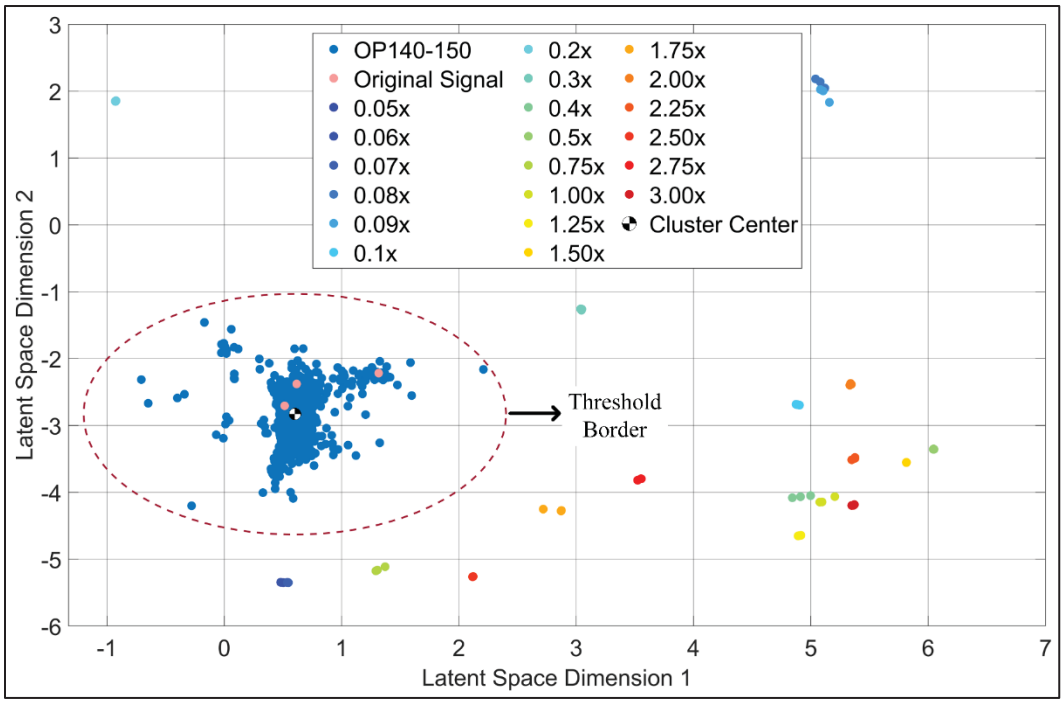

Figure 5.14 Visualization of artificially faulty data points vs. the OP140-150 cluster

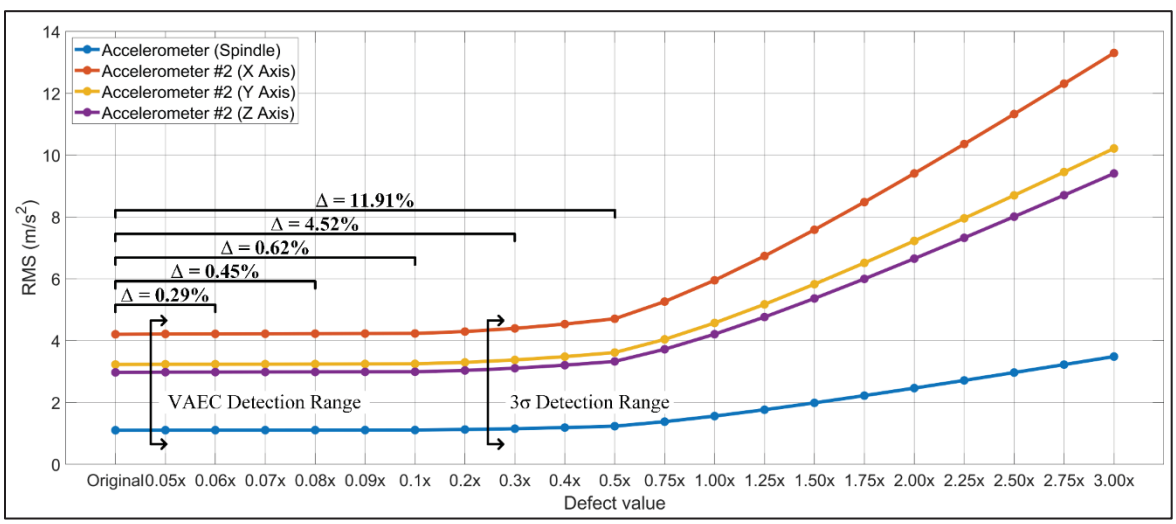

Figure 5.15 Evolution of the *RMS* value against the defect level

5.7 Conclusion

In this paper, we investigated the use of a VAEC method in a machining context. The approach was to use a two-steps training methodology (unsupervised then supervised) to predict the cutting operation label based on features extracted from signal data. We demonstrated that it was possible to achieve this with 99.24% accuracy and showed that, in accordance with the current state of the literature, a strong physical interpretation of the machining process can help improve the performance of an artificial neural network. Through that training process, we also showed that it was possible to reduce the dimensions of the dataset from 168 to 2, which was shown to be better than a PCA, in order to provide a visualization support. Henceforth, improving the interpretability of the network and reducing the black-box effect. Moreover, this 2D visualization support was shown to be a capable tool for doing the monitoring of a machining process and to detect changes of state in that machining process earlier than the monitoring of the RMS value.

However, even though we were able to achieve the objectives set out in this paper, there is still work to be done in order to achieve a general, real-time, system capable of predicting the state of a machining process and its quality level in a production environment. To achieve this, further work should include applying this methodology to a dataset that includes the quality level of each workpiece. In addition, this dataset should include workpieces that have clearly been labeled as non-conforming (i.e., faulty workpieces). Furthermore, another direction we propose would be to investigate if the two-dimensional latent space distribution can be used to reflect the level of degradation. This could provide an efficient 2D visualization tool of the level of defect in the process. This could be done in conjunction with our hypothesis that the VAEC model trained such as to measure the level of defects might be able to distribute the latent space in such a manner. It might also be interesting to apply a more conventional approach such as an autocorrelation one to compare with the performance of the proposed VAEC one. Moreover, two additions could be made to the dataset: first, another type of sensor (e.g., acoustic emission), to see if the conflict zone shown in Figure

5.12 can be reduced by adding a different dimension; second, add another product to the dataset to see if these results can be transferred and repeated with another machining process.

Nonetheless, the proposed methodology was developed and applied in an industrial context. From the results, we can therefore see that this approach could already provide benefits to a machining company by allowing it to better understand its processes, and to monitor their states visually. Consequently, a company should be able to work to reduce unexpected breakdown or production shutdowns, and furthermore, reduce the financial burden imposed by such unwanted events.

5.8 Acknowledgement

The authors would like to thank APN Inc. and their employees for the knowledge and the data shared in this project. We would also like to acknowledge the financial support of the *Fonds de Recherche du Québec – Nature et Technologies* (FRQNT) to this project through grant #257668. In addition, this research was enabled in part by the support provided by *Calcul Québec* (www.calculquebec.ca) and Compute Canada (www.computecanada.ca).

CHAPITRE 6

PREDICTING THE QUALITY OF A MACHINED WORKPIECE WITH A VARIATIONAL AUTOENCODER APPROACH

Antoine Proteau[a], Antoine Tahan[a], Ryad Zemouri[a, b], Marc Thomas[a]

[a]Département de génie mécanique, École de technologie supérieure, Montréal, Qc, H3C 1K3, Canada
[b]Laboratoire CÉDRIC du Conservatoire National des Arts et Métiers (CNAM), HESAM Université, 750141, Paris Cedex 03, France

Soumis à *Journal of Intelligent Manufacturing*, Décembre 2020

6.1 Résumé

Dans cet article, nous démontrons qu'il est possible de réaliser le pronostic de la mesure des requis de qualité, géométriques et dimensionnels, en nous basant sur une approche par apprentissage machine qui s'alimente seulement de données provenant de capteurs (vibration et consommation de courant) et ce, dans un contexte industriel. Nous utilisons premièrement une méthodologie basée sur une approche par autoencodeur variationnel et nous proposons ensuite une métrique basée sur le concept de distance euclidienne et l'espace latent 2D produit par l'autoencodeur variationnel. Le modèle proposé est capable de prédire les mesures de la qualité avec une erreur quadratique moyenne de 5.2573×10^{-4} mm. Le système de mesure proposé présente aussi un intervalle de confiance (C.I.) de ± 0.05 mm. De plus, l'espace latent de deux dimensions est capable de distribuer et structurer les données selon le niveau de qualité et fournit un outil de support visuel rapide. En comparaison avec la méthode *t*-SNE, l'espace latent présente une meilleure structure. De surcroît, la métrique de distance euclidienne proposée est corrélée au niveau de qualité autant au niveau des données prédites qu'observées. Ces travaux sont aussi basés sur un jeu de données industrielles ce qui augmente le potentiel de transfert technologique. En retour, ceci permet également une meilleure surveillance du processus d'usinage, ainsi que la réalisation du pronostic de la qualité du produit.

6.2 Abstract

In this article, it is shown that a machine learning approach based only on data from sensors (vibration and current consumption) can be used to predict the geometric dimensioning and tolerancing quality measurement values of machined workpieces in an industrial context. First, a methodology based on a variational autoencoder approach is used, and then a metric based on the concept of Euclidean distance and the 2D latent space produced by the variational autoencoder is proposed. The proposed variational autoencoder regression (VAER) model is shown capable of predicting the quality measurement values, with a mean square error of 5.2573×10^{-4} mm. The proposed measurement system also displays a confidence interval (C.I.) of ± 0.05 mm. Moreover, the resulting 2D latent space is capable of distributing and structuring data based on the quality level and of providing a quick visual support. Compared to the t-SNE method, this latent space displays a better structure. Furthermore, the proposed Euclidean distance metric is correlated to the quality level in both the predicted and observed subsets. This work is also based on an industrial dataset, thus increasing its potential for technological transfer; that in turn allows a better monitoring of the machining process, as well as the prediction of the workpiece quality.

6.3 Introduction

Today, globalization, forced price reductions, ever-increasing quality requirements and production rate improvements are all factors that exert tremendous pressure on the manufacturing industry (Takaya, 2013). Companies operating in the industry are in a never-ending race for innovation in a bid to keep ahead of the competition and to generate positive financial results (Wuest, Irgens, & Thoben, 2014). Even with the positive innovations that have been brought about by the fourth industrial revolution (Industry 4.0) (Baur et al., 2020; T. Han et al., 2019; Huang et al., 2019; Kohler & Weisz, 2016; Martínez-Arellano et al., 2019; Voisin et al., 2018), in the specific context of machining, companies are still plagued with challenges in the form of unexpected Computer Numerical Control (CNC) machine downtime, cutting tool breakage and nonconforming products, which ultimately, increase variances in the production process and burden the companies' financial health (Chadha et

al., 2019; Park & Tran, 2014; Y. Zhou & Xue, 2018). Monitoring and prognostic systems developed to monitor machine health (including that of critical components such as cutting tools or bearings) or to predict the remaining useful life are in effect assets that could help solve the aforementioned problems faced by the industry and ensure better financial performance (Laloix et al., 2016).

There is a direct relationship between the quality level, the productivity and the financial health of a manufacturing company since a nonconforming workpiece must be reworked anew, thereby increasing production costs. The quality of the workpiece (conformity with requirements and specifications) is ultimately a crucial factor. The ability to monitor and predict the quality level of a workpiece can thus improve productivity, lower the quantity of unexpected nonconforming workpieces and improve the financial health of a machining company. The main aim of this article is to propose a method to predict the quality of a workpiece based on a machine learning (ML) approach. In this context, it must be understood that the workpiece quality is still a complex concept, and that it is affected by multiple elements. Figure 6.1 shows a non-exhaustive list of factors influencing the machining process, and thus the workpiece quality. These elements are based on the work of Benardos et Vosniakos (2003), Park et Tran (2014) and Ouafi et Barka (2014).

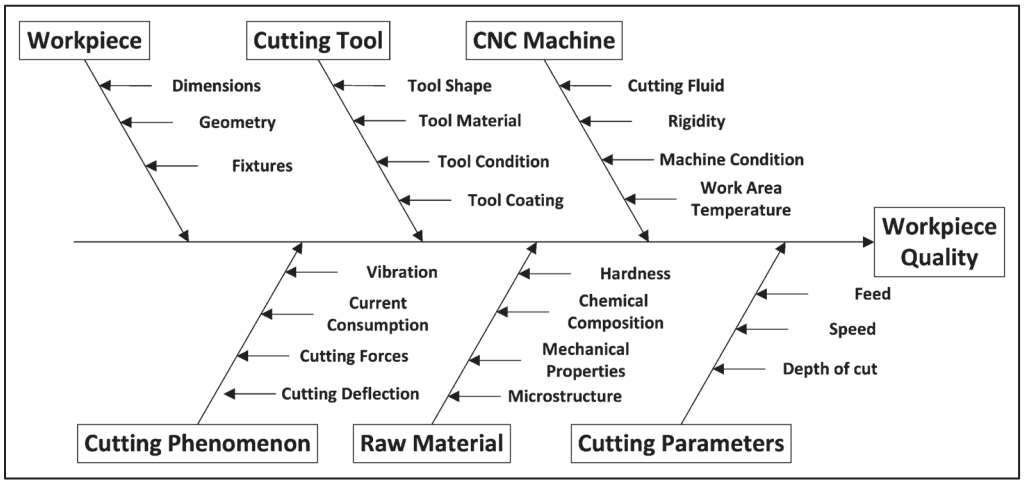

Figure 6.1 Workpiece quality cause and effects diagram

To control quality, two measurement methods (direct and indirect) can be used (Laloix et al., 2016; Ouafi & Barka, 2014). Direct methods relate either to a posteriori measurements carried out with metrology equipment following the machining process or those carried out during the process using equipment such as probes (Takaya, 2013). A posteriori measurement methods are the most common, and in the case of mechanical workpieces, are often carried out with a Coordinate Measuring Machine (CMM), a costly piece of equipment, which commonly represents a bottleneck during the production process. An indirect approach involves the measurement of physical quantities such as vibration, current consumption, acoustic emissions, etc., which can be used to infer the quality characteristics of the product. Indirect methods represent a less expensive and more flexible approach when used in combination with the appropriate modeling capabilities (Ouafi & Barka, 2014), and allow both online and in-process quality evaluation.

While indirect quality measurements have been explored in the literature, past works, however, attribute different meanings to the health monitoring or prognostic of the quality measurement of a workpiece. For instance, almost three decades ago, Irgens (1991) was already interested in the subject, and wanted to predict the quality at the design phase in terms of conformity with the functionalities of the workpiece, not its geometric or dimensional aspects. More recently, in his review, Takaya (2013) suggests that quality is related to a process output based on Statistical Process Control (SPC). Laloix et al. (2016) support this idea in their work and insist that quality evaluation is usually performed with SPC or statistical quality control after the machining process. However, Papananias et al. (2019) assert that the problem with SPC is that the complexity of control chart monitoring increases as the number of variables rises. Instead, they propose an intelligent monitoring system to monitor the quality based on an ML approach. Park et Tran (2014) support the idea of a quality monitoring and quality prediction system, but in their work, they propose a different vision of quality prediction: they define the workpiece quality as a prediction based on the cutting tool wear and surface roughness. This is supported by Bakker, Ratchev, et Popov (2015), who assume that the quality of the workpiece and of the process is derived

from the cutting tool condition. As can be seen in Figure 6.1, both do not represent the overall workpiece quality.

Both tool condition monitoring (TCM) and surface roughness prediction are active research domains that have been the focus of many studies (Abellan-Nebot & Romero Subirón, 2010; Benardos & Vosniakos, 2003; He, Gao, & Zhao, 2019; Kuntoğlu et al., 2021; X. Liang, Liu, & Wang, 2019; Serin, Sener, Ozbayoglu, & Unver, 2020; Y. Zhou & Xue, 2018) and several applications (Chen et al., 2018; Duo et al., 2019; Khorasani & Yazdi, 2017; Martínez-Arellano et al., 2019; Y. Zhang, Zhu, Duan, & Li, 2021). However, while both affect the geometrical and dimensional quality of the workpiece, they do not represent it.

In a machining process, the final quality is generally related to its conformity with Geometrical and Dimensional Tolerancing (GD&T) requirements. These requirements are usually governed by standards such as ASME (2018a), and are usually imposed by functional requirements. Few attempts have been made to predict quality based on this definition. In Laloix et al. (2016), the authors support the idea that a quality monitoring and prediction system would indeed reduce the need for a posteriori measurement. Voisin et al. (2018) successfully develop a health indicator based on vibration signals to monitor the evolution of two quality requirements, namely, surface location and parallelism. In the same vein, Papananias et al. (2019) develop an artificial neural network based on cutting forces to predict, with a low error, the true position and circularity requirements of a workpiece in an experimental context. However, in this last example, measuring cutting forces in an industrial context is difficult due to the high cost of implementing such a process, as well as its intrusive nature (Abellan-Nebot & Romero Subirón, 2010). Extensive work has been done to examine the health monitoring and prognostic of mechanical systems such as CNC machines. However, even given the positive impact of systems capable of monitoring and making workpiece quality predictions, a smaller number of applications were found in this regard. The hypothesis proposed herein is that an intricate connectivity between multiple systems (computer-aided design (CAD), computer-aided manufacturing (CAM), manufacturing execution system, CNC machine, etc.) is required to build the essential dataset needed to

achieve such predictions. Even with the availability of advanced technologies, these connections do not seem to be generally available in the industry. To fill this gap, authors such as Rauch, Laguionie, Hascoet, et Suh (2012), G. Zhao, Cao, Xiao, Liu, et Jun (2020) and Y. Zhang, Y. Zhang, et al. (2021) have made contributions using the STEP-NC standard. This standard proposes a new, information-rich model that could facilitate the exchange of information between the CAD-CAM-CNC systems (Rauch et al., 2012) and simplify data exchange, collection and contextualization.

As mentioned above, currently, the direct a posteriori method, in which measurements are carried out following the machining process, is still the most used approach. However, it is a reactive and costly method in terms of quality validation. To tackle this limitation and adopt a more proactive approach, transition to an indirect measurement methodology is needed.

Given that indirect measurements have successfully been applied in the specific areas of surface roughness prediction, TCM and Condition-Based Maintenance (CBM) (Haidong et al., 2018; Janssens et al., 2017; S. Wang et al., 2017) and in machining in general (Goyal, Mongia, & Sehgal, 2021), could the same methodology, which consists of monitoring, diagnostics and prognostic, be applied to the context of GD&T quality monitoring and prediction? The methodology could help establish a common definition regarding the prognostic of a workpiece quality, which is currently lacking in the field. Furthermore, it would be extremely advantageous for a machining company to have an online monitoring system capable of predicting a quality estimate in real time and of carrying out diagnostics (e.g., of cutting tool wear or machine health degradation) to determine causes of workpiece quality degradation. This would in turn help them lessen the impact of the aforementioned problem.

This paper thus intend to demonstrate that it is possible to predict the GD&T quality measurement value by using sensor data (such as vibration, current consumption, etc.) and an ML approach based on a Variational AutoEncoder (VAE) architecture. It should be pointed out that an ML approach is suited to the machining context as ML methods perform well in a

non-linear environment (S. Lee et al., 2019), as well as in situations where a human being cannot process all the different variables (Ouafi & Barka, 2014). Even with the great success enjoyed by ML applications in the industry and in other domains (Bao, Yue, & Rao, 2017; Gensler, Henze, Sick, & Raabe, 2016; K. Han et al., 2019; Pang, Zhang, Xiao, Qi, & Xue, 2021), the ML approaches often face three drawbacks: a lack of data in sufficient quantity and of good quality, the curse of dimensionality (the machining industry being a good example here) (San Martin et al., 2019), and their black-box effect (S. Yu & Príncipe, 2019).

In order to reduce the impacts of the dimensionality of this problem and minimize the black-box aspect of an ML approach and enhance the model interpretability, a VAE architecture is used. This type of Neural Network (NN) architecture has been shown to possess excellent dimensionality reduction capabilities, and it can be used for two-dimensional (2D) visualization, thus providing visual support to allow a better understanding of data distribution (Mancisidor, Kampffmeyer, Aas, & Jenssen, 2021; Proteau et al., 2020; Shahid & Ghosh, 2019; R. Zemouri et al., 2020). It also provides a simple architecture and can be trained quickly (Doersch, 2016) and behaves well in a non-linear situation (S. Lee et al., 2019), which is also ideal for a context such as that of the machining industry. The fact that the VAE provides a well-regularized latent space further improves the 2D visualization capability, as compared to a classical AutoEncoder (AE) approach. The literature provides multiple examples of prediction models based on an AE (Bampoula, Siaterlis, Nikolakis, & Alexopoulos, 2021; Bao et al., 2017; Gensler et al., 2016; Xu, Yang, Fei, Huang, & Tsui, 2021; W. Yu, Kim, & Mechefske, 2019; W. Yu, Kim, & Mechefske, 2021), but they are mainly used for their feature extraction capability, are paired with other types of NN architecture, and are not used for visualization purposes. Furthermore, the VAE also exhibits excellent generative properties as compared to other approaches (Doersch, 2016; Mancisidor et al., 2021). A trained VAE and its latent representation could thus be used to generate new data based on the assumptions made from the training dataset.

Therefore, the second aim of this paper is to illustrate that the proposed methodology will provide a convenient 2D visualization capability. This capability will prove useful for

improving the acceptance and transferability of the suggested methodology to an industrial context by providing a visual tool to help shop floor workers better understand the model's behavior and prediction. This is important because technology transfer does not seem to feature prominently in the reviewed literature. By successfully achieving these two goals, machining companies avail themselves with a novel measurement system allowing them to free up capacity on their existing, post-process, measurement systems (e.g., CMM, optical comparator, etc.), while providing an efficient and easy-to-use visualization tool. Moreover, the proposed approach is based on an industrial dataset, which helps provide a real and industrial application example and shows that the connectivity required to build the necessary dataset can be achieved. Figure 6.2 below summarizes this paper's proposal.

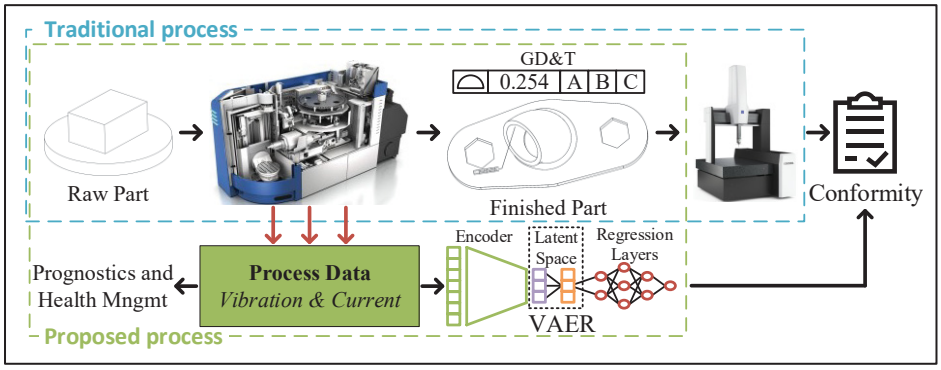

Figure 6.2 Traditional versus proposed process[6]

Specifically, the objectives of this article are, first, to show that a signal processing methodology similar to the one used in TCM or in CBM combined with a VAE approach to predict the GD&T quality measurement value of a workpiece can be used. Second, it aims to demonstrate that the VAE-trained latent space can be used as a tool for the visual monitoring of the quality level of a workpiece. Third, it attempts, and indeed succeeds, to illustrate that the trained latent space distribution is highly correlated to the quality level of a workpiece, thus showing that a well-trained latent space can also be used to quickly predict an estimate of the quality level of a workpiece. Finally, the paper intends to show that the method is

[6] Photos: ZEISS and Grob-Werke

highly transferable to an industrial context as it uses a dataset acquired entirely in the course of the regular production activities of an industrial partner. While some authors have successfully predicted the quality in terms of GD&T while using experimental data, to the best of the current knowledge, an industrial application based on a VAE approach such as the one proposed herein is scarce.

The remainder of this article is structured as follows: section 6.4 presents the methodology, and highlights the industrial context and the dataset used in this work, as well as the signal processing and feature extraction approach. In section 6.5, the ML approach and the architecture of the NN are described. The results are presented and discussed in section 6.6. Finally, the article is concluded in section 6.7.

6.4 Methodology

In this section, four elements essential to this work are elaborated: first, the industrial context and the industrial dataset acquired from the industrial partner for this project are described. Then, the methodology proposed to achieve the objectives is described. Next, inspired by work done in TCM and CBM, a signal processing and feature extraction methodology is proposed. Finally, the data preparation methodology is presented.

6.4.1 Industrial Context and Dataset

For this project, a collaboration was made with an industrial partner, APN Inc. (Quebec, Canada), a machining company specializing in the manufacture of high precision products made from exotic alloys (Inconel, titanium, etc.) for the aerospace, defence and high tech industries. They are also a national leader in Industry 4.0, and are the first technological window for the province of Quebec.

The dataset was acquired during the partner's regular production schedule. Specifically, it was done during the production of a component made from Inconel 625, a nickel-based alloy (as per AMS-5666), over three work orders and intended for use in the aerospace industry.

The machining process was realized on a G352 5-axis CNC machine from GROB company (see Figure 6.2). Following the machining process, the partner used an a posteriori direct measurement method with a Zeiss Contura CMM to measure the GD&T quality of the workpiece. In accordance with manufacturing and quality requirements, 21 GD&T specifications needed to be measured for each sample, and each of them had to fall within the established tolerance limits to be deemed conforming. Of these 21 specifications, 17 did not show enough variation throughout the manufacturing process or did not have nonconforming measurements. From the remaining four specifications, the total number of nonconforming workpieces per specifications over the three work orders was gathered. The unilateral process performance index (P_{pk}) was also calculated for each specification according to equation (6.1) (ISO, 2006; Tahan & Levesque, 2009). A lower P_{pk} indicates a less stable production process:

$$P_{pk} = \frac{USL - \hat{x}_{50\%}}{\hat{x}_{99.865\%} - \hat{x}_{50\%}} \tag{6.1}$$

where USL and LSL are respectively the upper and lower specification limit of the customer, $\overline{x}$ is the average of the measurements and σ is the standard deviation of the measurements.

A summary is provided in Tableau 6.1 for all three acquired work orders. For the purpose of this study and as a starting point, the GD&T characteristic #31, which is a profile of a surface (d), was chosen based on its poor performance results from the remaining four specifications. This specification allows up to a 0.254 mm [0.010 in] 3D profile deviation related to three data: A, B and C. To illustrate the workpiece and its requirement, Figure 6.2 also presents an isometric view of the raw material, an isometric view of the finished workpiece, and the location of the GD&T #31. For reasons of confidentiality, the 3D models were altered to only give an idea of the geometric shape of the workpiece, and limited information is shown.

Tableau 6.1 Specifications statistics summary

Characteristic number	Type of GD&T	P_{pk}	Number of noncoformances
16	Profile of a Surface	0.90	0
23.2	Radius	0.80	4
28.Max	Length	0.78	2
31	Profile of a Surface	0.45	11

To be considered within the tolerance limits, an observed GD&T measurement value (y) had to be between the nominal value of 0 mm and the maximum limit of 0.254 mm [0.010 in] ($0 \leq y \leq 0.254$). If the measurement exceeded the tolerance limit ($y > 0.254$), then the workpiece was considered out of tolerance and nonconforming (red area). To illustrate this behaviour, Figure 6.3 displays the measurements made for each workpiece for the GD&T #31 during the production of one out of three work orders. The green area represents the conforming workpieces, the yellow one shows workpieces that are conforming, but within a warning zone (20% of the allowed tolerance as per the industrial partner data), and the red one represents the nonconforming area. It can be seen that during this work order's production, three workpieces were outside the tolerance limits, and were thus considered nonconforming.

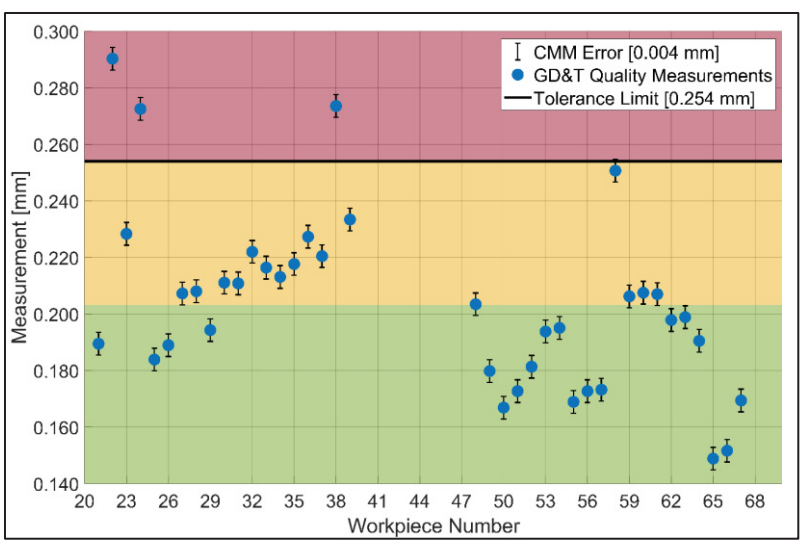

Figure 6.3 Examples of measurements for GD&T #31 per workpiece

In Tableau 6.2, the cutting parameters of the four cutting operations affecting specification #31 are presented. This association between the affected GD&T #31 and the cutting operations was determined by the experts at the industrial partner's. To perform the operations on the CNC machine, a 6.35 mm, 4-flute ball nose cutting tool was used.

Tableau 6.2 Cutting operations details

Name	Spindle speed [RPM]	Feed [mm/s]	Depth of cut [mm]	Est. cutting time [sec]	Volume removed [cm^3]
OP280	6035	858.52	0.152	123.770	0.0427
OP290	6035	858.52	0.064	77.470	0.0248
OP430	6035	858.52	0.165	36.641	0.0258
OP440	6035	858.52	0.165	39.727	0.0103

For the dataset, the data acquired was obtained from a previously discussed data acquisition (DAQ) system implemented at the industrial partner's, and used in Proteau et al. (2019b) and Proteau et al. (2020). This system allows the physical quantities (vibration, current consumption) provided by sensors to be automatically contextualized with the operational data (CNC program, cutting parameters, cutting operations, quality measurements data, etc.) in real time. Bakker et al. (2015) assert that these two types of information and their fusion should be used in order to predict the quality of a workpiece. Two types of physical phenomena were recorded: first, vibration, where a triaxial accelerometer (PCB model 356A33[7]) was mounted on the housing of the CNC machine spindle and an uniaxial accelerometer (IFM model VSA004[8]) which was already installed by the manufacturer in the spindle, was also used. Then, the current consumption, with four current transducers (LEM model LF 210-S[9]) installed on one phase of the spindle motor and on one phase of each motor of the main axes (X, Y and Z). For the relative position of each sensor, the reader is referred to Proteau et al. (2020). Additionally, Figure 6.4 shows an overview of the database acquired at the industrial partner's.

[7] Technical specifications are provided at https://www.pcb.com/products?model=356a33
[8] Technical specifications are provided at https://www.ifm.com/ca/en/product/VSA004
[9] Technical specifications are provided at https://www.lem.com/en/lf-210ssp5

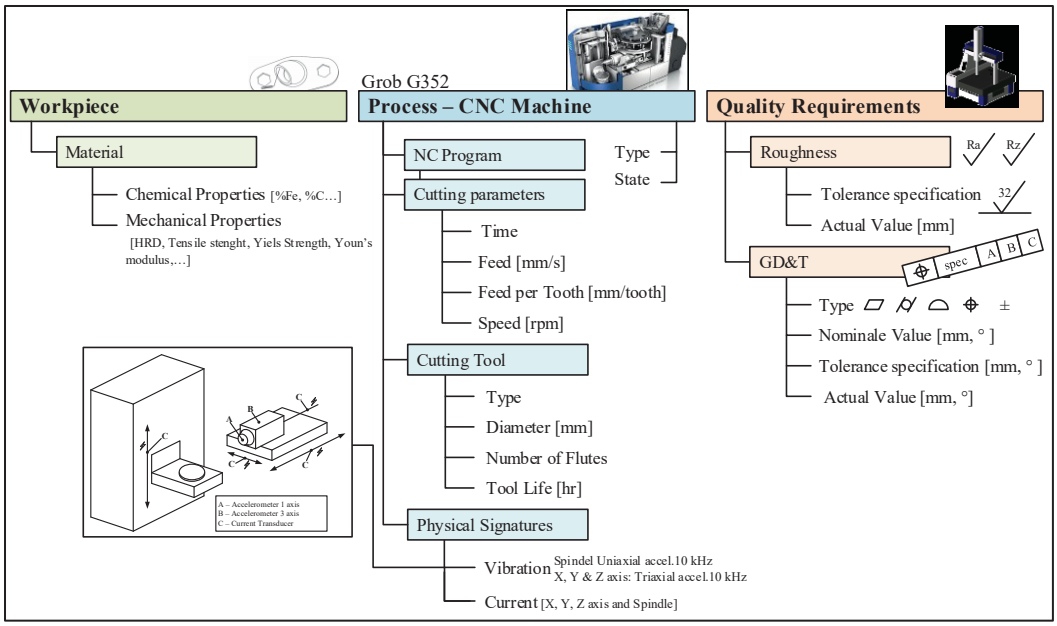

Figure 6.4 Acquired database information overview

The DAQ system process was then paced by the real-time state and context of the CNC machine (material cutting, feed stop, in error, etc.). Each sensor signal file was thus "attached" to an operation context, such as the cutting tool being used, the cutting operation being executed, the workpiece number, etc. The acquisition process was also performed only while the CNC machine was cutting the raw material, which meant that all transition phases (spindle start, cutting tool change, etc.) of the process have been removed. This capability of the DAQ system thus decreases the number of potential signal error sources. The acquired dataset covered the production of three work orders, with a total of 166 workpieces produced (~2.2 GB of raw data). Of these, 11 were considered nonconforming, as per the aforementioned logic.

6.4.2 Proposed Methodology

The methodology proposed to achieve the objectives is as follows: for the first objective, a signal processing method (see section 6.4.3) is applied to generate a dataset that will be used in conjunction with the VAE approach to predict the GD&T #31 quality measurement value of each workpiece. Here, a regression approach is used, which means that the model will

predict the workpiece GD&T measurement value in millimetres (mm). In other words, the goal here is to predict a measurement value by proceeding in a fashion similar to the current measurement system at the industrial partner's. To evaluate the model's ability to accurately make these predictions, and actually replace the current measurement system, the Mean Square Error (MSE) metric in equation (6.2) is used as the prediction model performance evaluation metric:

$$MSE = \frac{1}{n}\sum_{i=1}^{n}(y_i - \hat{y}_i)^2 \tag{6.2}$$

where y is the observed GD&T measurement value [mm] and $\hat{y}$ is the predicted GD&T measurement value [mm] for the workpiece number i out of n test samples.

Not only is it important to demonstrate that this model can accurately predict a GD&T measurement value, the model also needs to correctly predict whether a workpiece is conforming or nonconforming. If the model predicts a conforming workpiece when, in fact, it is nonconforming, such a false negative influences the output of the manufacturing process. It is less critical if the measurement system predicts a false positive than if it predicts a false negative. Therefore, after the regression, a confusion matrix will be used to display the model's capability to predict conforming and nonconforming workpieces accurately. Moreover, a prediction is considered conforming not only when its observed measurement is within the tolerance limit, but also when its predicted measurement is within that tolerance limit ($0 \leq \hat{y} \leq 0.254$). The same applies for a nonconforming prediction: a workpiece is predicted to be nonconforming when its observed GD&T measurement is outside the tolerance limits and the GD&T measurement value predicted by the model is also outside the tolerance limits ($\hat{y} > 0.254$).

To further validate the model behaviour, its error and prediction confidence must be quantified. To that end, the same model is trained 100 times, with each cycle representing a complete training of the model. This allows to approximate the "true" error of the prediction

model. The error will be reported in terms of average MSE and its related standard deviation (σ). Then, a nonparametric distribution is also used to define the 95% confidence level of the distribution. By quantifying the model error, not only will it be possible to quantify the behaviour of the measurement system, but the quantification will also be useful in the industrial context. For instance, the quantification allows to know when a workpiece is getting to be nonconforming and would require validation. It should also be noted that this proposal is not expected to be free of error. In fact, even the measurement systems already in place in the industry have error intervals.

Once the behaviour and performance of the prediction model are evaluated, attention is turned to the latent space created by the VAE. Therefore, for the second objective, the trained VAE 2D latent space is used, and shows that its distribution of every subset of the dataset, including the test one, reflects the quality level of each GD&T specification. To this end, it is graphically shown that the distribution of the predicted and the observed GD&T measurement values follow a logic related to the quality level in the 2D latent space.

Then, to further illustrate that the approach is capable of correctly distributing the data according to the quality level logic, it is compared with the popular 2D visualization *t*-distributed Stochastic Neighbor Embedding (*t*-SNE) method (Maaten & Hinton, 2008).

For the third objective, a new metric based on the trained VAE latent space and on the concept of Euclidean distance is proposed to demonstrate that the VAE latent space distribution is correlated to the observed and predicted quality levels. Figure 6.5 is used to illustrate this proposal. In order to calculate this metric, the well-known *k*-means algorithm (Ghosal, Nandy, Das, Goswami, & Panday, 2020; MacQueen, 1967) is used to group the training subset into clusters. It was arbitrarily decided to use 10 clusters to split the data into groups each representing 10% of the data. The centroid of the cluster consisting of the most conforming workpieces in terms of their observed GD&T quality measurement values is then used to calculate the Euclidean distance between the positions of each test workpiece in the latent space and this centroid. The distances are obtained with equation (6.3):

$$d(c, wp) = \sqrt{(wp_1 - c_{1)}{}^2 + (wp_2 - c_2)^2} \tag{6.3}$$

where $d(c, wp)$ is the 2D Euclidean distance d between the centroid $c = (c_1, c_2)$ and a test workpiece $wp = (wp_1, wp_2)$.

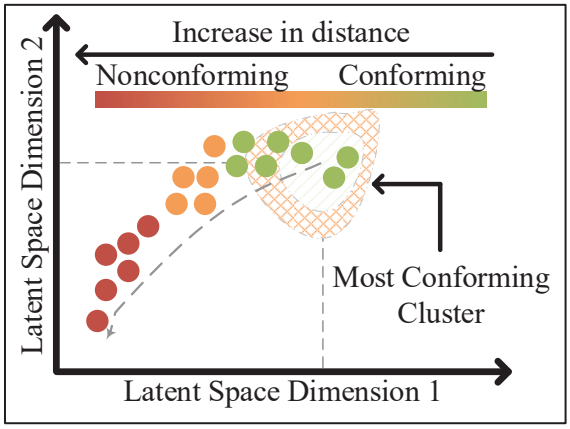

Figure 6.5 Visualization of the distance metric

It is then established that both the observed and predicted quality values are correlated with these distance values in the latent space by doing both a Pearson's correlation (r) and a Spearman's correlation (ρ) analysis. The respective *p-values* for each analysis are also reported. To show that this work is highly transferable to an industrial context, it is reiterated that this entire methodology is conducted using the previously described acquired industrial dataset.

6.4.3 Signal Processing

This section presents the signal processing methodology applied. The different features extracted from the raw signal acquired from the sensors that are going to be used in the input vector are explained. Features based on physical concepts are mainly focused on to better understand the physical phenomenon occurring during the machining process. This choice is

also guided by the works of Abellan-Nebot et Romero Subirón (2010), Elattar et al. (2016), Ahmad et al. (2020), Duo et al. (2019) and S. Y. Liang, Hecker, et Landers (2004).

Equations (6.4) to (6.10) define the features used to describe a raw signal (x). They respectively are the redressed Root Mean Square (RMS), the kurtosis (K), the peak ($Peak$), the peak-to-peak (PTP), the crest factor (x_{crest}), the cutting tool frequency amplitude (A_{ct}), and the Specific Cutting Energy (k_c):

$$RMS = \sqrt{\frac{1}{N}\sum_{i=1}^{N}(x_i - \overline{x})^2} \tag{6.4}$$

where N is the number of samples, x_i is the value of a sample and $\overline{x}$ is the average of the signal.

$$K = \frac{\sum_{i=1}^{N}(x_i - \bar{x})^4}{\frac{1}{N}\left[\sum_{i=1}^{N}(x_i - \bar{x})^2\right]^2} \tag{6.5}$$

$$Peak = \max(x_i) \tag{6.6}$$

$$PTP = \max(x_i) - \min(x_i) \tag{6.7}$$

$$x_{crest} = \frac{Peak}{RMS} \tag{6.8}$$

$$A_{ct} = \sqrt{\sum_{i=a}^{b} A_i^2} \tag{6.9}$$

A_i is the amplitude of the signal at the ith frequency and a and b are the two corners of the window. In this case, the corners of the window are ± 5 Hz of the cutting tool frequency, which, here, is equal to: 402.33 Hz ($6035[RPM] \times 4$ [flutes]).

$$k_c = \frac{P[\mathrm{W}]}{Q[\mathrm{cm}^3\mathrm{s}^{-1}]} = \frac{[\mathrm{J\ s}^{-1}]}{[\mathrm{cm}^3\mathrm{s}^{-1}]} = [\mathrm{J\ cm}^{-3}] \tag{6.10}$$

where P [W] is the power consumed and Q $[\mathrm{cm}^3\mathrm{s}^{-1}]$ is the material removal rate.

The reader is referred to Thomas (2011) and Proteau et al. (2019a) for equations (6.9) and equation (6.10), respectively. Also, these features are extracted on three different domains: the time domain, the frequency domain and the cyclostationarity domain (Antoni, 2009). For the cyclostationarity domain, the signals are not obtained by using the spindle encoder signal (M. Lamraoui, Thomas, El Badaoui, & Girardin, 2012), but rather, are estimated by doing an angular sampling of the acquired signals.

Tableau 6.3, below shows the features extracted according to the type of sensor signal and the domain.

Tableau 6.3 Features per type of signal

Signal	RMS	K	$Peak$	PTP	x_{crest}	A_{ct}	k_c
Vibration	T, C	T, C	T, C	T, C	T, C	F	-
Current	T	-	-	-	-	-	T

T: Time domain, F: Frequency domain, C: Cyclostationarity domain (first and second orders)

These features were then used for the input vector according to equation (6.11):

$$\boldsymbol{x} = [RMS^i, K^i, Peak^i, PTP^i, x^i{}_{crest}, A^i{}_{ct}, k^i{}_c] \tag{6.11}$$

where i is an index indicating the channel number, which, in this context, goes from 1 to 8 (4 channels for the vibration sensors and 4 channels for the current transducers).

6.4.4 Data Preparation

This section presents the data preparation approach used. Even though the acquired dataset is of good quality, this preparation step was required in order to correct the anomalies that had been captured, and that are inherent to the industrial nature of the production process.

First, data containing abnormal signals were removed from the 2.2 GB database. These outlier data files are inherent to the industrial nature of this dataset, and were the result either of an electrical anomaly in the DAQ setup or of external stimuli in the machining process. Then, each input vector for each sensor data file was grouped together by workpiece into one input vector. In other words, instead of having multiple input vectors for each workpiece, they were grouped together to ensure that each workpiece corresponded to one input vector. Next, for the smaller workpiece input vectors, they were padded with zeros in order to have even-length input vectors.

Furthermore, to compensate for the uneven ratio between conforming and nonconforming workpieces, three temporary groups were created: very good, good and nonconforming. These groups were defined as follows: workpieces with a measurement lower than 0.178 mm (closer to the nominal value of 0 mm) belonged to the first group, higher than 0.178 mm, but lower than 0.254 mm belonged to the second group and lastly, workpieces with measurements greater than 0.254 mm belonged to the nonconforming group. Decisions regarding the number of groups and their thresholds were based on the frequency distribution of the measurements. Then, random signal files were removed in each group to reduce the influence of the conforming-to-nonconforming ratio.

In addition, two normalization methods were applied. For the input vector, a standardization approach, in which the mean is subtracted and then divided by the standard deviation ($(x - \overline{x})/\sigma$), was used. For the output data, a min-max approach to normalize the data between -1 and 1 was used.

Finally, any remaining smaller signal errors were discarded during the training process of the model because an NN-based approach provides such a capacity (Abellan-Nebot & Romero Subirón, 2010; Elattar et al., 2016).

6.5 Neural Network Background and Architecture

This section provides background information on the VAE approach used in this work. Furthermore, the architecture and structure of the VAE model on which the prediction model is based and its training methodology are presented.

6.5.1 VAE Background

A VAE is a variation of an AE introduced by Kingma et Welling (2013), which, at its core, is an NN trained to output a reproduction of its input (Cheng et al., 2019; R. Zemouri et al., 2020). Basically, the encoder part of the AE encodes the input data with function $z = f_\phi(x)$ into a latent space z, which is then returned to the decoder, which decodes it with function $\hat{x} = h_\theta(z)$. Figure 6.6 (a) shows the architecture of an AE:

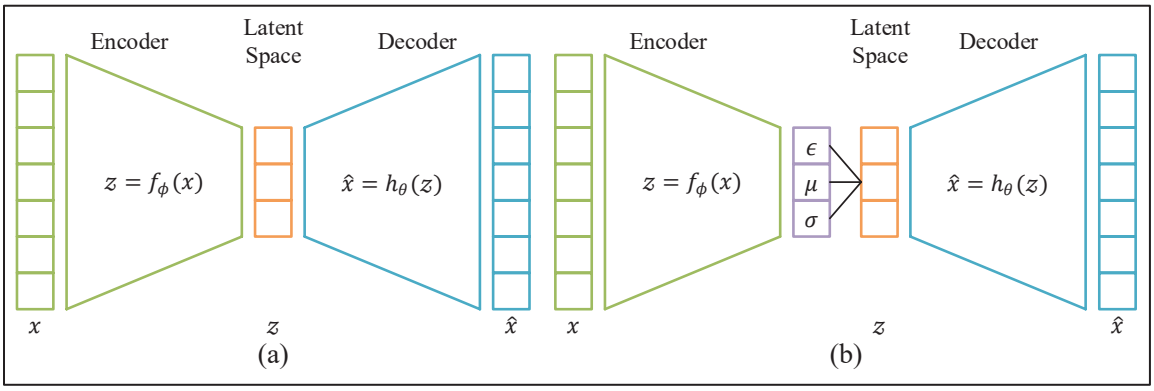

Figure 6.6 Structure of an AE (a) and of a VAE (b);
from Proteau et al. (2020)

Figure 6.6 (b) presents the architecture of the VAE. The difference between a classical AE and the VAE is that the AE lacks a well-regularized latent space. Therefore, a re-

parameterization trick is used. This allows each z_i to be sampled with equation (6.12) (Doersch, 2016; S. Lee et al., 2019; R. Zemouri et al., 2020):

$$z_i = \mu_i + \sigma_i \cdot \epsilon \tag{6.12}$$

where μ_i is the mean, σ_i is the standard deviation, i is an element of the vector and ϵ is a random variable following a Gaussian distribution $\epsilon \sim \mathcal{N}(0,1)$.

The loss function ($\mathcal{L}$) of a VAE is given by equation (6.13), which has two terms: the first one is the reconstruction cross-entropy and the second is the Kullback-Leibler (KL) divergence, which enforces the model to produce a latent space with a Gaussian distribution (R. Zemouri et al., 2020).

$$\mathcal{L} = \mathcal{L}_{rec} - \mathcal{L}_{KL} = E_{q\phi(z|x)} \log[P_\theta(x|z)] - KL[q_\phi(z|x) \parallel P(z)] \tag{6.13}$$

For more details about the VAE and its underlying mechanisms, the reader is referred to the work of Doersch (2016).

6.5.2 VAER Architecture

This section describes the VAE architecture used in this article and the strategies used to diminish the effects of overfitting. The proposed model is founded on two components, which are discussed below: a VAE's encoder and a regression NN. The encoder projects the input vector in a 2D, well-regularized, latent space that is then used as the input for the regression NN. The decoder part of the VAE was intentionally not used because this work is not interested in the generative properties of the VAE, but rather, in its latent space representation properties. Furthermore, based on equation (6.2) and equation (6.13), the loss function of the whole model is defined as per equation (6.14). Finally, Figure 6.7 summarizes the model's architecture:

$$\mathcal{L} = \mathcal{L}_{rec} - \mathcal{L}_{KL} = \frac{1}{n}\sum_{i=1}^{n}(y_i - \hat{y}_i)^2 - KL[q_\phi(z|x) \parallel P(z)] \tag{6.14}$$

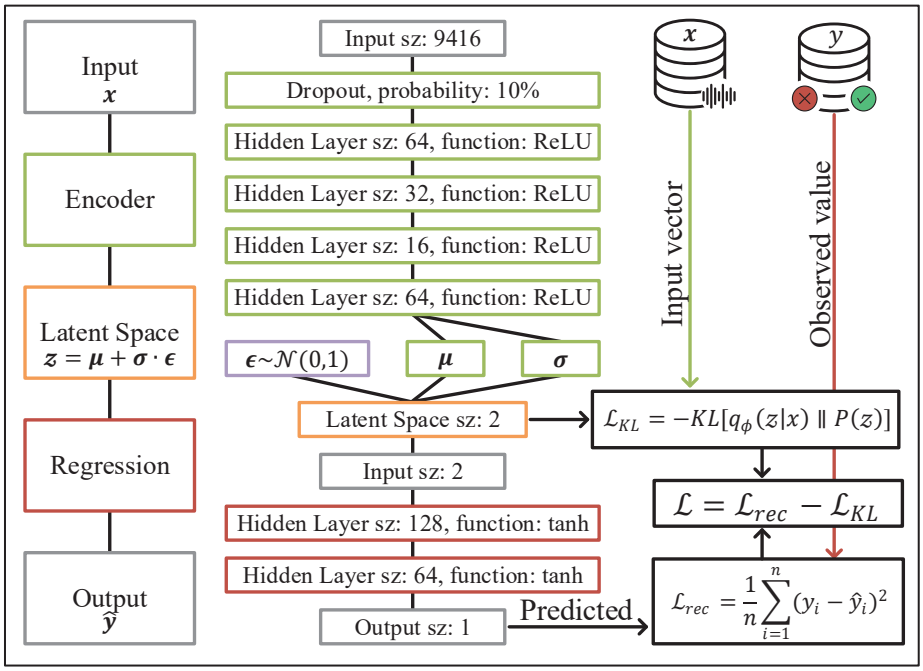

Figure 6.7 VAER architecture. NN structure visualization inspired by Hemmer et al. (2020).

6.5.2.1 Encoder Architecture

The VAE's encoder proposed architecture focuses on the dimensionality reduction capability and the ability to produce a well-regularized latent space distribution. Specifically, it is comprised of one input layer of size 9416, four hidden layers respectively of sizes 64, 32, 16, 64 and a 2D latent space layer. Each hidden layer uses the ReLU activation function.

It is also important to note that, in order to achieve a well-regularized latent distribution, the *KL* portion of equation (6.13) is used as the function for the latent space. This 2D latent space is then considered to be the output of the encoder component.

6.5.2.2 Regression Architecture

Based on the work of R. Zemouri et al. (2020) and the previous work of Proteau et al. (2020), a regression NN is directly attached to the VAE's encoder latent space output. In other words, the input vector is going through the encoder and is reduced to two dimensions ($\mathbb{R}^2$) within the latent space distribution. This 2D output vector is then fed to the regression layers as its input vector. The regression NN component's objective is then to output a GD&T quality measurement value prediction. To measure the error between the predicted and the observed values, the MSE is calculated according to the aforementioned equation (6.2).

For its structure, the regression NN is comprised of one input layer of size two, of two hidden layers respectively of sizes 128 and 64 and, finally, an output layer of size 1. The hyperbolic tangent function is used as the activation function for the two hidden layers.

6.5.2.3 Diminishing Overfitting

It is essential to include a strategy to diminish the negative effects of overfitting. Since it has been shown that the dataset used is unbalanced in terms of conforming to nonconforming workpieces cases, the authors conjecture that a strategy to prevent and reduce overfitting is necessary. Thus, based on the work of Ghojogh et Crowley (2019), Goodfellow et al. (2016) and Ying (2019), several strategies were included in the proposed architecture and training methodology to diminish the impact of overfitting on the results.

First, within the encoder's scope, the strategy was to add a dropout layer (Srivastava, Hinton, Krizhevsky, Sutskever, & Salakhutdinov, 2014) right after the input vector, with a drop probability of 10%. To further reduce overfitting, the second adopted strategy was to add an L^2 regularization to the regression hidden layers (Goodfellow et al., 2016). The third strategy applied was to include an early stop of the training process based on the loss value of the validation subset. In other words, when the validation subset calculated loss starts to increase, the training process is halted.

6.5.3 Training Methodology

As for the training methodology, the dataset was first separated into three subsets: training, validation and test. The acquisition process covered three work orders. Each of these was then assigned to the training, validation and test subsets. To approximate the manufacturing reality as much as possible, the training subset represents the first work order that was manufactured (39 samples), the second is assigned to the validation subset (51 samples) and the last is used for the test subset (76 samples). A summary of the subsets is presented below in Tableau 6.4.

Tableau 6.4 Summary of the subsets

Subset	**Training**	**Validation**	**Test**
Number of Workpieces (samples)	39	51	76
Nonconforming Samples	3 (7.7%)	3 (5.9%)	5 (6.6%)
Conforming Samples	36 (92.3%)	48 (94.1%)	71 (93.4%)

Finally, to train the model, the RMSProp algorithm was used with a maximum of 1000 training epochs.

6.6 Results and Discussion

In this section, the results are presented and discussed. The results related to the VAER model and the different calculated performance metrics are first discussed, followed by those pertaining to the VAER latent space utilization.

6.6.1 Quality Measurement Prediction

As expressed in the proposed methodology, the first objective was to demonstrate that the quality measurement value of a workpiece can be predicted based on a VAE approach. By applying the signal processing strategy to the industrial dataset explained in section 6.4.1, combined with the VAER approach, it was possible to achieve these results. First, in Figure 6.8, the predicted and observed GD&T measurements are displayed for (a) the training subset, (b) the validation subset and (c) the test subset. In that figure, the regression model,

without being perfect, is shown to be able to predict measurement values close to the observed measurement.

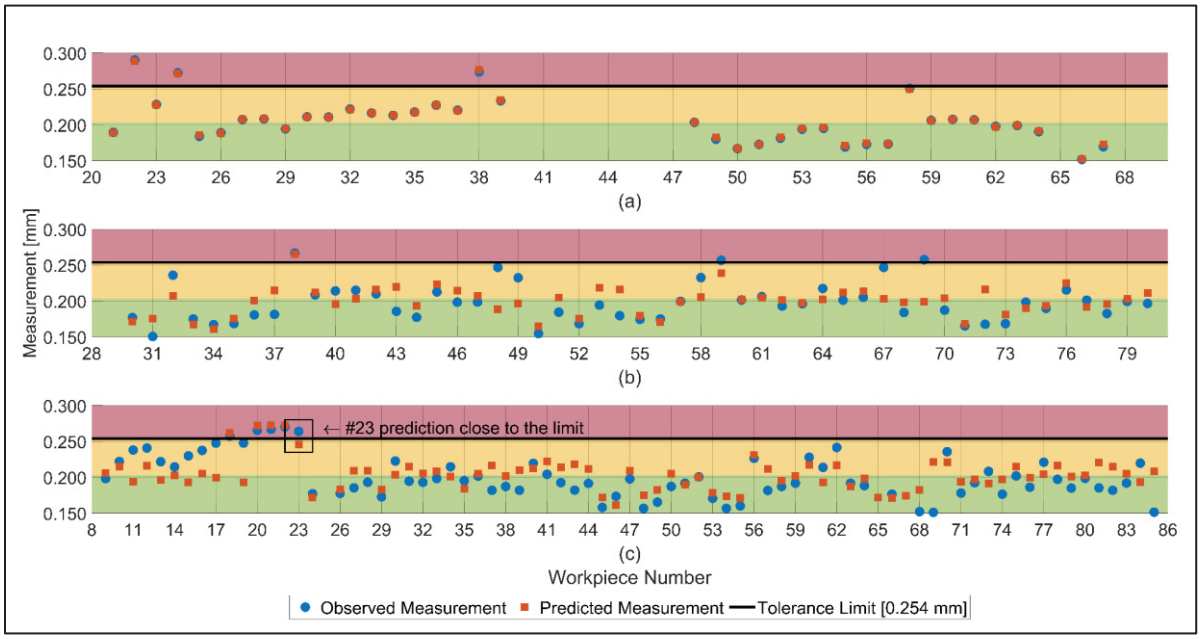

Figure 6.8 Observed and predicted quality measurements per workpiece and subset (a) training, (b) validation and (c) test

With the VAER model, an MSE of 5.2573×10^{-4} mm was achieved with the test subset. However, it is important that such a model accurately predict and detect a nonconforming workpiece, especially in an industrial context. Based on the methodology, a confusion matrix was used to classify each workpiece according to its status (conforming *vs*. nonconforming). In Figure 6.9, the confusion matrix is displayed for (a) the training subset, (b) the validation subset and (c) the test subset. From this figure, it can be seen that with this approach, it is possible to accurately predict four nonconforming workpieces out of five on the test subset. Furthermore, the model accurately predicted all 71 conforming workpieces. Having such unbalanced classes within the dataset is inherent to the nature of the industry, where a machining company cannot survive financially by producing a high number of nonconforming workpieces. Therefore, it is even more important to have an approach that can be adopted in this kind of environment. It is also interesting to note that during the experiments, a classification layer was attempted with the VAE instead of a regression one.

However, the results in that case were inconclusive, leading us to pursue the regression approach.

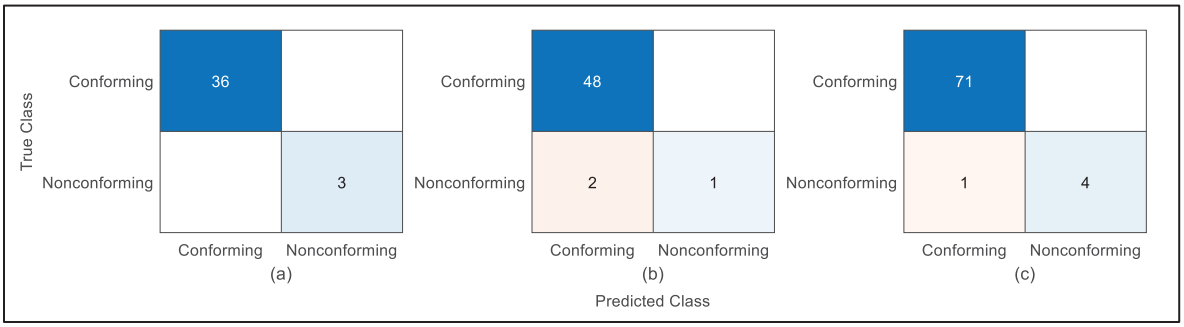

Figure 6.9 Confusion matrix of conforming vs. nonconforming prediction for all subsets (a) training, (b) validation and (c) test

In Figure 6.8, the nonconforming workpiece (#23), where the model was not able to accurately predict the measurement value ($\hat{y} = 0.2457$ mm vs. $y = 0.2639$ mm), is specifically considered, and it is agreed that the error between both values is relatively small. When the confidence interval of the prediction system ($\pm$ 0.05 mm) is factored in, it is plausible that if the model was in production at the industrial partner's, this workpiece would have been targeted as uncertain, and the system would have forced a measurement.

This confidence interval was obtained by applying a nonparametric distribution to the test subset residual error. Figure 6.10 display the results as well as the two boundary points corresponding to 95% limits of the distribution, which are equal to approximately $\pm$ 0.05 mm. This indicates that the measurement system error would not be greater than this interval 19 times out of 20. It is also shown that most residuals (~67%) span between $\pm$ 0.02 mm, which reinforces the assertion that the proposed model seems to be able to predict measurement values close to the observed measurement.

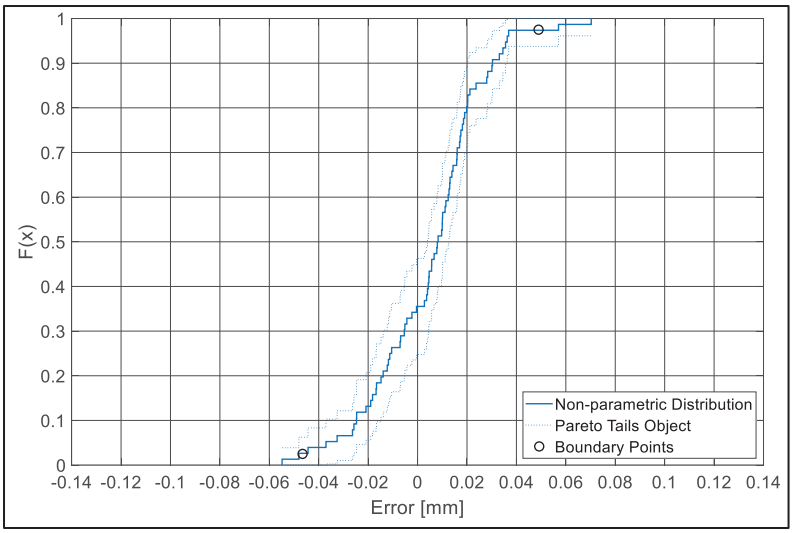

Figure 6.10 Cumulative non-parametric distribution results

To further investigate the confidence performance of the model, it was decided to train it 100 times and to measure its average MSE and its related standard deviation. This step resulted in an average MSE of 5.9434×10^{-4} mm, with a standard deviation of 5.2492×10^{-5} mm over the 100 training cycles. In addition, Figure 6.11 shows a box-and-whisker plot of the 100 training cycles for each subset. It can be seen that most of the training cycles are within the $1.5 \times$ IQR (Interquartile Range), and that only three training cycles in the training subset and one training cycle in the validation subset are out of the whisker.

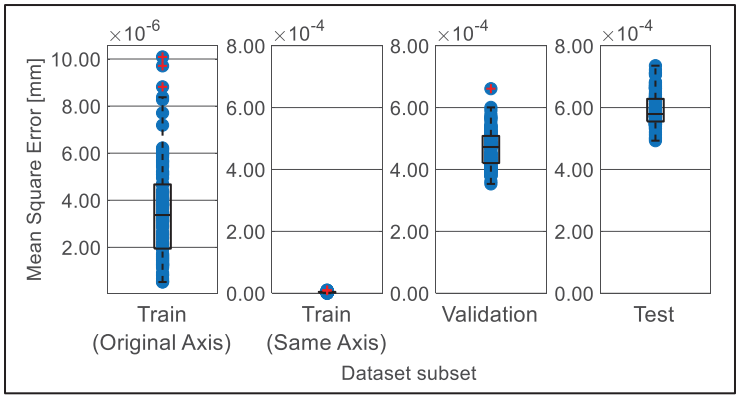

Figure 6.11 MSE per iteration for each subset

These results indicate that the VAER approach, while not perfect, can indeed predict the quality measurement values based solely on data obtained from sensors, which supports the first objective.

6.6.2 Latent Space Visualization

With respect to the second objective, which was to show that the VAER 2D latent space can accurately represent the quality level of a workpiece, the trained latent space of the model was used and its distribution examined. As a reminder to the reader, the colour underneath an element always refers to either the observed or the predicted quality measurement value: going from green (conforming) to red (nonconforming) means a decrease in the quality of the workpiece. In Figure 6.12, the latent space distribution is presented for (a) the observed measurement values and for (b) the predicted measurement values for all the subsets (training, validation and test). In Figure 6.13, the latent space distribution is shown, in more details, for (a) the training subset, (b) the validation subset and (c) the test subset. The figure indicates that each workpiece position in the latent space produced by the VAER seems to be linked to its predicted measurement ($\hat{y}$) in a sort of progression. *Progression*, here means that the quality level of a workpiece seems to worsen as it moves from right to left along the x-axis. This appears to be the pattern when the observed measurement values (y) are used for (a) the training subset, (b) the validation subset, and (c) the test subset in Figure 6.14.

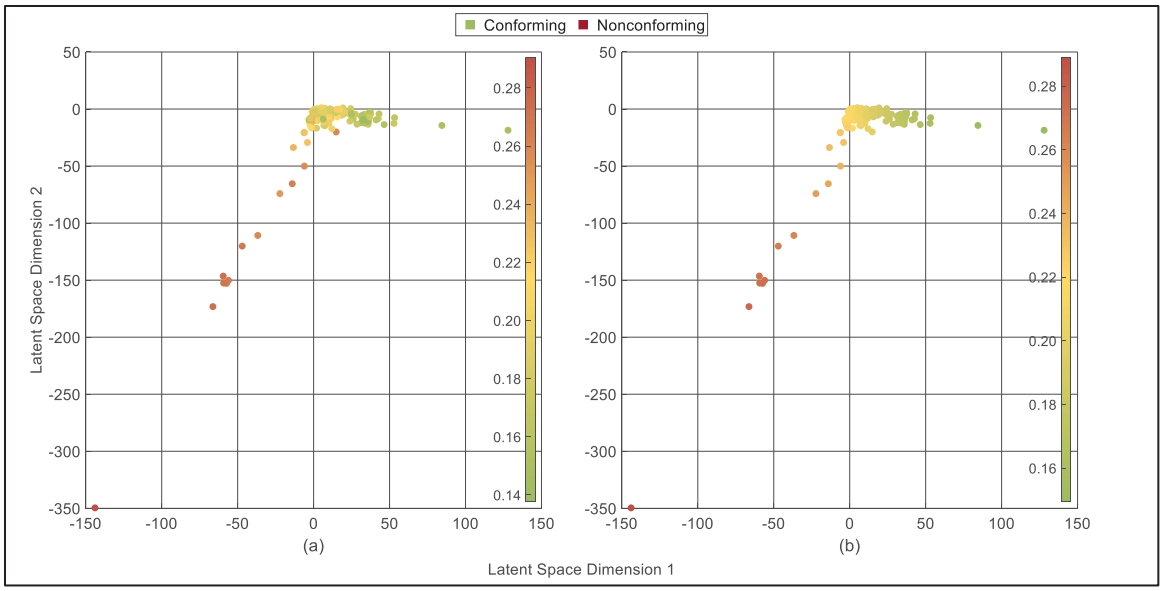

Figure 6.12 Latent space distribution for all subsets
(a) observed values and (b) predicted values

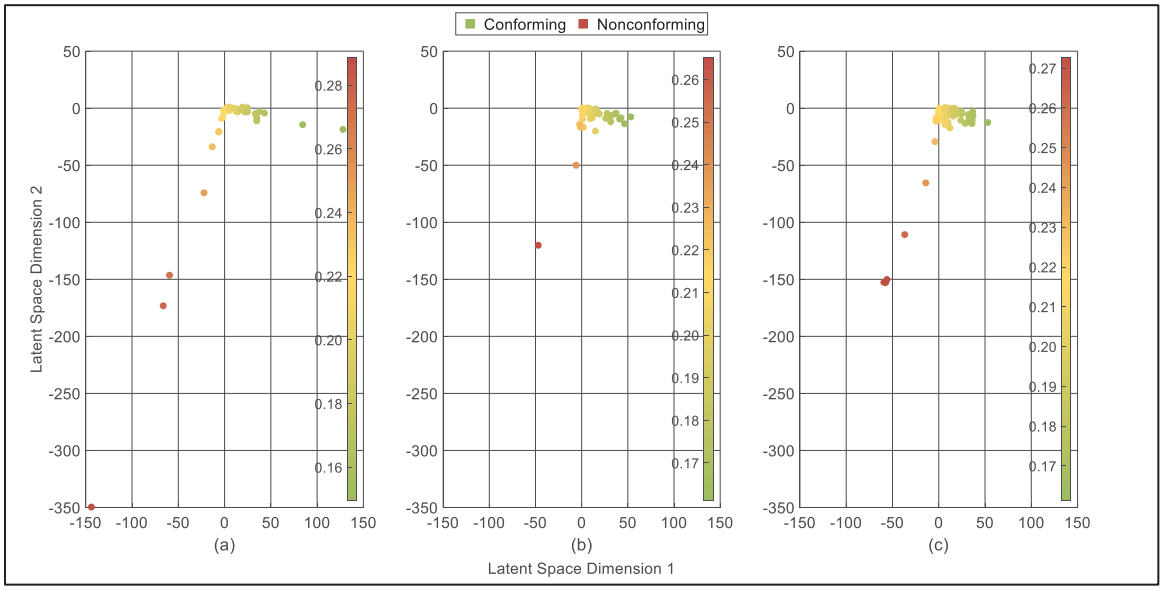

Figure 6.13 Latent space distribution for **predicted** values for all data subset
(a) training, (b) validation and (c) test

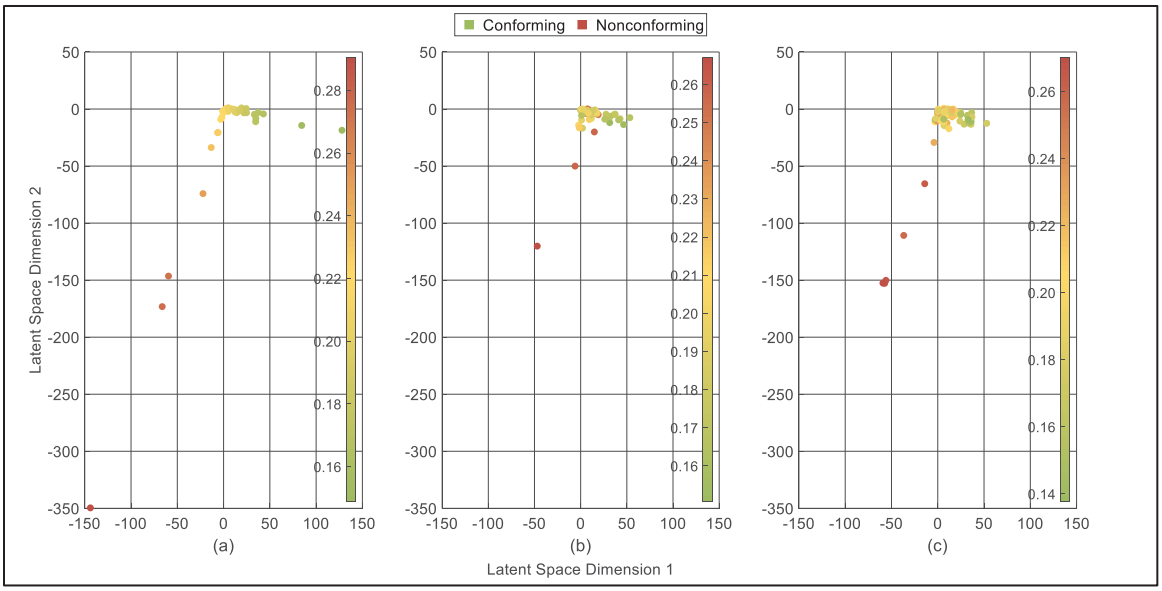

Figure 6.14 Latent space distribution for **observed** values for all data subset (a) training, (b) validation and (c) test

It is also interesting to see that the approximate area covered in the latent space of each subset for both the observed and predicted values seems to be related to the range between the maximum and minimum measurement values. For instance, the range for the training, validation and test subsets for the observed values is respectively 0.1415 mm, 0.1164 mm and 0.1323 mm, which appears to relate visually to the covered area of the distribution of the latent space for each subset in Figure 6.13 and Figure 6.14.

Furthermore, looking closely at Figure 6.14, it can be seen that there is an area around the origin where measurements seem to be *mixed up*, and tend to not follow this progression pattern. It can be conjectured that this is a transition area between conforming and soon-to-be nonconforming workpieces and that uncertainty is higher here, which could be due more to the model having difficulty interpreting the sensors' data with respect to the quality level in this area. In Figure 6.15, the transition area is zoomed in for the (a) predicted and (b) observed values of the test subset. Aside from this area, the model tends to accurately interpret highly conforming or highly nonconforming workpieces.

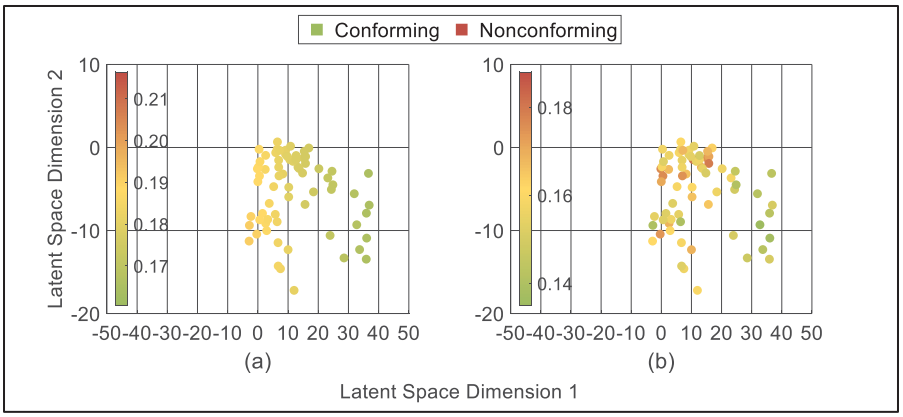

Figure 6.15 Transition area zoomed in for the test subset

To compare the VAER approach with the popular *t*-SNE method (Maaten & Hinton, 2008), the latter was applied to the training subset. Figure 6.16 shows the results of the projection in 2D with the *t*-SNE approach (the colours represent the observed measurement values in mm). In looking at the figure, it can be deduced that the clusters do not seem to be linked to the quality level of the workpieces. Hence, while the VAER approach requires a training phase, it was able to create a latent space with a distribution that represents the quality level of the workpieces. Furthermore, the trained VAER encoder can also be reused after its training, while the *t*-SNE cannot.

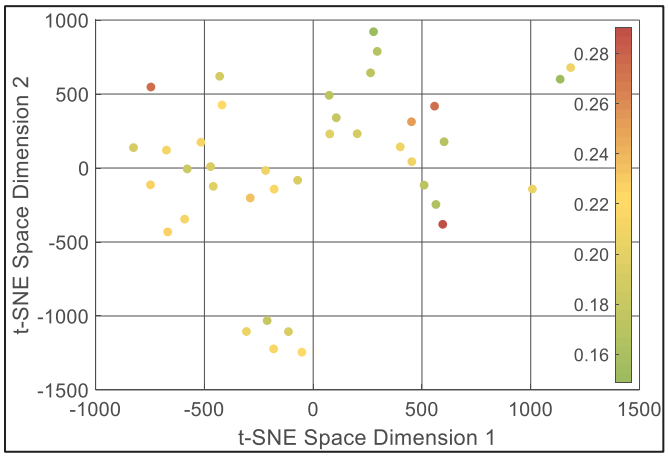

Figure 6.16 *t*-SNE projection

These results therefore strengthen the decision to use a VAE approach and the hypothesis that its trained latent space distribution is related to the workpiece quality level.

For the third objective, where a metric based on the Euclidean distance is proposed to quickly identify the quality level of a workpiece, an unsupervised *k*-means algorithm was trained to create 10 clusters based on the VAER trained latent space for the training subset. The results of this manipulation are shown in Figure 6.17. The next step was to calculate the Euclidean distances in the latent space between each VAER latent space's coordinates for the test subset and the cluster centroid of the highly conforming workpieces.

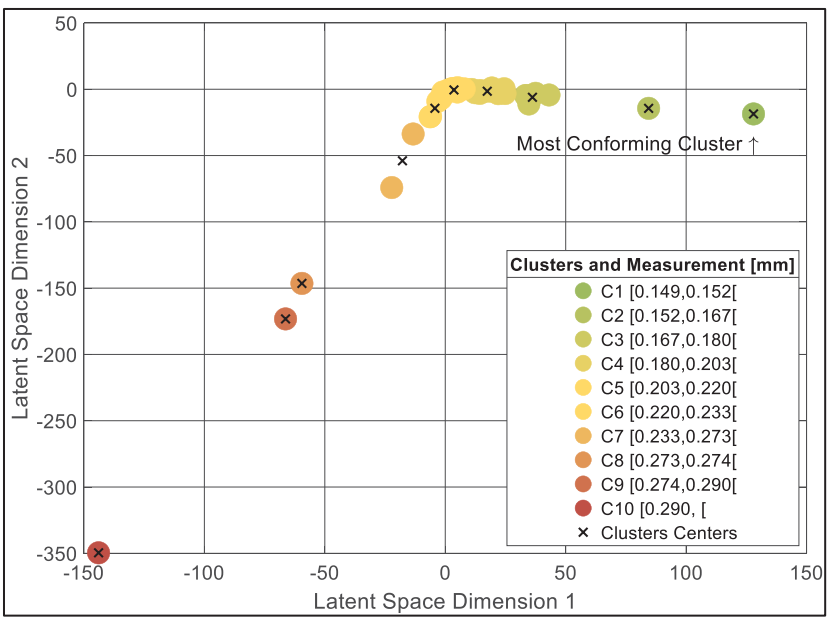

Figure 6.17 *k*-means cluster for the training subset

In Tableau 6.5 and Tableau 6.6, the results of the Pearson's and Spearman's correlation analyses between the calculated distances and the observed and predicted quality measurements values are respectively shown. A very good correlation coefficient based on the predicted measurement value and a moderate coefficient for the one based on the observed measurements can be identified. However, in both cases, the respective p-values are lower than the alpha level ($\alpha = 0.05$). It is hypothesized that the lower coefficient with the observed measurement might be due to the transition area mentioned above, where

uncertainty is higher. Figure 6.18 (a) shows the latent space distribution, while Figure 6.18 (b) shows the distribution of the Euclidean distance values and the observed measurement for the test subset. It can be seen that the highly conforming and highly nonconforming workpieces are well distributed in both Figure 6.18 (a) and Figure 6.18 (b). As conjectured above, it is indeed the transition area in the latent space that seems to diminish both the Pearson's (r) and the Spearman's (ρ) coefficients in Tableau 6.5.

Tableau 6.5 Pearson's (r) and Spearman's (ρ) correlation analysis results for the observed measurements

Subset	**Observed measurements**					
	r	C.I. [95%]	*p-value*	ρ	C.I. [95%]	*p-value*
Training	86.4%	[75.5, 92.7]	0.000	99.9%	[99.8, 100]	0.000
Test	66.8%	[52.4, 77.8]	0.000	51.7%	[31.7, 67.3]	0.000

Tableau 6.6 Pearson's (r) and Spearman's (ρ) correlation analysis results for the predicted measurements

Subset	**Predicted measurements**					
	r	C.I. [95%]	*p-value*	ρ	C.I. [95%]	*p-value*
Training	86.5%	[75.7, 92.8]	0.000	99.9%	[99.8, 100]	0.000
Test	94.3%	[91.2, 96.4]	0.000	98.7%	[97.7, 99.2]	0.000

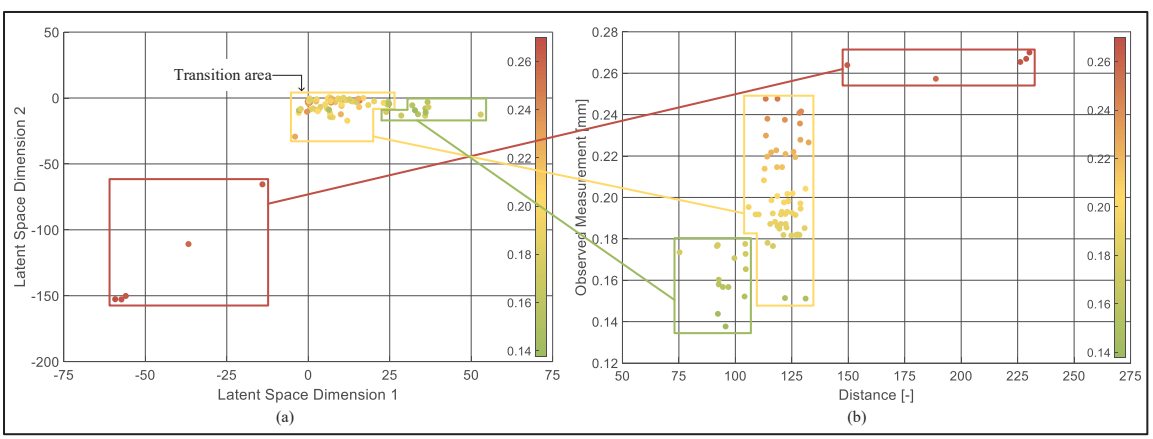

Figure 6.18 For the test subset, relationships between:
(a) the latent space distribution and (b) the metric distance distribution

6.6.3 Limitations of the Proposed Model

This section reviews and highlights some limitations of the proposed work and methodology. On the one hand, it is shown that this method is transferable to an industrial context as it uses a dataset acquired entirely in the course of the regular production activities of the industrial partner.

On the other hand, even though the results described above demonstrate the ability of this model to make a prognosis regarding the quality measurement of a workpiece, we must highlight the limitations of the proposed methodology. Firstly, due to the nature of ML in general, and of its training process in particular, the model's results are limited and dependent on the dataset used. Hence, the reader should be aware that the results are limited to the specific context in which the dataset was acquired and prepared (milling process, low cutting parameters, Inconel, etc.). The authors do not claim to propose a general prognostic model, but they are confident enough to posit the hypothesis that this same methodology applied to an extended and increased dataset (different cutting parameters, different materials, different machining processes, different GD&T specifications, etc.) could produce similar results. However, future work would be needed before claiming such contributions.

Secondly, another possible limitation of this work that must be taken into account is the extensibility of the model to predict, within the dataset used, a different set of measurement values related to a GD&T specification different from the one used in this work (specification #31). Similar to the previous limitation, the nature of the ML training process makes it dependent on the training examples. That is why future work should include working toward a general model or a framework that could be used to predict multiple GD&T specifications types.

Nevertheless, it is known that Inconel and other nickel-based alloys, on which this study is based, are hard-to-machine alloys and not necessarily deterministic between each material lot (E. Liu, An, Xu, & Zhang, 2020; Saleem & Mumtaz, 2020; Yin, Liu, Wang, Song, & Cai,

2020). The ability to provide a visual tool based on the latent space of the proposed methodology provides an opportunity for the industry to better monitor and follow production processes based on the milling of a nickel-based alloy. In addition to being able to benefit from this visual capability of the proposed framework, the ability to predict the quality measurement of a workpiece provides another opportunity for a machining company to be more proactive in the control and monitoring of its production processes. Hard-to-machine alloys can create situations in which degradation occurs faster than expected because the quality control sampling intervals are often based on statistical evaluations not on the dynamics of the actual production process. Therefore, both the visual and prognostic capabilities of the proposed approach provide an opportunity for the machining industry to become more proactive.

6.7 Conclusion

In this paper, the application of a VAER approach to a machining context was explored. The method was used to predict the GD&T quality measurement values of workpieces. It was shown to be capable of predicting measurement values based solely on data from sensors with an MSE of 5.2573×10^{-4} mm on the test subset, and that the average MSE was 5.9434×10^{-4} mm for 100 training cycles. Furthermore, the investigation showed the confidence interval of the model to be ± 0.05 mm 19 times out of 20. It was also demonstrated that the 2D latent space is distributed according to the quality level of each workpiece. In this context, this space also behaved better than in the *t*-SNE approach. Additionally, the proposed metrics based on the 2D latent space and the Euclidean distance were shown to be correlated to the observed and predicted measurement values, thus providing a quick way to estimate the quality level of a machining process.

Nevertheless, the model's results were not perfect, and the limitations of the proposed work were highlighted. For instance, uncertainty appeared to be higher in a certain area in the results. To help improve these results, it is suggested that further work include the acquisition of more data, and if possible, specifically more data related to nonconforming workpieces. In

order to improve the distribution of the data in the transition zone, adding one or more types of sensors (e.g., acoustic emission) could help by adding another dimension to the input vector. To improve the distance metric, it is also recommended to try using a curvilinear distance instead of a Euclidean distance. The curvilinear distance value between the cluster centroid and a new data point should be more accurate since it would work its way through all clusters, which could better represent the degradation process a workpiece would go through. It is also suggested to consider the use of a generative adversarial network approach to the VAER model to see if it could improve the capacity of the model to better predict the quality measurement. Additionally, it is proposed to explore if there is a relationship between the *k*-means clusters and the input vector features. This could be helpful to better understand the relationship between the machining process and its impact on workpiece quality. To increase the transferability and diminish the limitations of this study, it is advised that future work include applying this methodology to different types of GD&T from the one used here. This could increase the ability to propose a more general approach or framework for the prognostics of the quality measurements values. An increase in the use and sharing of industrial datasets is also advised in order to improve the technology transfer to the industry. It is also recommended to extend the dataset to include more training cases belonging to different machining contexts (different raw materials, cutting parameters, processes, etc.).

Notwithstanding these shortcomings, it was demonstrated, with the current state of this research, that not only is it possible to monitor and predict the quality measurement value of a workpiece, but that it is also possible to do so with only two types of sensors (vibration and current consumption), which can be easily mounted on a machine at low cost. It is also interesting to see that this was achieved without measuring the cutting forces with a dynamometer, which according to research such as that of Abellan-Nebot et Romero Subirón (2010), is best used to describe the cutting process. This work was performed in an industrial context, which increases the probability of technology transfer to industry. Finally, even in its current state, the work described could still help a machining company better control its production through visual support, thus increasing productivity while decreasing unexpected process degradation.

6.8 Acknowledgement

The authors would like to thank APN Inc. and their employees for the knowledge and the data shared in this project. We would also like to acknowledge the financial support of the *Fonds de Recherche du Québec – Nature et Technologies* to this project through Grant #257668. In addition, this research was enabled in part by the support provided by *Calcul Québec* (www.calculquebec.ca) and Compute Canada (www.computecanada.ca).

CONCLUSION GÉNÉRALE

Les travaux entrepris dans le cadre de cette thèse portent sur le développement d'un modèle de pronostic de la qualité d'un produit usiné et ce, basé sur une approche par apprentissage machine. Nous avons soulevé en introduction l'importance pour l'économie mondiale de l'industrie manufacturière et plus précisément du secteur de l'usinage par retrait de matériau. Bien que d'une importance capitale pour l'économie et les chaînes logistiques mondiales, cette industrie est sans cesse en proie à diverses pressions comme la mondialisation, l'augmentation des requis de la qualité ou les demandes de réductions des coûts.

Pour pallier aux effets de certaines de ces pressions, dans le cadre de cette thèse, nous nous sommes donc questionnés sur la faisabilité d'un système de surveillance du procédé de fabrication basé seulement sur les données de capteurs installés à même l'équipement de fabrication. Plus précisément, nous avons émis trois questions de recherche :

1) Est-ce possible de déterminer un ou plusieurs descripteurs issus des capteurs de la machine-outil CNC et qui sont fortement reliés à la dégradation du processus de fabrication (niveau de qualité)?
2) Est-ce qu'il existe un lien causal entre les signaux des phénomènes physiques à l'œuvre durant l'usinage d'un produit et les données d'inspection (GD&T et rugosité) de celui-ci? Si oui, quels sont les meilleurs descripteurs? Et quelle est la méthode de surveillance la mieux adaptée à ce cas?
3) Est-ce possible de fournir un support permettant de suivre visuellement, d'une manière conviviale et adaptée pour un usage industriel, la dégradation (ou l'évolution) du processus de fabrication et donc, de la conformité du produit?

Ces trois questions nous ont permis de nous fixer quatre objectifs devant être atteints :

1) Proposer une méthodologie d'acquisition et de traitement des données pour le suivi et la surveillance d'un processus d'usinage sur une machine-outil CNC. Autant que possible, le formalisme doit intégrer la consolidation des variables sur des bases liées à la physique des phénomènes en cours (ex. : concept d'énergie spécifique, ergodicité des signaux,

etc.), le prétraitement (ex. : filtrage) et les processus de traitement des signaux à l'aide des outils, techniques ou méthodes inspirées par l'état de l'art;

2) Déterminer et proposer un ou plusieurs descripteurs fortement corrélés à la dégradation du processus de fabrication (et par conséquent à l'état de conformité des produits usinés);
3) Proposer une méthodologie basée sur l'apprentissage machine pour démontrer qu'il est possible de réaliser le pronostic de la conformité d'un produit en se basant uniquement sur la captation des phénomènes physiques durant le processus d'usinage (captation des paramètres du procédé et non pas des mesures sur des produits);
4) Fournir pour un usage industriel un support visuel facilitant le diagnostic et le pronostic rapides de l'état du processus de fabrication.

En relation avec notre premier objectif, nous avons proposé et implanté un système d'acquisition de données sur une machine-outil CNC chez un partenaire industriel. Les données acquises via des capteurs ont été mises en relation avec les données opérationnelles et les données de métrologie du partenaire permettant ainsi le développement d'un jeu de donnée. Ce jeu de données industriel d'une grosseur de plus de 2TB représente plus de 600 heures de fabrication et des dizaines d'outils et d'opérations de coupe différentes. Sur la base de celui-ci, nous avons été en mesure de répondre à notre premier objectif et donc, de permettre à ce projet de recherche de s'articuler.

Notre deuxième objectif de recherche a pu être atteint par notre proposition d'un descripteur physique basé sur le concept d'énergie spécifique de coupe. Ce concept, basé sur les travaux de Debongnie (2006), nous permet donc de quantifier l'énergie nécessaire à l'enlèvement d'1 cm^3 de matière. Nos résultats ont démontré que celui-ci est fortement corrélé (> 90%) à l'usure d'un outil de coupe et donc, à l'évolution du processus de fabrication. Nous avons également établi que ce descripteur fourni un apport significatif à notre approche de modélisation par apprentissage machine (performance augmentée de 14.67%).

L'atteinte de cet objectif nous permet donc de conclure que nous sommes en mesure de répondre à la première question de recherche posée dans le cadre de cette thèse. Sur la base

de notre hypothèse que la dégradation de l'outil de coupe engendre la majorité de la dégradation du processus de fabrication, notre proposition de descripteur basée sur l'énergie spécifique de coupe permet de suivre et quantifier adéquatement l'évolution de l'usure d'un outil de coupe et donc, du processus. De plus, cette conclusion est également en adéquation avec les travaux d'auteurs comme Agrawal et al. (2020), Z. Zhu et al. (2019) et Shen et al. (2018) qui supportent qu'une définition physique sur la base du concept de l'énergie fournit une approche adéquate pour modéliser un processus de fabrication.

Notre exercice de modélisation par apprentissage machine a permis de développer un modèle de pronostic de la qualité d'un produit usiné basé sur une architecture de type VAE. Notre troisième objectif a pu être atteint grâce aux résultats de notre modèle de pronostic : une faible erreur de prédiction MSE de 5.2573×10^{-4} mm, un intervalle de confiance de ± 0.05 mm, ainsi qu'une capacité à prédire adéquatement les produits avec des mesures non conformes par rapport aux mesures conformes. De plus, nous soutenons qu'il est possible d'atteindre ces résultats en utilisant seulement les données provenant de deux types de capteurs : un accéléromètre et un capteur de consommation de courant. De surcroît, ce choix de capteurs rend notre méthodologie d'autant plus abordable du fait que ces deux types de capteurs soient des technologies matures, abordables et puissent être aisément installées de manière non intrusive sur un équipement de production.

Les résultats du modèle de pronostic supportent et répondent aussi à notre deuxième question de recherche puisqu'il est non seulement possible de faire le pronostic de la qualité d'un produit usiné en termes du respect de celui-ci par rapport à ses requis GD&T, mais que cette prédiction peut se faire sur la base seule de données provenant de capteurs de vibration et de consommation de courant. Ce lien de causalité entre données des phénomènes physiques et niveau de qualité ne semble pas être linéaire comme démontré à l'ANNEXE I ce qui supporte notre hypothèse et notre approche qu'une modélisation par apprentissage machine soit adéquate dans ce contexte. Nos travaux permettent donc de supporter la direction et les conclusions d'auteurs comme J. Lee et al. (2013), Voisin et al. (2018) et de Papananias et al. (2019).

Dans notre processus de modélisation, nous avons également fait le choix d'utiliser un espace latent à deux dimensions afin d'explorer l'utilisation d'un support visuel pour faire la surveillance et le diagnostic rapide du processus de fabrication. Nous avons démontré que la distribution de cet espace latent, lorsque combinée à une approche de régression supervisée, est fortement reliée au niveau de qualité. De plus, en se basant sur cette distribution et le concept de distance euclidienne, nous avons proposé une métrique permettant d'estimer rapidement le niveau de qualité d'un produit. Cette métrique s'est également avérée être en corrélation quant au niveau de qualité autant avec les valeurs observées (r = 66.8%) qu'avec les valeurs prédites de la qualité (r = 94.3%). Ces résultats nous ont donc permis d'atteindre le quatrième objectif de cette thèse.

Les choix faits tout au long de nos travaux ont également permis que cette modélisation par apprentissage machine ne soit pas une boîte noire. En effet, comme mentionné ci-haut par l'utilisation d'une architecture de type VAE et d'un espace latent, il est possible d'obtenir un support visuel. Ceci nous permet donc de répondre à notre troisième et dernière question de recherche. En plus de fournir un support intéressant et utile pour faire la surveillance rapide de processus de fabrication, nous conjecturons que cette approche permettra de faciliter l'acceptabilité sociale de celle-ci pour la mise en production de ces travaux sur un plancher de production. En effet, « l'explicabilité » de ce type de système devient de plus en plus important pour faciliter leur implantation et leur utilisation. C'est pourquoi des auteurs comme Ribeiro et al. (2016) proposent des méthodologies afin d'expliquer le comportement et la logique derrière les prédictions des systèmes basés sur l'intelligence artificielle. Sans pour autant fournir une explication, le support visuel créé par notre proposition vient tout de même, selon nous, diminuer l'effet boîte noire.

L'atteinte de chacun de nos objectifs de recherche a permis de fournir une réponse à chacune de nos questions de recherche. Nous résumons donc nos contributions significatives à notre domaine d'intérêt ci-dessous :

1) Nous avons proposé une architecture et un processus d'acquisition de données permettant de faire l'acquisition de données issues de capteurs à même la machine-outil CNC tout en

contextualisant ces données physiques avec les données opérationnelles et les données de métrologie;

2) Cette acquisition a été faite dans un contexte industriel facilitant ainsi le transfert technologique de nos conclusions;
3) Nous avons proposé une stratégie de consolidations des signaux sous une base physique et statistique en plus de proposer un descripteur physique fondé sur le concept de l'énergie spécifique de coupe;
4) Nous avons démontré que ce dernier est fortement corrélé à l'usure d'un outil de coupe;
5) Nous avons démontré qu'il était possible d'utiliser un VAE afin de diminuer la dimensionnalité de notre jeu de données à deux dimensions;
6) Nous avons démontré que ces deux dimensions sont suffisantes pour prédire les types d'opérations de coupe lorsque combinées à un classificateur;
7) Nous avons démontré qu'il était possible avec cette même approche de prédire les mesures de la qualité d'un produit usiné;
8) Nous avons démontré que l'espace latent de deux dimensions permettait de visualiser la distribution des données et que cette distribution reflète le niveau de qualité d'un produit;
9) Nous avons proposé une nouvelle métrique basée sur cet espace latent et sur le concept de distance euclidienne et établi que celle-ci était corrélée au niveau de qualité;
10) Finalement, ces contributions ont été matérialisées par la soumission et la publication de nos travaux dans un article de conférence et trois articles de journaux avec comité de révision. Dans l'ordre chronologique :
    a) Proteau, A., Tahan, A., & Thomas, M. (2019). Specific cutting energy: a physical measurement for representing tool wear. The International Journal of Advanced Manufacturing Technology, 103(1), 1-10.
    b) Proteau, A., Tahan, A. S., & Thomas, M. (2019). Toward the quality prognostic of an aircraft engine workpiece in Inconel Alloy 625: case study and proposed system architecture. Dans Surveillance, Vishno and AVE conferences.
    c) Proteau, A., Zemouri, R., Tahan, A., & Thomas, M. (2020). Dimension reduction and 2D-visualization for early change of state detection in a machining process with a

variational autoencoder approach. The International Journal of Advanced Manufacturing Technology, 111(11), 3597-3611.

d) Proteau, A., Tahan, A., Zemouri, R., & Thomas, M. (2021). Predicting the quality of a machined workpiece with a variational autoencoder approach. Soumis à Journal of Intelligent Manufacturing, décembre 2020.

Pour conclure, malgré nos contributions et l'atteinte de nos objectifs, nous avons, aux sections 4.8, 5.7 et 6.7, soulevé certaines limitations de nos travaux. En effet, notre modélisation n'étant qu'une approximation de la réalité de ces phénomènes, des erreurs persistent et provoquent des prédictions imprécises. Néanmoins, les systèmes de mesure déjà établis en industrie (comme les CMM) sont également imparfaits et présentent des limitations avec lesquelles les entreprises manufacturières doivent toujours composer aujourd'hui. Nos conclusions étant basées sur des données industrielles, à défaut des autres travaux recensés dans cette thèse, faciliteront donc un transfert technologique vers l'industrie. Ce faisant, malgré les limitations de nos travaux, nos résultats permettent de répondre adéquatement à notre problématique et fournissent donc un point de départ pour la mise en place de méthode de mesures alternatives permettant de tirer profit des plus récentes avancées technologiques et ainsi aider les entreprises manufacturières à améliorer leur qualité et leur productivité. Toute conclusion n'étant que le point de départ pour de nouveaux travaux, la section suivante présente une série de recommandations pour quiconque désirerait construire sur les fondements que nous venons aujourd'hui de poser.

RECOMMANDATIONS

Nous avons conclu au chapitre précédent que nous avons été en mesure d'atteindre nos objectifs et de répondre à notre problématique. Malgré tout, nous avons aussi soulevé que le modèle proposé n'est pas parfait et présente certaines lacunes. Ce faisant et dans le but d'améliorer celui-ci, cette section vise à fournir un point de départ pour quiconque désirerait poursuivre les travaux entrepris dans cette thèse.

Comme première avenue, nous avons mis en évidence à la section 6.6.2 la présence d'une zone d'incertitude où le modèle semble avoir plus de difficulté à ordonner les données en fonction du niveau de qualité. Nous proposons donc trois directions qui, selon nous, pourraient aider à amener de la clarté dans cette zone et ainsi augmenter les performances du modèle. Premièrement, nous suggérons l'ajout d'un autre type de capteur. Plusieurs auteurs comme Abellan-Nebot et Romero Subirón (2010) font la promotion de l'utilisation d'une table dynamométrique pour mesurer les efforts de coupe. Ce type de capteur reste néanmoins plus intrusif et dispendieux pour un industriel. Nous suggérons donc, comme premier ajout, l'utilisation d'un capteur d'émission acoustique. Ce type de capteur permettrait de couvrir une plage de fréquences qui n'est pas encore couverte par notre système d'acquisition (i.e. MHz). De plus, il est connu que ce type de capteur peut être utilisé pour la détection des plus petits défauts comme les microfissures. Ce faisant, nous conjecturons que cette information pourrait aider à procurer une nouvelle dimension à notre jeu de données et ainsi potentiellement aider le modèle à augmenter ses performances et améliorer la distribution de l'espace latent.

Nous suggérons également l'acquisition de plus de données. En termes de quantité, nous avons démontré que le jeu de données proposé comporte suffisamment de données pour obtenir des résultats intéressants. Néanmoins, nous avons également mis en lumière à la section 6.4.1 qu'il existe un ratio inégal entre le nombre de produits conformes et le nombre de produits non conformes. Acquérir davantage de données non conformes permettrait de rétablir un ratio plus égal et ainsi aider le modèle de pronostic à mieux détecter les

phénomènes menant à un produit non-conforme. Cependant, nous devons émettre deux mises en garde pour cette recommandation : premièrement, il est normal, dans un contexte industriel, que ce ratio soit inégal puisqu'il est improbable qu'une entreprise manufacturière soit performante si elle fabrique autant de produits conformes que de produits non conformes. Il faudra donc tout de même que le modèle soit en mesure de composer avec un ratio inégal. Deuxièmement, obtenir un ratio égal dans un contexte industriel requière un investissement financier de la part de l'industriel, puisqu'il devra volontairement laisser dévier son processus pour que celui-ci produise des produits non conformes. Il n'en reste pas moins que d'un point de vue académique, c'est une avenue intéressante afin de capter correctement ces données pour permettre de futures améliorations au modèle de pronostic.

En ce qui a trait à la généralisation de nos résultats, nous avons mentionné à la section 6.4.1 que, comme point de départ, nous allions nous concentrer sur la spécification #31 qui est un requis de déviation du profil d'une surface. Cependant, il existe plusieurs autres types de GD&T : positionnement, diamètre, planéité, parallélisme, etc. Par conséquent, pour augmenter la validation et la généralisation de nos travaux, nous suggérons d'appliquer cette même méthodologie, mais au pronostic d'autres types de GD&T. Le jeu de données acquis contient d'ailleurs d'autres types de requis, ce qui en fait un bon point de départ. Il sera également intéressant de valider si un même modèle peut prédire plusieurs types de requis GD&T ou bien un système de pronostic « complet » nécessiterait la génération et l'apprentissage d'un modèle par type. À ce niveau, le lecteur intéressé à cette avenue pourrait également explorer les concepts « d'apprentissage par transfert ». Un point de départ pourrait être la lecture de Goodfellow et al. (2016) (section 15.2) et Zhuang et al. (2021).

Dans le même ordre d'idées, afin de mieux comprendre les phénomènes d'usinage et de généraliser nos résultats, nous suggérons d'appliquer cette même méthodologie à d'autres produits. Dans le cadre de cette thèse, nous nous sommes concentrés sur un produit relativement petit et usiné à partir d'un alliage de nickel. Obtiendrions-nous des résultats similaires avec un produit de dimensions ou géométries différentes fait à partir d'un alliage

différent (aluminium, acier inoxydable, etc.)? Répondre à cette question passe invariablement par l'acquisition de données reflétant ces différences.

De plus, tel qu'illustré à la section 3.4.1, notre banc de test spécifique était un centre d'usinage. Nos résultats sont donc fondés sur le pronostic de la qualité dans un contexte de fraisage. Toujours dans l'optique de généraliser nos résultats et notre méthodologie, il devient intéressant et important de vérifier si nos conclusions sont transférables à un autre contexte d'usinage tel que le tournage ou la rectification. Très rependu, le cas du tournage devient un point de départ intéressant, d'autant plus qu'il présente certaines différences avec le fraisage. Par exemple, le partenaire industriel possède des équipements de tournage multiaxes pouvant exécuter plusieurs opérations d'usinage en même temps. L'instrumentation de ce type d'équipement présente donc, selon nous, des défis différents et donc un point de départ pour l'application de notre méthodologie à ce contexte différent.

Toujours dans le but de généraliser nos conclusions et d'augmenter la validation externe, il serait intéressant d'appliquer cette même méthodologie, mais chez un autre partenaire qu'APN. Il est connu que chaque entreprise possède ses propres méthodes et stratégies d'usinage. Il serait donc intéressant de comparer les résultats obtenus avec les données d'APN versus les résultats chez un autre partenaire. Des résultats positifs dans un cas externe à celui-ci augmenteraient indubitablement la validation externe et les possibilités d'un transfert technologique vers l'industrie. Ces tests chez un autre partenaire pourraient également permettre de mettre en évidence des lacunes du modèle ou de notre méthodologie qui n'auraient pas pu être mises en lumière dans le cadre spécifique de ce projet.

Notre proposition d'une métrique basée sur l'espace latent et le concept de distance euclidienne a mis en évidence le lien entre la distribution des données et les différents groupes créés. Afin d'augmenter notre compréhension de l'impact des phénomènes d'usinages sur la qualité du produit, il serait également intéressant d'explorer s'il existe un lien entre les groupes créés dans l'espace latent et les différents descripteurs utilisés. Une forte corrélation entre l'évolution des groupes et l'évolution des descripteurs permettrait

sûrement de mieux comprendre la relation entre les phénomènes d'usinage et le niveau de qualité. Un point de départ à ce niveau serait la mise en relation des descripteurs obtenus suite à l'application de notre stratégie de consolidation des signaux avec les différents groupes de l'espace latent. Malheureusement, dû à des contraintes logistiques et temporelles, nous n'avons pas pu mener à bien cette analyse.

Dans le cadre de ce projet, nous avons utilisé des métriques de performance bien établies comme le MSE. Par contre, plusieurs auteurs comme Goebel, Saxena, Saha, Saha, et Celaya (2011) ou Saxena, Celaya, Saha, Saha, et Goebel (2010) proposent une revue des différentes métriques de performance pour les modèles de pronostic, ainsi qu'un cadre d'application. Il devient donc intéressant d'établir une définition plus large de la performance du modèle de pronostic que celle présentée dans ce projet. L'application de certaines des recommandations pourrait probablement mener à mettre de l'avant certaines faiblesses de notre proposition et ainsi donner une direction aux améliorations possibles.

Pour terminer, nous avons pu démontrer que la proposition faite dans ce projet de thèse permet de faire le pronostic de la qualité d'un produit usiné grâce à une approche par apprentissage machine de type VAE. Malgré les résultats positifs et nos contributions, cette section a levé le voile sur plusieurs avenues d'améliorations qui permettraient de répondre à certaines questions toujours en suspens : est-ce que les résultats du modèle sont généralisables à d'autres types de requis GD&T? À d'autres types de produits et/ou de procédés? Pouvons-nous transférer nos résultats à un autre partenaire industriel que celui de ce projet? Existe-t-il un lien entre les groupes créés dans l'espace latent et les descripteurs proposés? Serions-nous en mesure de faciliter la généralisation de nos résultats grâce à une approche d'apprentissage par transfert? Bien que ces questions soient toujours irrésolues, l'approche proposée dans cette thèse permet déjà de fournir un point de départ, ainsi que des outils concrets pouvant aider les entreprises manufacturières à faire face au contexte socio-économique mondial d'aujourd'hui et de demain. Finalement, nous espérons que les propositions d'améliorations énumérées et décrites à cette section permettront de fournir un

point de départ à quiconque voudrait faire progresser le domaine du pronostic et ainsi contribuer au cheminement des travaux présentés dans le cadre de cette thèse.

ANNEXE I

TOWARD THE QUALITY PROGNOSTIC OF AN AIRCRAFT ENGINE WORKPIECE IN INCONEL ALLOY 625: CASE STUDY AND PROPOSED SYSTEM ARCHITECTURE

Antoine Proteau[a], Marc Thomas[a], Antoine Tahan[a]

[a]Département de génie mécanique, École de technologie supérieure, Montréal, Qc, H3C 1K3, Canada

Article publié dans « Surveillance, Vishno and AVE conferences », juillet 2019

Publication originale disponible à: https://hal.archives-ouvertes.fr/hal-02188568/

Abstract

Manufacturing companies are under a constant pressure due to multiple factors: new competition, disruptive innovations, cost reduction request, etc. To survive, they must strive to innovate and adapt their business model to improve their productivity. Recent developments based on the concept of Industry 4.0 such as big data, new communication protocols and artificial intelligence provide several new avenues to explore. In the specific context of machining, we are working toward the development of a system capable of making the prognostic of the quality (in terms of dimensional conformance) of a workpiece in real time while it is being manufactured. The goal of this paper is to showcase a prototype of the data acquisition aspect of this system and a case study presenting our first results. This case study has been conducted at our industrial partner facility (Quebec, Canada) and is based on the manufacturing of an aircraft component made from Inconel alloy 625 (AMS5666). The proposed prototype is a data acquisition system installed on a 5 axis CNC machines (GROB model G352) used to acquire and to contextualize the vibration signal obtained from the CNC machine sensor. The contextualization of the data is a key component for future work regarding the development of a prognostic system based on supervised machine learning algorithms. In the end, this paper depicts the system architecture as well as its interactions between the multiple systems and software already in place at our industrial partner. This paper also shows preliminary results describing the relationship

between the workpiece quality (in terms of respect toward the dimensional requirements) and the extracted features from the sensors signals. We conclude that it is now possible to do the diagnostic of a cutting operation. Additionally, with the same information we show that it is possible to quickly do the general diagnostic of the health state of the machine. Future work regarding this project will include data acquisition from a wider range of products (i.e. different shapes, materials, processes, etc.) and the development of a machine learning based prognostic model.

1 Introduction

Fuelled by the rapid evolution and introduction of new technologies and new philosophies such as Industry 4.0, the manufacturing industry is quickly transforming. This new manufacturing era brings a lot of possibilities to an industry that is under constant pressure for cost reduction and better quality caused by a global competition (Kohler & Weisz, 2016). In the specific context of machining; automation and methodologies such as lean manufacturing were the go to solutions to decrease process cost and improve quality output. However, in this new age, possibilities brought by artificial intelligence, more affordable technologies such as sensing technologies and collaborative robotic offer new improvements directions.

In this context, the objective of our research project is to see if we can connect the operational information of a machining process to the physical phenomenon happening during the machining of a workpiece on a CNC machine in order to be able to predict the quality of this workpiece in real-time. Thus, the objective of this paper is to propose a data acquisition system architecture based on the prototype we built, showcase that it is now possible to do the diagnostics of a cutting operation with this system and that we are now able to put in relationship the quality, in terms of the conformity towards a workpiece's G&DT specifications, and the physical phenomenon happening during the machining process.

In a general manufacturing context, attempts have been made to try to predict the quality of a production process. For instance, D. Wang (2011) tried to predict the quality of a chemical batch process operation. However, their results are based on simulated data and not industrial data such as what we propose. Closer to the machining industry, through our exploration of the literature we have not yet found authors who have proposed a methodology to predict the quality of a whole machining process and the produced workpiece. Nevertheless, we can find articles related to the prognostic of some aspect of a machining process such as predicting the surface roughness. In that context, Benardos et Vosniakos (2003) propose a review of the works that have been done in that domain and more recently, Balamurugamohanraj, Vijaiyendiran, Mohanaraman, et Sugumaran (2016) used a machine learning approach and data from an accelerometer to predict the surface roughness in terms of its Ra value.

Even though we have not found many publications with industrial application of prognostic methodology related to the quality of a workpiece, we clearly see an interest for the concept of prognostic in the manufacturing industry. Reviews and publications by authors such as Vogl et al. (2016), K.-S. Wang (2013), J. Lee et al. (2017); Peng et al. (2010) are all dedicated to the state of the prognostic concept or the proposal of a framework related to manufacturing. Thus, we are not the only one with interest in applying these concepts to a manufacturing context. Still, one of the biggest challenge to the industrial application of such concept and the development of prognostic methodologies is the access to data of good quality and in sufficient quantity. The foremost challenge is addressed in this article.

We also see that, in our research domain, the interest related to applying prognostic methodologies is strong in fields related to tool wear prediction and condition-based maintenance. For instance, Proteau et al. (2019a) showed that it is possible to predict the tool wear with a Long Short-Term Memory (LSTM) neural network. Balan et Epureanu (2008a, 2008b) and Aghazadeh et al. (2018a) also proposed different methodologies based on artificial intelligence approaches to monitor and predict the cutting tool condition. Related to condition-based maintenance, Waqar et Demetgul (2016) and Aydin et Guldamlasioglu

(2017) also suggested methodologies based on artificial intelligence to predict the state of an equipment or a component (e.g. bearing, gears, etc.).

To improve the state of this research domain and to make a step toward the industrial application of prognostic methodologies, this paper will present our most recent work to show that it is now possible to put the workpiece quality in relationship with the physical phenomenon happening during the machining process. We also want to prove that we are now making a step forward to go from being able to diagnose a cutting operation toward being able to predict the quality of that process. To do so, this article is structured as follows: section 2 will introduce our research partner as well as our research environment and equipment. Then, in section 3, we propose a data acquisition (DAQ) system architecture and describe the dataset built. In section 4, we present our signal processing methodologies and the different features that we extracted from the acquired signals. In section 5, we detail our results and show that it is now possible to do the diagnostic of a cutting operation as well as working toward the prognostic of the quality of a workpiece. Finally, in section 6, we make our conclusions.

2 Research environment

To pursue this research project, we are collaborating with an industrial partner: APN Inc.[10] APN is a leader of the machining industry as well as at the forefront of the Industry 4.0 movement in Quebec, Canada. They are specialized in the machining of complex products in exotic material (i.e. titanium, Inconel, etc.) for the aerospace and high-tech industry.

In our research context, our work was done on a 5 axis CNC machine made by GROB, model G352 (see Figure-A I-1). This machine was acquired in 2017.

[10] More information here : http://apnglobal.ca/en/apn/

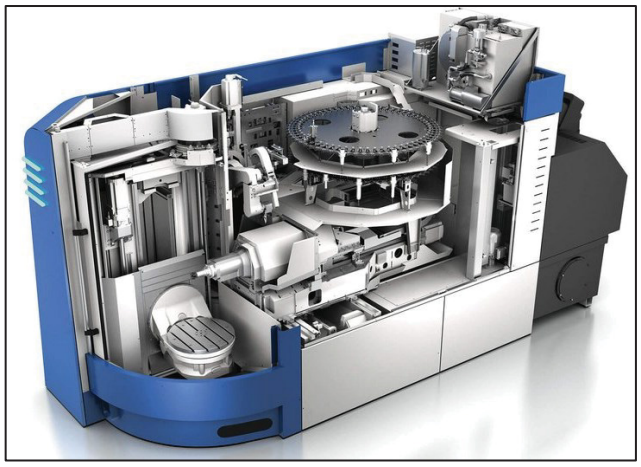

Figure-A I-1 GROB G352 CNC machine[11]

It is also important to state that, to be able to acquire a vibration signal, we worked with the GROB employees to have access to the accelerometer already installed into the machine's spindle. Thus, the signal was acquired through an IFM VSA004[12] accelerometer on which the signal was amplified with a Phoenix Contact signal conditioner model MACX MCR-UI-IU[13]. From Figure-A I-2, we can see where the accelerometer was installed by the manufacturer (as indicated by the bubble #1). This information was provided by the GROB documentation available at APN Inc. In the next section, we present our DAQ system architecture.

[11] Picture source : https://www.grobgroup.com/en/products/product-range/universal-machining-centers/milling-centers/g350/
[12] Specifications : https://www.ifm.com/ca/en/product/VSA004
[13] Specifications : https://www.phoenixcontact.com/online/portal/ca?uri=pxc-oc-itemdetail:pid=2811446&library=caen&tab=1

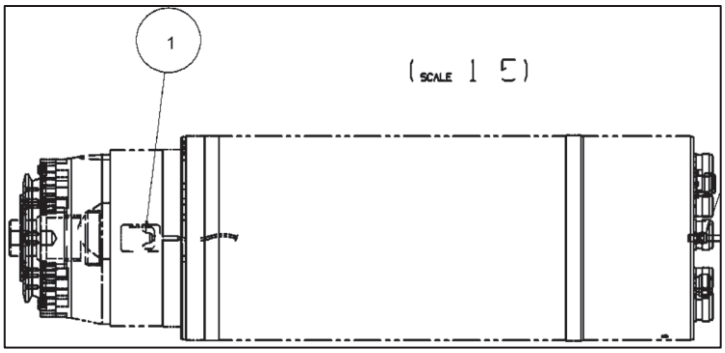

Figure-A I-2 Accelerometer location in the spindle

3 Data acquisition system architecture

One of our hypothesis is that, in order to be able to predict the quality of a workpiece based on the physical information of the CNC machine, we must contextualize the signals acquired from sensors. Therefore, we developed a data acquisition system to automatically execute this operation. Figure-A I-3 shows the contextualization of the data in terms of its relationships.

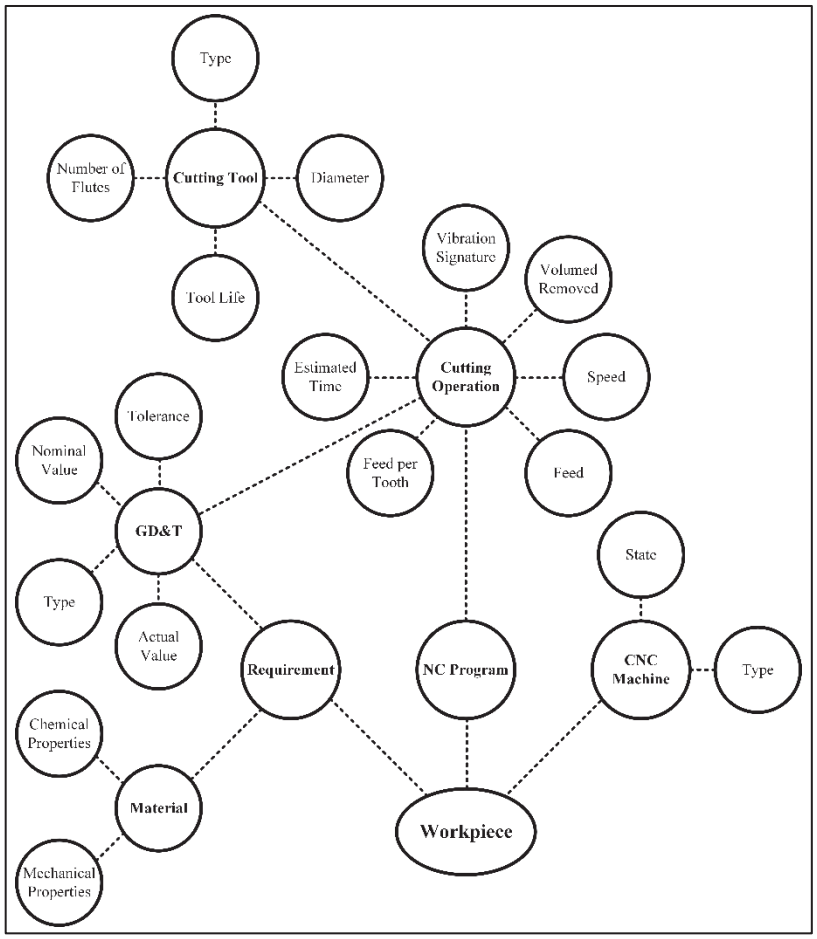

Figure-A I-3 Relationships between data sources

Whit this figure, we can see that, through this system, it is possible to create a relationship that goes from the workpiece requirements (including the actual measurements made on a finished workpiece) up to the vibration signature of a specific cutting operation. This means that at every moment during the machining process, we can know which cutting operation was being executed, its vibration signature, what was the cutting tool and its cutting parameters as well as which GD&T was influenced. To achieve these relationships, multiple data sources must be integrated. Tableau-A I-1 shows the source of each data types.

Tableau-A I-1 Data sources by data types

Data types	**Sources**
Workpiece Requirements	APN Quality System (From the technical drawing)
Actual Measurements	APN Quality System
Material Properties	APN Quality Documents System
CNC Machine information	Machine controller through OPC Protocol
Cutting Operation	CAM Software
Cutting Tool	CAM Software
Vibration signal	Accelerometer and National Instruments Card

To automatically integrate these data sources and create the relationships between the data, we developed an acquisition system that had to take into account the state of the machine (cutting or not, on idle, etc.). To illustrate our acquisition system, Figure-A I-4 shows an overview of the acquisition process. On this figure, we can also see the isometric view of the workpiece as well as the quality data flow.

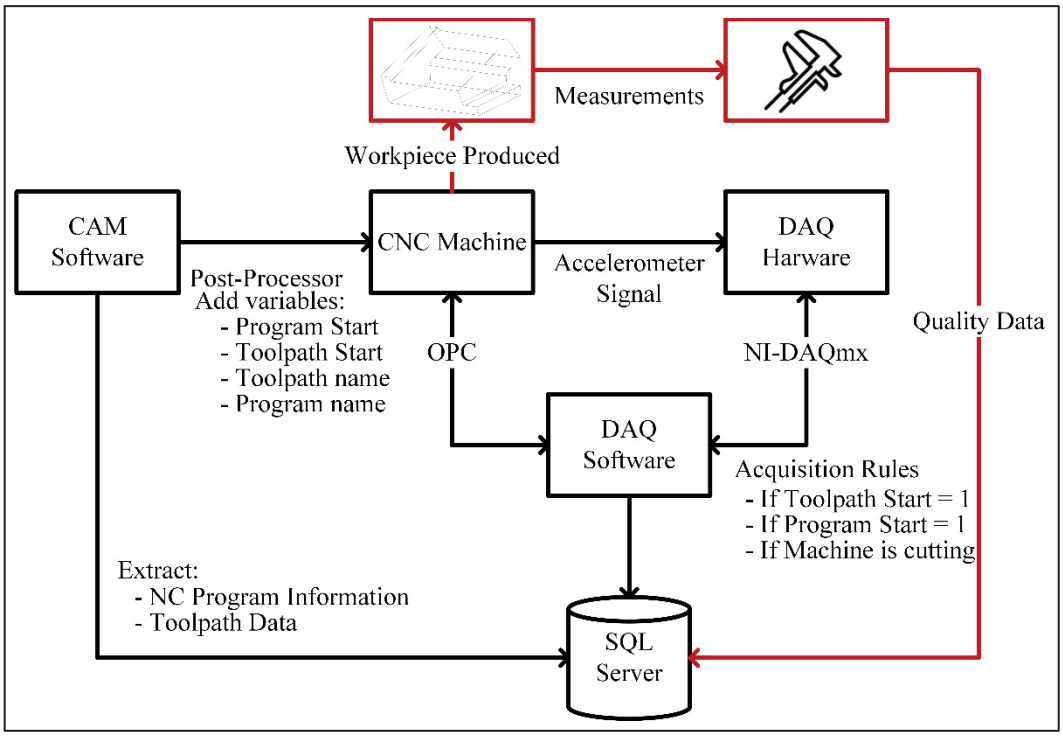

Figure-A I-4 DAQ System architecture

We worked with our industrial partner to modify their post-processor program to add four variables: when the NC Program start/stop, when a cutting operation start/stop, the cutting

operation name and the NC Program name for reference. This modification allowed us to control the behaviour of the National Instruments data acquisition card by sampling the signal only when the machine was actually cutting the workpiece. However, since we are in a production environment, different machine states can also arise: the machine is in idle during a cutting operation, an alarm is raised, etc. Therefore, in our acquisition rules, we added some logic based on variables extracted in real-time from the CNC machine controller through the OPC communication standard. The reader can refer himself to the Siemens Sinumerik 840D SL documentation for a complete list of all available variables.

During the acquisition process, the raw signal is thus contextualized and attached to the current workpiece and the current cutting operation being executed on the CNC machine. This, consequently, gives us a contextualized vibration signal suited to model the relationships between the physical and operational data (the model input) and the actual measurement in terms of GD&T (the model output). The next section presents an overview of the data collected.

3.1 Dataset overview

To prove the concept and functionalities of our proposed system, we conducted a first acquisition process. The acquisition was made during the machining of an Inconel 625 (AMS5666) workpiece intended for the aerospace industry. During our acquisition process, we were able to cover the entirety of the machining process which means:

- 22 different cutting tools;
- 140 cutting operations of multiple types;
- 135 GD&T to be respected for a workpiece to be considered conform.

The acquired data covers five finished workpieces which represents approximately 13 hours of machining process. Unfortunately, due to industrial constraints, we were not able to gather more workpiece. However, this information is sufficient to prove our concept and start our analysis. In this article, we focused on one specific operation where measurements were made for every workpiece to showcase our results. Information related to this operation can

be found in Tableau-A I-2. Information regarding the cutting tool used during the cutting operation can be found in Tableau-A I-3. The cutting tool was new at the beginning of the machining process and was not changed during the machining of the five workpieces. For visualization, Figure-A I-5 shows the cutting operation strategy obtained from the CAM software and Figure-A I-6 shows the difference between the finished workpiece and the raw material used. Due to confidentiality, the 3D model shown in this paper have been redesign to showcase the overall shape of the workpiece and not the actual geometry.

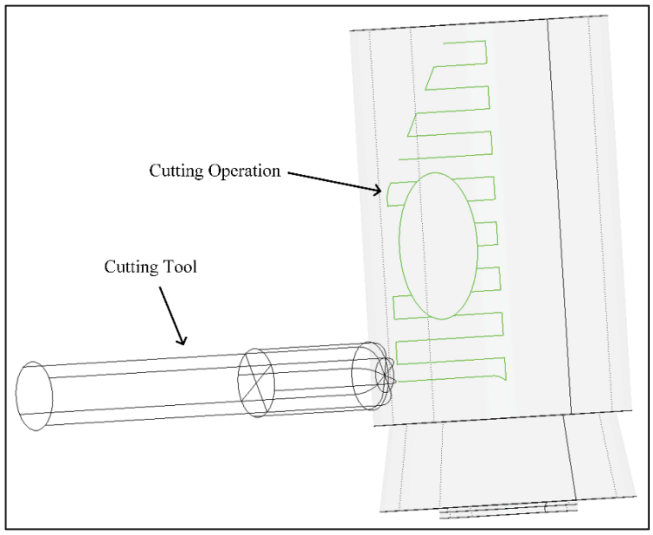

Figure-A I-5 Cutting operation *OP_510*

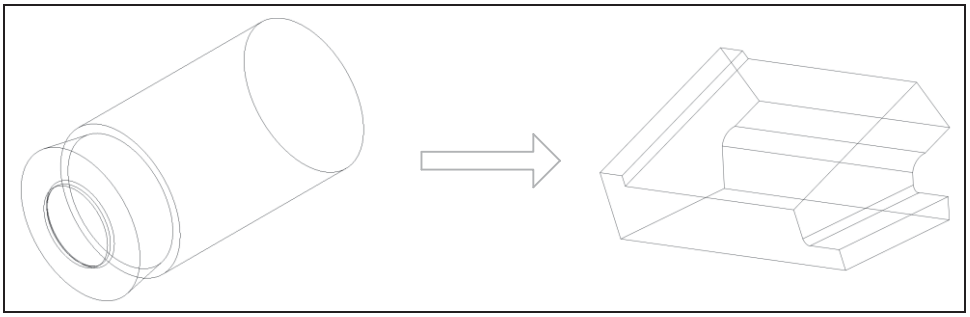

Figure-A I-6 Difference between the raw material and the finished workpiece

Tableau-A I-2 Cutting operation information

Name	Type	Spindle speed [RPM]	Feed [mm/s]	Est. cutting time [min]	Volume removed [cm^3]	Coolant pressure [MPa]
OP_510	Face Milling	1047	233.934	2.5	0.078	6

Tableau-A I-3 Cutting tool information

Name	Type	Diameter [mm]	Radius [mm]	Number of flutes
EMR0.500R0.125L4LG1.100	Radius End Mill	12.7	3.175	4

By connecting our system to the quality system of APN, we are able to associate the cutting operation with the specifications (GD&T) influenced by that operation. These associations are made by expert employees at APN. Thus, for this project, we assumed that the associations are good. Through these associations, we know that the *OP_510* operation influences the specification #15. Details about this specification is found in Tableau-A I-4.

Tableau-A I-4 Details of the GD&T specification #15

Number	GD&T type	Minimum value [µm]	Maximum value [µm]	Severity	Illustration [µm]	Inspection tool used
15	Flatness	0	25.4	Critical	▱ 25.4	CMM

The interpretation of this type of GD&T was made according to the standard Y14.5 (ASME, 2009). The reader can refer to ASME (2009) for further details.

For the five workpieces, Figure-A I-7shows each actual measurements made by the operator after each workpiece was produced.

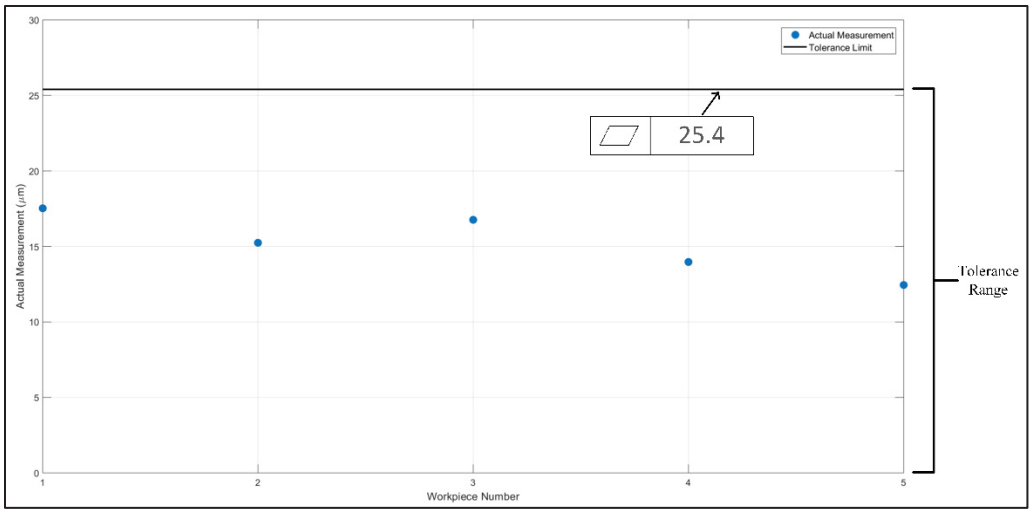

Figure-A I-7 Actual measurement per workpiece for the specification #15

The next section will present the signal processing methodology applied to the data acquired.

4 Signal processing methodology

We have shown in the previous section that we can now acquire a signal that is well contextualized. The objective of this section is to describe our signal processing methodology in order to be able to do the diagnostic of the machining process as well as the production equipment itself; taking a step toward a predictive methodology.

Our methodology is segmented in two sections: a time domain methodology and a frequency domain methodology. Once acquired, each signal sampled file is cleaned and has several features extracted. The signal features used are described below and are chosen according to the work of Lei et al. (2018), Elattar et al. (2016) and Abellan-Nebot et Romero Subirón (2010).

4.1 Time domain

To describe the signal in the time domain, we used equation (A I-1) to equation (A I-5) which refer respectively to the Root Mean Square (RMS), the Kurtosis (K), the Peak value ($Peak$), the Peak-to-Peak value (PTP) and the Crest Factor (CF).

$$RMS = \sqrt{\frac{1}{N}\sum_{i=1}^{N}(x_i - \overline{x})^2} \tag{A I-1}$$

$$K = \frac{\sum_{i=1}^{N}(x_i - \bar{x})^4}{\frac{1}{N}\left[\sum_{i=1}^{N}(x_i - \bar{x})^2\right]^2} \tag{A I-2}$$

$$Peak = \max(x) \tag{A I-3}$$

$$PTP = \max(x) - \min(x) \tag{A I-4}$$

$$CF = \frac{Peak}{RMS} \tag{A I-5}$$

Where x is a signal of N samples, x_i is the value of ith sample and $\overline{x}$ is the average of x.

4.2 Frequency domain

In the frequency domain, we are interested in following the evolution, through time, of the cutting tool frequency (A_{CT}). This is because the degradation of the tool is one of the major cause of the degradation of a machining process. To do so, we used equation (A I-6). This equation is similar to the RMS equation in the sense that we could interpret its result as being the energy content of the signal around a specific frequency.

$$A_{CT} = \sqrt{\sum_{i=a}^{b} A_i^2} \tag{A I-6}$$

Where A_i is the amplitude of the signal at the ith frequency and a and b are the two corners of the window. In our case, we assigned $a = 64$ Hz and $b = 75$ Hz, which correspond to

±5 Hz around the frequency of interest (f_i). We are also interested in making the same measurement at the different harmonics of the cutting tool frequency, thus we also applied the same equation at the 2nd, 3rd, 4th and 5th harmonics ($2f_i$, $3f_i$, $4f_i$ and $5f_i$).

To improve the physical meaning of this feature we use the work of Proteau et al. (2019a). In Proteau et al. (2019a), the authors proposed an adaptation of the specific cutting energy (SCE, k_c) metric first established by Debongnie (2006). In their work, the authors used their version of the SCE to show that it can adequately represents tool wear degradation. Their version is defined by equation (A I-7).

$$k_c = \frac{P_{Tool}[\mathrm{W}]}{Q[\mathrm{cm^3 s^{-1}}]} = \frac{[\mathrm{Js^{-1}}]}{[\mathrm{cm^3 s^{-1}}]} = [\mathrm{Jcm^{-3}}] \qquad \text{(A I-7)}$$

Where P_{Tool} is the power [W] consumed by the cutting tool and Q is the material removal rate express in $\mathrm{cm^3 s^{-1}}$.

SCE is therefore defined in terms of the energy required to remove and keep a certain rate of material removal in a specific material (aluminum, Inconel, etc.). The reader can refer himself to Proteau et al. (2019a) for the details. Since we do not have the actual power transmitted to the cutting tool, we can estimate this value by using the energy contained in the signal at the frequency related to the cutting tool (A_{CT}). For the same material and a constant material removal rate, k_c should be constant. In case of tool wear, k_c increase through time. The next section will present the results of our analysis.

5 Results and discussion

We first present the results of our analysis in the time domain. Figure-A I-8 shows the values of the RMS, $Peak$ and PTP values through time for each workpiece.

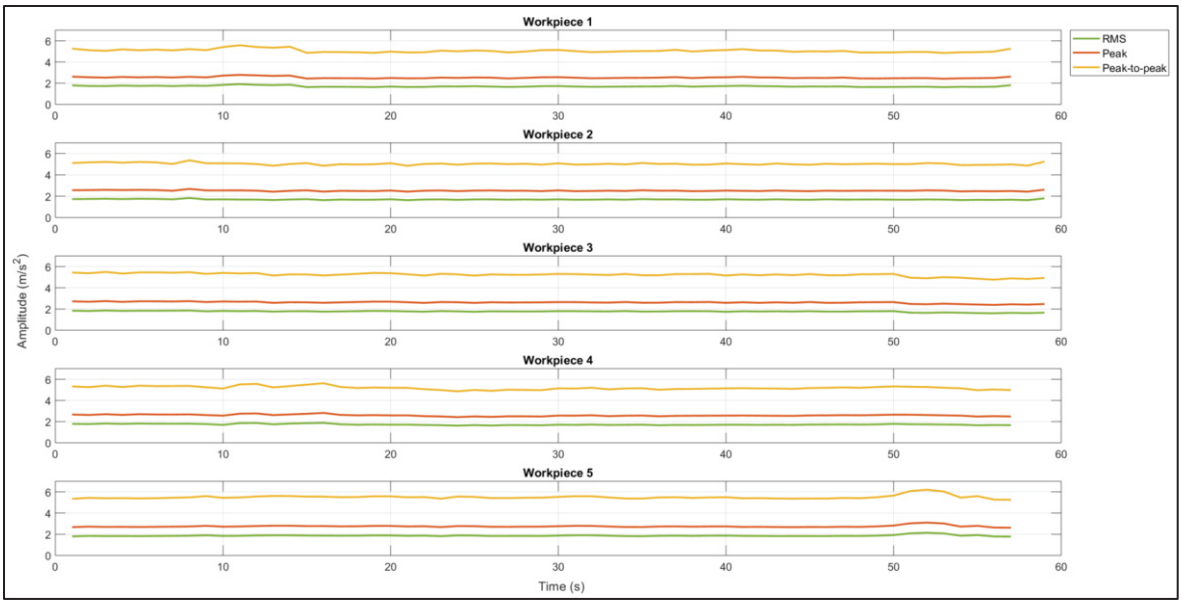

Figure-A I-8 RMS, $Peak$ and PTP values through time per workpiece

Then, Figure-A I-9 presents the average values for the RMS, $Peak$ and PTP value per workpiece. We also included the evolution of the actual measurement per workpiece for the specification #15 to see if there is a direct relationship between the evolutions of the two phenomenon that could be visually witnessed.

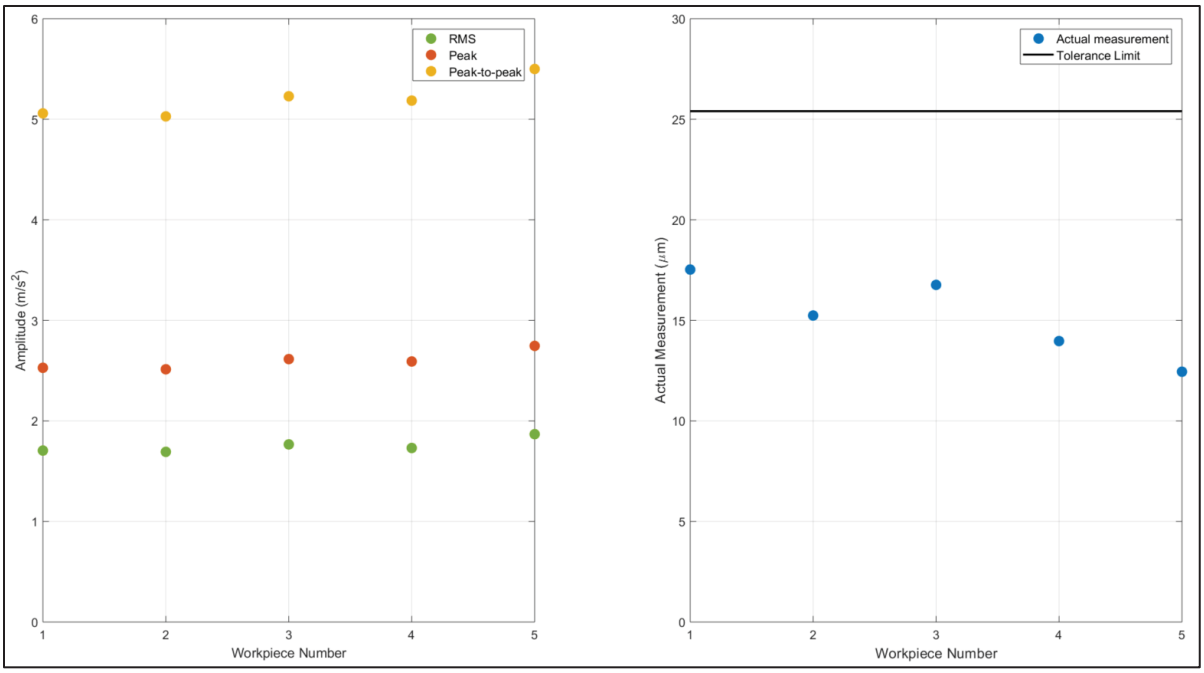

Figure-A I-9 RMS, $Peak$ and PTP values per workpiece and actual measurement per workpiece

We did the same analysis with the kurtosis and the crest factor. Results are shown in Figure-A I-10 and Figure-A I-11.

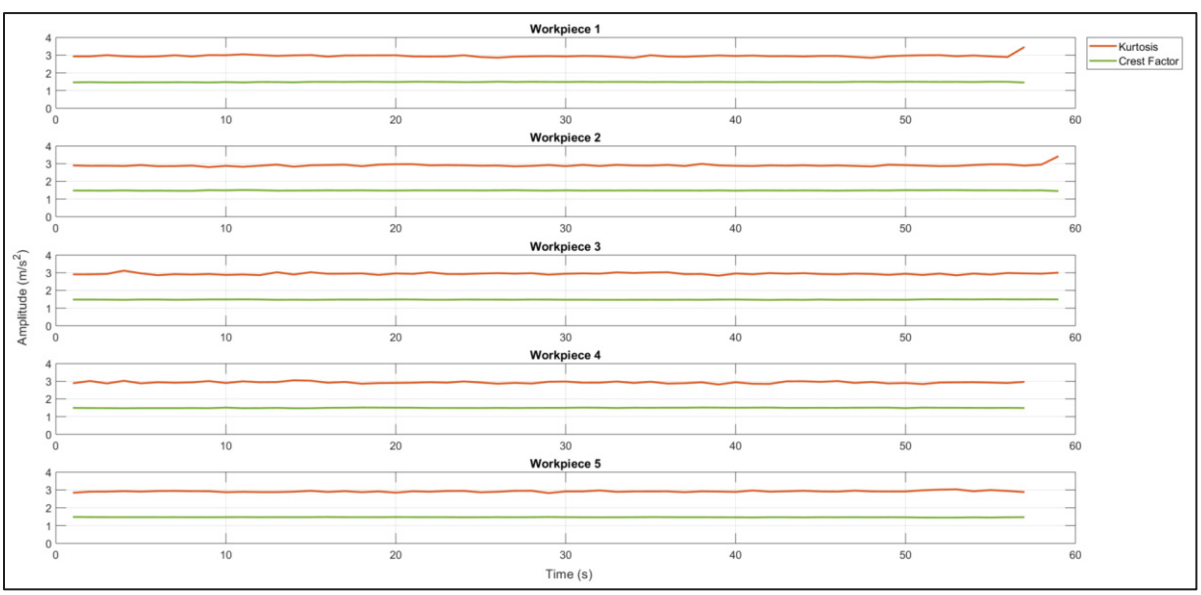

Figure-A I-10 K and CF values through time per workpiece

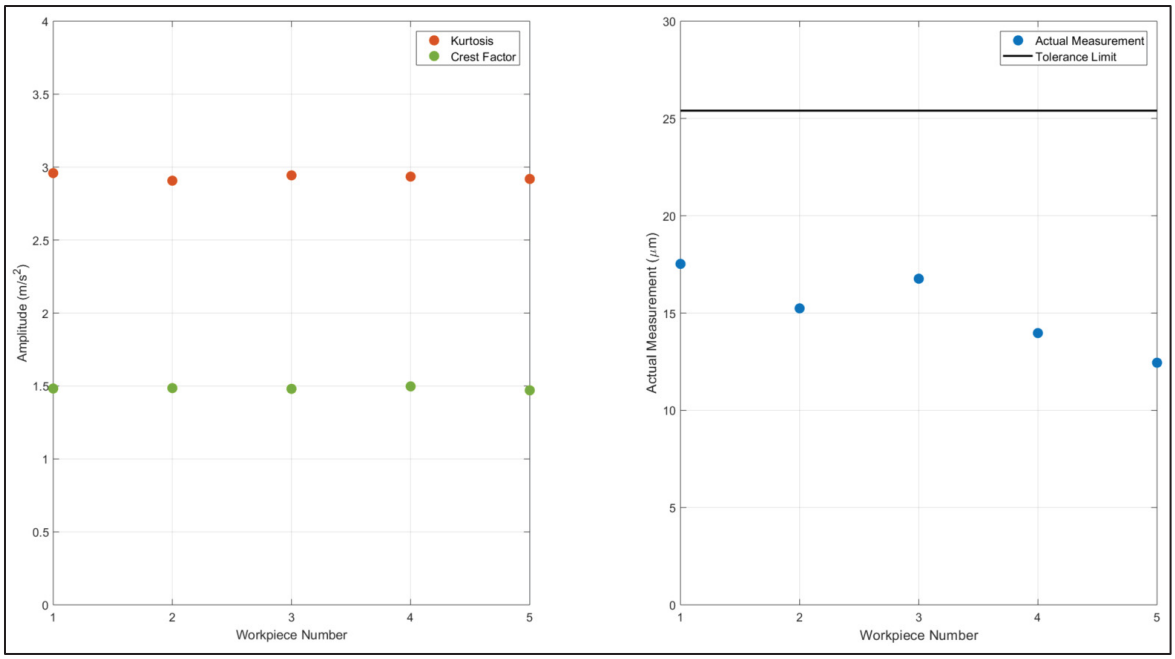

Figure-A I-11 K and CF values per workpiece and actual measurement per workpiece

We then did the same analysis in the frequency domain. Results of the SCE values for each harmonics are shown in Figure-A I-12 and Figure-A I-13.

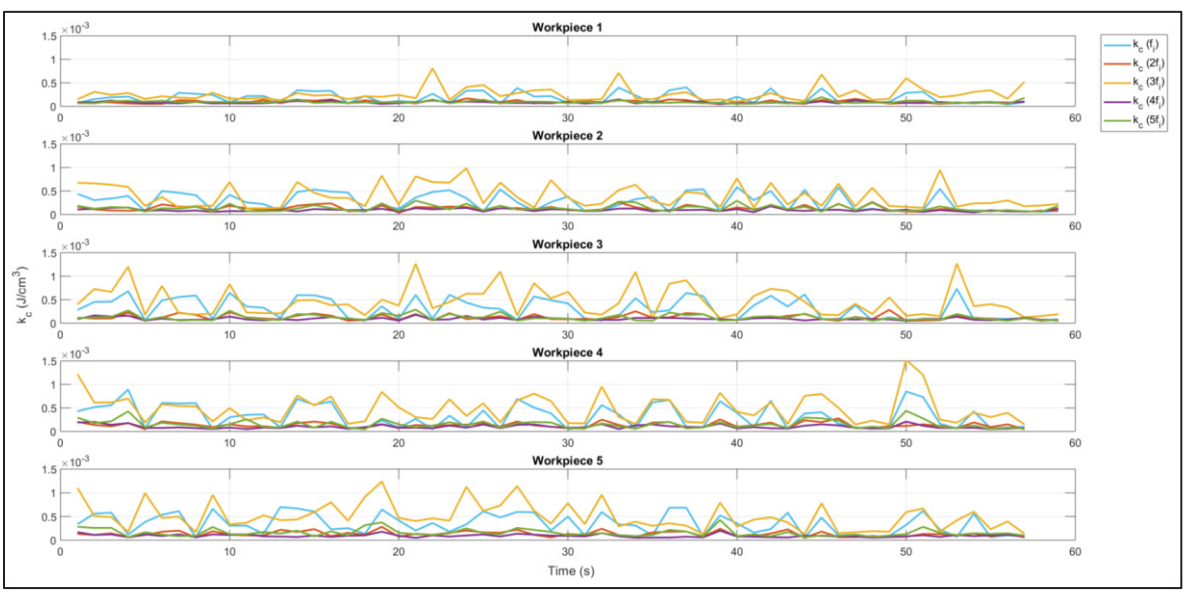

Figure-A I-12 k_c values for each harmonics of f_i through time per workpiece

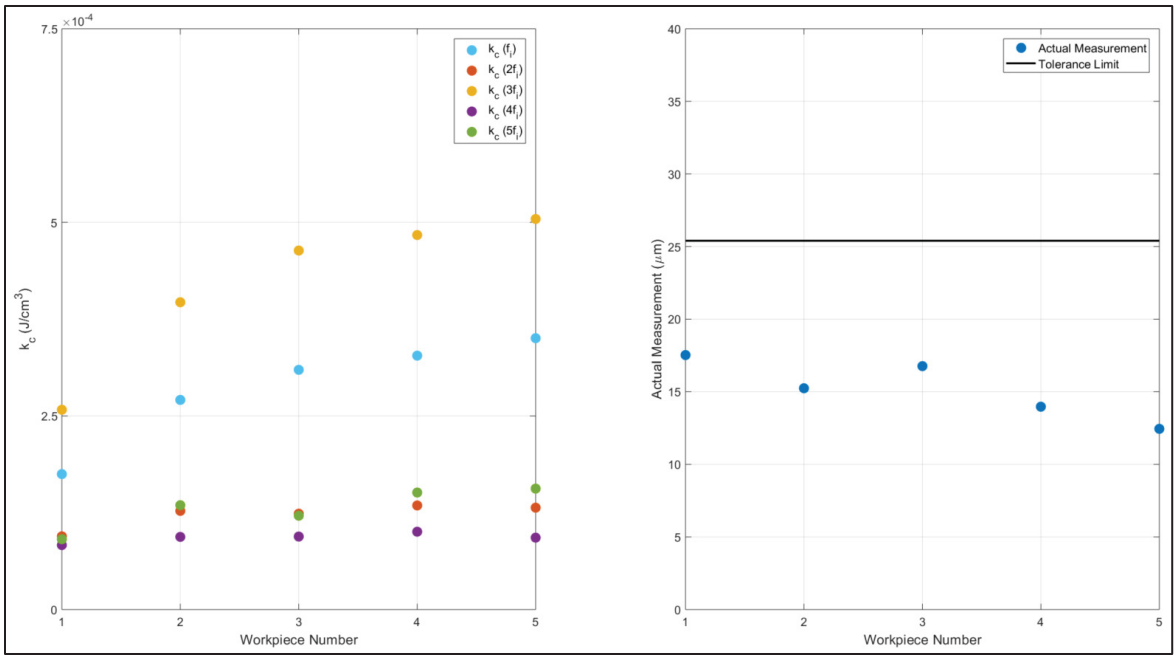

Figure-A I-13 k_c values for each harmonics of f_i per workpiece and actual measurement per workpiece

Finally, we also did a time-frequency analysis where we looked at the frequency domain of the signal through time. Figure-A I-14 presents the spectrogram we obtained. The white lines represent the separation between each workpiece; starting to the left with workpiece 1 up to the right with workpiece 5. In a) we gave the spectrogram for the frequencies between 0 and 400 Hz and in b) for the frequencies 400 to 1000 Hz. Most frequencies of interest are located in the range of 0 to 1 kHz.

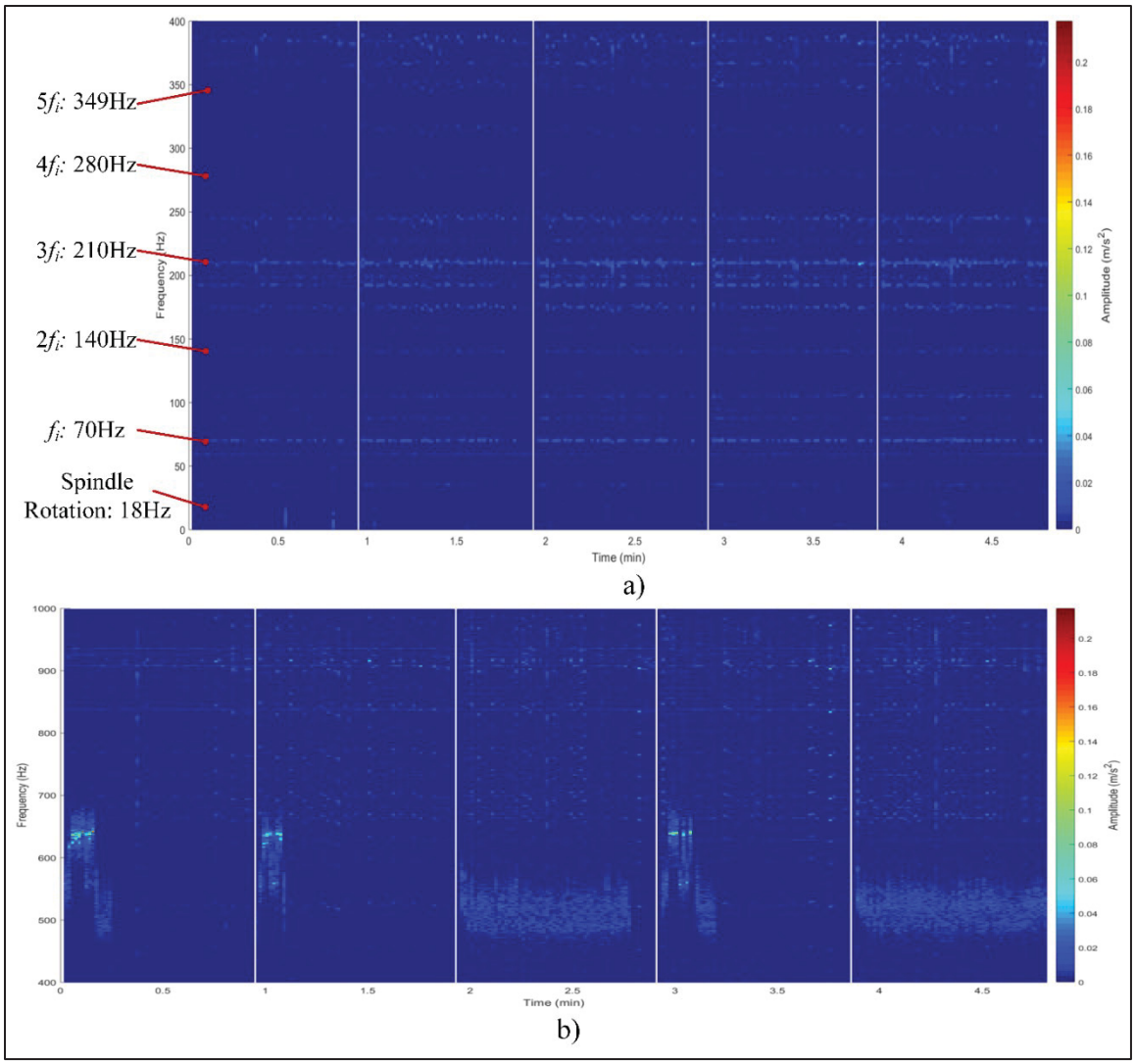

Figure-A I-14 Time-frequency analysis for all the workpiece

From Figure-A I-8, we can see that, for all workpieces, most values are comprised between an amplitude of 0 and 6 m/s^2; with some peaks during the machining process of each workpiece. However, we cannot clearly see that there was either a degradation or an improvement regarding the machining process in a part-to-part point of view. Also, when we look at the average values per part in Figure-A I-9, we cannot clearly state that there is a direct relationship between the actual measurement and the evolution of the RMS, $Peak$ or PTP.

We could conclude the same thing regarding the evolution of the K and CF through time with the results shown in Figure-A I-10 and Figure-A I-11. However, it is interesting to also use these results to do the diagnostic of the machine health state. Based on these results, we could conclude that the machine is in a good health state. From Thomas (2011), a kurtosis value around a value of 3 means a random signal, hence a machine in good health where no spike or impact were recorded. Values higher than that would start to indicate that impacts are being recorded. This is also supported by the values of the crest factors which are low and near the value indicating a good condition ($CF = 1.41$). We also tried to look at the fundamental frequencies related to the bearings installed in the spindle. However, since the machine and its component are relatively new, the amplitudes related to the typical fault (FTF, BPFI, etc.) do not stand out. This could indicate that they are in good condition and that their signal is lost in the noise of the machine during the machining process. A diagnostic when the machine is not cutting could probably help us identify with better accuracy these frequencies.

From Figure-A I-12, we can see that the variation in terms of amplitude seems to increase between the workpiece 1 and workpiece 5. This would seems to be consistent with the claim of Proteau et al. (2019a) that the energy required to keep a material removal rate is increasing with tool wear. When we look at Figure-A I-13, we can see that the values are increasing with every workpiece; for the first and third harmonics (f_i and $3f_i$). The 2nd, 4th and 5th harmonics ($2f_i$, $4f_i$ and $5f_i$) seems to have a low amplitude throughout the data we collected.

Moreover, when we look at the scale of the amplitude of the data, we can see that they are pretty low. This is somewhat counter intuitive to our belief. We believed that because the Inconel 625 is a very hard and difficult material to work with, we would have seen very high amplitudes due to the force required to remove the material. It was not possible to get the exact depth of cut used in this operation, therefore, maybe the engineers responsible of this product at APN used a very low depth of cut parameter in order to create less friction between the material and the cutting tool in order to facilitate the machining process.

When we look at the spectrogram shown in Figure-A I-14, we can quickly see that the overall frequencies' amplitudes are consistent with our previous claim; it is low across most frequencies. We can still detect some frequencies of interest such as the spindle rotation (1047 RPM = 17.45 Hz), the cutting tool frequency (with 4 flutes: 69.8 Hz) and its harmonics (139.6 Hz, 209.4 Hz, 279.2 Hz and 349 Hz).

Aside from these specific frequencies, this low amplitude claim seems to hold true except for some spontaneous peak between 600 and 700 Hz. In fact, if we look at the graph in b), we see a phenomenon where we have not yet found the source. No video recording was made during the acquisition process. This kind of data would surely help us to correlate such phenomenon with actual events during the machining process. Additionally, this phenomenon is not consistent across all workpiece. Cutting parameter and overall machining strategy were not changed between the workpieces, hence we would have expected a similar pattern for each workpiece. However, we can denote two patterns: one related with workpiece 1, 2 and 4 and the other with the workpiece 3 and 5. The peaks in amplitude are also related to the first pattern for workpiece 1, 2 and 4.

In a diagnostic point of view, our conclusion related to the kurtosis and crest factor values seems to hold in the frequency domain since we do not seem to detect traces of impact during the utilization of the equipment.

The objective of this paper was to demonstrate that we can now have access to data allowing us to describe and diagnose a machining process and its cutting operations as well as making a step toward being able to do the prognostic of the overall quality of a workpiece. With the results shown in this section we can conclude that the propose data acquisition architecture enable us now to adequately contextualize, in real-time and automatically, signals acquired through sensing devices. However, when we look at the final objective of our project; that is the prognostic of the quality of a workpiece in term of the respect of its GD&T requirements, we have not seen a clear linear relationship or pattern between the cutting operation vibration signal and the evolution of the actual measurement of the specification #15 neither in the

time and frequency domain. Throughout this article, we have been looking at one operation influencing the specification #15; in fact, there is a total of 11 cutting operations influencing this specific requirement. In other words, we conjuncture that a clear linear relationship cannot be establish between only one operation and the evolution of a specific requirement. On the contrary, it is maybe the "sum" or sequence of all these operations that could influence the conformity of a workpiece specific requirements. In other words, all the variations across all these operations could explain the evolution of a specification. Consequently, we believe that only through a machine learning approach we could be able to predict the quality of a workpiece. Our strategy to apply such approach to this research project still hold to this point.

5 Conclusion

To conclude this article, we wanted to showcase our data acquisition system architecture and demonstrate that we can now adequately contextualize a vibration signal to better do the diagnostic of a cutting operation to, in the end, facilitate the development of a prognostic methodology for the quality of a workpiece. We believe that we have successfully achieve these objectives by showing multiple results related to the cutting operation *OP_510*. However, we have not yet been able to showcase a linear relationship between the vibration signal of this operation and the evolution of the quality of the workpiece. The use of a machine learning approach could probably help us achieve this objective. Further work in order to close the gap between our current status and our final objective to predict the quality of a workpiece will include adding sensors to the GROB CNC machine: a tri-axial accelerometer, an acoustic emission sensor, current and voltage sensors to the motor of the spindle as well as the ones of the three main working axis of the CNC machine and try to apply cyclostationarity analysis based on the work of M. Lamraoui et al. (2012). We will also expand our system capacity to have it works in a more autonomous way and we will finally use and apply multiple machine learning approaches to perform sensors fusion and the actual prediction of a workpiece quality.

Acknowledgments

The authors would like to thank APN Inc.: their owners, Jean and Yves and all their employees related to this project for their support and time in helping our research team. Special thanks to Alain, Jonathan, Michel, David, Daniel, Raphael, Maxim and Mathieu for the many questions they answered and their help to make this project happen. We would also like to acknowledge the financial support of the *Fonds de Recherche du Québec – Nature et Technologies* (FRQNT) to this project through Grant #257668.

BIBLIOGRAPHIE

Abellan-Nebot, J. V., & Romero Subirón, F. (2010). A review of machining monitoring systems based on artificial intelligence process models. *The International Journal of Advanced Manufacturing Technology, 47*(1), 237-257.

AFNOR. (2002). *Moyens de production - Indicateurs de performances - Taux de rendement synthétique (TRS) - Taux de rendement global (TRG) - Taux de rendement économique (TRE)*. NF E60-182. France: Association Française de Normalisation.

Afshari Behzad, M., Abedi, M., & Shahryari, M. (2017). Optimization of a radiator for a MPFL system in a GEO satellite. *Advances in aircraft and spacecraft science, 4*(6), 701-709.

Aghazadeh, F., Tahan, A., & Thomas, M. (2018a). Tool Condition Monitoring Using Spectral Subtraction Algorithm and Artificial Intelligence Methods in Milling Process. *International Journal of Mechanical Engineering and Robotics Research, 7*(1), 30-34.

Aghazadeh, F., Tahan, A., & Thomas, M. (2018b). Tool condition monitoring using spectral subtraction and convolutional neural networks in milling process. *The International Journal of Advanced Manufacturing Technology, 98*(9), 3217-3227.

Agogino, A., & Goebel, K. (2007). Milling Data Set Repéré à https://ti.arc.nasa.gov/tech/dash/groups/pcoe/prognostic-data-repository/#milling

Agrawal, C., Khanna, N., Pruncu, C. I., Singla, A. K., & Gupta, M. K. (2020). Tool wear progression and its effects on energy consumption and surface roughness in cryogenic assisted turning of Ti-6Al-4V. *The International Journal of Advanced Manufacturing Technology, 111*(5), 1319-1331.

Ahmad, M. I., Yusof, Y., Daud, M. E., Latiff, K., Kadir, A. Z. A., & Saif, Y. (2020). Machine monitoring system: a decade in review. *The International Journal of Advanced Manufacturing Technology, 108*, 1-15.

Albertelli, P., Goletti, M., Torta, M., Salehi, M., & Monno, M. (2016). Model-based broadband estimation of cutting forces and tool vibration in milling through in-process indirect multiple-sensors measurements. *The International Journal of Advanced Manufacturing Technology, 82*(5), 779-796.

Antoni, J. (2009). Cyclostationarity by examples. *Mechanical Systems and Signal Processing, 23*(4), 987-1036.

Arinez, J. F., Chang, Q., Gao, R. X., Xu, C., & Zhang, J. (2020). Artificial Intelligence in Advanced Manufacturing: Current Status and Future Outlook. *Journal of Manufacturing Science and Engineering, 142*(11).

ASME. (2009). *Dimensioning and Tolerancing; Engineering Drawing and related documentation practices*. ASME Y14.5-2009. New York, NY: American Society of Mechanical Engineers.

ASME. (2018a). *Dimensioning and Tolerancing; Engineering Drawing and related documentation practices*. ASME Y14.5-2018. New York, NY: American Society of Mechanical Engineers.

ASME. (2018b). *Surface Texture Symbols*. Y14.36. New York, NY: American Society of Mechanical Engineers.

Aydin, O., & Guldamlasioglu, S. (2017). Using LSTM networks to predict engine condition on large scale data processing framework. Dans *2017 4th International Conference on Electrical and Electronic Engineering (ICEEE)* (pp. 281-285).

Azimi, M., Mirjavadi, S. S., Asli, S. A., & Hamouda, A. (2017). Fracture analysis of a special cracked lap shear (CLS) specimen with utilization of virtual crack closure technique (VCCT) by finite element methods. *Journal of Failure Analysis and Prevention, 17*(2), 304-314.

Bakker, O. J., Ratchev, S. M., & Popov, A. A. (2015). Towards a Condition-Monitoring Framework for Quality Assurance in Intelligent Multistage Manufacturing Environment. *IFAC-PapersOnLine, 48*(3), 2089-2094.

Balamurugamohanraj, G., Vijaiyendiran, K., Mohanaraman, P., & Sugumaran, V. (2016). Prediction of Surface Roughness Based on Machining Condition and Tool Condition in Boring Stainless Steel-304. *Indian Journal of Science and Technology, 9*(47), 1-6.

Balan, G. C., & Epureanu, A. (2008a). The monitoring of the turning tool wear process using an artificial neural network. Part 1: The experimental set-up and experimental results. *Proceedings of the Institution of Mechanical Engineers, Part B: Journal of Engineering Manufacture, 222*(10), 1241-1252.

Balan, G. C., & Epureanu, A. (2008b). The monitoring of the turning tool wear process using an artificial neural network. Part 2: The data processing and the use of artificial neural network on monitoring of the tool wear. *Proceedings of the Institution of Mechanical Engineers, Part B: Journal of Engineering Manufacture, 222*(10), 1253-1262.

Bampoula, X., Siaterlis, G., Nikolakis, N., & Alexopoulos, K. (2021). A Deep Learning Model for Predictive Maintenance in Cyber-Physical Production Systems Using LSTM Autoencoders. *Sensors, 21*(3), 972.

Bao, W., Yue, J., & Rao, Y. (2017). A deep learning framework for financial time series using stacked autoencoders and long-short term memory. *PloS one, 12*(7), e0180944.

Baur, M., Albertelli, P., & Monno, M. (2020). A review of prognostics and health management of machine tools. *The International Journal of Advanced Manufacturing Technology, 107*(5), 2843-2863.

Benardos, P. G., & Vosniakos, G. C. (2003). Predicting surface roughness in machining: a review. *International Journal of Machine Tools and Manufacture, 43*(8), 833-844.

Bousdekis, A., Magoutas, B., Apostolou, D., & Mentzas, G. (2015). A proactive decision making framework for condition-based maintenance. *Industrial Management & Data Systems, 115*(7), 1225-1250.

Bureau de Normalisation du Québec. (2018). *BNQ6545-200/2018: Vitrine 4.0 - Programme de certification*. Québec, Qc.

Cai, W., Zhang, W., Hu, X., & Liu, Y. (2020). A hybrid information model based on long short-term memory network for tool condition monitoring. *Journal of Intelligent Manufacturing*.

Cambron, P., Tahan, A., Masson, C., & Pelletier, F. (2017). Bearing temperature monitoring of a Wind Turbine using physics-based model. *Journal of Quality in Maintenance Engineering, 23*(4), 1-12.

Chadha, G. S., Rabbani, A., & Schwung, A. (2019). Comparison of Semi-supervised Deep Neural Networks for Anomaly Detection in Industrial Processes. Dans *2019 IEEE 17th International Conference on Industrial Informatics (INDIN)* (Vol. 1, pp. 214-219).

Chen, Y., Jin, Y., & Jiri, G. (2018). Predicting tool wear with multi-sensor data using deep belief networks. *The International Journal of Advanced Manufacturing Technology, 99*(5), 1-10.

Cheng, F., He, Q. P., & Zhao, J. (2019). A novel process monitoring approach based on variational recurrent autoencoder. *Computers & Chemical Engineering, 129*, 106515.

Chollet, F. (2017). Keras (2015). Repéré à https://keras.io

Cui, Y., Kara, S., & Chan, K. C. (2020). Manufacturing big data ecosystem: A systematic literature review. *Robotics and Computer-Integrated Manufacturing, 62*, 101861.

de-Felipe, D., & Benedito, E. (2017). Monitoring high complex production processes using process capability indices. *The International Journal of Advanced Manufacturing Technology, 93*(1), 1-11.

Debongnie, J.-F. (2006). *Usinage*. Editions du CEFAL.

Doersch, C. (2016). Tutorial on variational autoencoders. *arXiv preprint arXiv:1606.05908*.

Du, R., Elbestawi, M., & Wu, S. (1995a). Automated monitoring of manufacturing processes, part 1: Monitoring methods. *Journal of Engineering for Industry, 117*(2), 121-132.

Du, R., Elbestawi, M., & Wu, S. (1995b). Automated monitoring of manufacturing processes, part 2: Applications. *Journal of Engineering for Industry, 117*(2), 133-141.

Duo, A., Basagoiti, R., Arrazola, P. J., Aperribay, J., & Cuesta, M. (2019). The capacity of statistical features extracted from multiple signals to predict tool wear in the drilling process. *The International Journal of Advanced Manufacturing Technology, 102*(5), 2133-2146.

Elattar, H. M., Elminir, H. K., & Riad, A. (2016). Prognostics: a literature review. *Complex & Intelligent Systems, 2*(2), 125-154.

Elsevier. (2021). Engineering Village. Repéré le 10 Janvier à www.engineeringvillage.com

Ertekin, Y. M., Kwon, Y., & Tseng, T.-L. (2003). Identification of common sensory features for the control of CNC milling operations under varying cutting conditions. *International Journal of Machine Tools and Manufacture, 43*(9), 897-904.

Fu, P., Hope, A., & King, G. (1998). *Intelligent tool condition monitoring in milling operation*.

Fu, Y., Zhang, Y., Gao, Y., Gao, H., Mao, T., Zhou, H., & Li, D. (2017). Machining vibration states monitoring based on image representation using convolutional neural networks. *Engineering Applications of Artificial Intelligence, 65*, 240-251.

Gao, R., Wang, L., Teti, R., Dornfeld, D., Kumara, S., Mori, M., & Helu, M. (2015). Cloud-enabled prognosis for manufacturing. *CIRP Annals - Manufacturing Technology, 64*(2), 749-772.

Gao, S., Pang, S., Jiao, L., Yan, P., Luo, Z., Yi, J., & Wang, X. (2017). Research on specific cutting energy and parameter optimization in micro-milling of heat-resistant stainless steel. *The International Journal of Advanced Manufacturing Technology, 89*(1-4), 191-205.

García, V., Sánchez, J. S., Rodríguez-Picón, L. A., Méndez-González, L. C., & Ochoa-Domínguez, H. d. J. (2018). Using regression models for predicting the product quality in a tubing extrusion process. *Journal of Intelligent Manufacturing, 30*(6), 2535-2544.

Gebremariam, M. A., Xiang Yuan, S., Azhari, A., & Lemma, T. A. (2017). Remaining Tool Life Prediction Based on Force Sensors Signal During End Milling of Stavax ESR Steel. Dans *ASME 2017 International Mechanical Engineering Congress and Exposition* (Vol. 58356, pp. V002T002A094).

Gensler, A., Henze, J., Sick, B., & Raabe, N. (2016). Deep Learning for solar power forecasting - An approach using AutoEncoder and LSTM Neural Networks. Dans *2016 IEEE International Conference on Systems, Man, and Cybernetics (SMC)* (pp. 002858-002865).

Ghojogh, B., & Crowley, M. (2019). The theory behind overfitting, cross validation, regularization, bagging, and boosting: tutorial. *arXiv preprint arXiv:1905.12787*.

Ghosal, A., Nandy, A., Das, A. K., Goswami, S., & Panday, M. (2020). A Short Review on Different Clustering Techniques and Their Applications. Dans *Emerging technology in modelling and graphics* (Vol. 937, pp. 69-83). Springer Singapore.

Girardin, F., Rémond, D., & Rigal, J.-F. (2010). Tool wear detection in milling—An original approach with a non-dedicated sensor. *Mechanical Systems and Signal Processing, 24*(6), 1907-1920.

Goebel, K., Saxena, A., Saha, S., Saha, B., & Celaya, J. (2011). Prognostic Performance Metrics. Dans *Machine Learning and Knowledge Discovery for Engineering Systems Health Management* (Vol. 147, pp. 20).

Goodfellow, I., Bengio, Y., & Courville, A. (2016). *Deep Learning*. The MIT Press.

Goyal, D., Mongia, C., & Sehgal, S. (2021). Applications of Digital Signal Processing in Monitoring Machining Processes and Rotary Components: A Review. *IEEE Sensors Journal, 21*(7), 8780-8804.

Gugulothu, N., TV, V., Malhotra, P., Vig, L., Agarwal, P., & Shroff, G. (2017). Predicting Remaining Useful Life using Time Series Embeddings based on Recurrent Neural Networks. *arXiv preprint arXiv:1709.01073*.

Guillén, A. J., Crespo, A., Gómez, J. F., & Sanz, M. D. (2016). A framework for effective management of condition based maintenance programs in the context of industrial development of E-Maintenance strategies. *Computers in Industry, 82*, 170-185.

Haber, R. E., Jiménez, J. E., Peres, C. R., & Alique, J. R. (2004). An investigation of tool-wear monitoring in a high-speed machining process. *Sensors and Actuators A: Physical, 116*(3), 539-545.

Haidong, S., Hongkai, J., Xingqiu, L., & Shuaipeng, W. (2018). Intelligent Fault Diagnosis of Rolling Bearing Using Deep Wavelet Auto-encoder with Extreme Learning Machine. *Knowledge-Based Systems, 140*, 1-14.

Han, K., Wen, H., Shi, J., Lu, K.-H., Zhang, Y., Fu, D., & Liu, Z. (2019). Variational autoencoder: An unsupervised model for encoding and decoding fMRI activity in visual cortex. *NeuroImage, 198*, 125-136.

Han, T., Liu, C., Yang, W., & Jiang, D. (2019). A novel adversarial learning framework in deep convolutional neural network for intelligent diagnosis of mechanical faults. *Knowledge-Based Systems, 165*, 474-487.

Hanachi, H., Yu, W., Kim, I. Y., Liu, J., & Mechefske, C. K. (2019). Hybrid data-driven physics-based model fusion framework for tool wear prediction. *The International Journal of Advanced Manufacturing Technology, 101*(9), 2861-2872.

Hassan, M., Sadek, A., Attia, M. H., & Thompson, V. (2018). Intelligent machining: real-time tool condition monitoring and intelligent adaptive control systems. *Journal of Machine Engineering, 18*(1), 5-17.

He, K., Gao, M., & Zhao, Z. (2019). Soft Computing Techniques for Surface Roughness Prediction in Hard Turning: A Literature Review. *IEEE Access, 7*, 89556-89569.

Hemmer, M., Klausen, A., Khang, H. V., Robbersmyr, K. G., & Waag, T. I. (2020). Health Indicator for Low-Speed Axial Bearings Using Variational Autoencoders. *IEEE Access, 8*, 35842-35852.

Hou, P., Wen, C., & Dong, D. (2017). Rolling bearing fault diagnose based on stacked sparse auto encoder. Dans *2017 36th Chinese Control Conference (CCC)* (pp. 7027-7032).

Hou, X., Sun, K., Shen, L., & Qiu, G. (2019). Improving variational autoencoder with deep feature consistent and generative adversarial training. *Neurocomputing, 341*, 183-194.

Huang, Y., Chen, C., & Huang, C. (2019). Motor Fault Detection and Feature Extraction Using RNN-Based Variational Autoencoder. *IEEE Access, 7*, 139086-139096.

Iglesias-Martínez, M. E., Córdoba, P. F. d., Antonino-Daviu, J. A., & Conejero, J. A. (2019). Detection of Nonadjacent Rotor Faults in Induction Motors via Spectral Subtraction and Autocorrelation of Stray Flux Signals. *IEEE Transactions on Industry Applications, 55*(5), 4585-4594.

Irgens, C. (1991). A Feature Based KBS for Quality Prediction of Machined Parts and Products. Dans *Computer Integrated Manufacturing* (pp. 385-396). Springer London.

ISO. (2006). *Statistical methods : process performance anc capability statistics for measured qualilty characteristics*. ISO 21747. Genève, Suisse: International Organization for Standardization.

Janssens, O., Walle, R. V. d., Loccufier, M., & Hoecke, S. V. (2017). Deep Learning for Infrared Thermal Image Based Machine Health Monitoring. *IEEE/ASME Transactions on Mechatronics, 23*(1), 151-159.

Jia, F., Lei, Y., Guo, L., Lin, J., & Xing, S. (2017). A neural network constructed by deep learning technique and its application to intelligent fault diagnosis of machines. *Neurocomputing, 272*, 619-628.

Jia, S., Yuan, Q., Cai, W., Lv, J., & Hu, L. (2019). Establishing prediction models for feeding power and material drilling power to support sustainable machining. *The International Journal of Advanced Manufacturing Technology, 100*(9-12), 2243-2253.

Jiang, X., Li, B., Mao, X., Hao, C., & Liu, H. (2018). Tool condition monitoring based on dynamic sensitivity of a tool-workpiece system. *The International Journal of Advanced Manufacturing Technology, 98*(5), 1441-1460.

Jiang, Z., Gao, D., Lu, Y., Kong, L., & Shang, Z. (2019). Electrical energy consumption of CNC machine tools based on empirical modeling. *The International Journal of Advanced Manufacturing Technology, 100*(9-12), 2255-2267.

Khan, S., & Yairi, T. (2018). A review on the application of deep learning in system health management. *Mechanical Systems and Signal Processing, 107*, 241-265.

Khorasani, A., & Yazdi, M. R. S. (2017). Development of a dynamic surface roughness monitoring system based on artificial neural networks (ANN) in milling operation. *The International Journal of Advanced Manufacturing Technology, 93*(1), 141-151.

Kingma, D. P., & Welling, M. (2013). Auto-encoding variational bayes. *arXiv preprint arXiv:1312.6114*.

Kohler, D., & Weisz, J.-D. (2016). *Industrie 4.0 Les défis de la transformation numérique du modèle industriel allemand*. France.

Kong, D., Chen, Y., Li, N., & Tan, S. (2017). Tool wear monitoring based on kernel principal component analysis and v-support vector regression. *The International Journal of Advanced Manufacturing Technology, 89*(1), 175-190.

Kundu, P., Chopra, S., & Lad, B. K. (2017). Multiple failure behaviors identification and remaining useful life prediction of ball bearings. *Journal of Intelligent Manufacturing, 30*(4), 1795-1807.

Kundu, P., Darpe, A. K., & Kulkarni, M. S. (2020). A review on diagnostic and prognostic approaches for gears. *Structural Health Monitoring*.

Kuntoğlu, M., Aslan, A., Pimenov, D. Y., Usca, Ü. A., Salur, E., Gupta, M. K., . . . Sharma, S. (2021). A Review of Indirect Tool Condition Monitoring Systems and Decision-Making Methods in Turning: Critical Analysis and Trends. *Sensors, 21*(1), 108.

Kwon, D., Hodkiewicz, M. R., Fan, J., Shibutani, T., & Pecht, M. G. (2016). IoT-based prognostics and systems health management for industrial applications. *IEEE Access, 4*, 3659-3670.

Laloix, T., Iung, B., Voisin, A., & Romagne, E. (2016). Towards the control of product quality from the process deviation monitoring: Overview and investigation in automotive sector. *IFAC-PapersOnLine, 49*(28), 79-84.

Lamraoui, M., Thomas, M., & El Badaoui, M. (2014). Cyclostationarity approach for monitoring chatter and tool wear in high speed milling. *Mechanical Systems and Signal Processing, 44*(1), 177-198.

Lamraoui, M., Thomas, M., El Badaoui, M., & Girardin, F. (2012). Cyclostationarity analysis of instantaneous angular speeds for monitoring chatter in high speed milling. Dans *IECON 2012 - 38th Annual Conference on IEEE Industrial Electronics Society* (pp. 3868-3873).

Lamraoui, M., Thomas, M., El Badaoui, M., Zaghbani, I., & Songmene, V. (2011). New indicators based on cyclostationarity approach for machining monitoring. *Proceedings of Surveillance, 6*, 1-27.

Larousse. (2015). *Dictionnaire Larousse*. Paris: Larousse.

Lee, J., Jin, C., & Bagheri, B. (2017). Cyber physical systems for predictive production systems. *Production Engineering, 11*(2), 155-165.

Lee, J., Lapira, E., Bagheri, B., & Kao, H.-a. (2013). Recent advances and trends in predictive manufacturing systems in big data environment. *Manufacturing Letters, 1*(1), 38-41.

Lee, J., Ni, J., Djurdjanovic, D., Qiu, H., & Liao, H. (2006). Intelligent prognostics tools and e-maintenance. *Computers in Industry, 57*(6), 476-489.

Lee, S., Kwak, M., Tsui, K.-L., & Kim, S. B. (2019). Process monitoring using variational autoencoder for high-dimensional nonlinear processes. *Engineering Applications of Artificial Intelligence, 83*, 13-27.

Lei, Y., Li, N., Guo, L., Li, N., Yan, T., & Lin, J. (2018). Machinery health prognostics: A systematic review from data acquisition to RUL prediction. *Mechanical Systems and Signal Processing, 104*, 799-834.

Li, L., Tang, J., Wen, Y., & Shao, W. (2019). Characterization of ultrasonic-assisted grinding surface via the evaluation of the autocorrelation function. *The International Journal of Advanced Manufacturing Technology, 104*(9), 4219-4230.

Li, R., Verhagen, W. J. C., & Curran, R. (2020). A systematic methodology for Prognostic and Health Management system architecture definition. *Reliability Engineering & System Safety, 193*, 106598.

Li, X., Ding, Q., & Sun, J.-Q. (2018). Remaining useful life estimation in prognostics using deep convolution neural networks. *Reliability Engineering & System Safety, 172*, 1-11.

Liang, M., Cao, P., & Tang, J. (2021). Rolling bearing fault diagnosis based on feature fusion with parallel convolutional neural network. *The International Journal of Advanced Manufacturing Technology, 112*(3), 819-831.

Liang, S. Y., Hecker, R. L., & Landers, R. G. (2004). Machining Process Monitoring and Control: The State-of-the-Art. *Journal of Manufacturing Science and Engineering, 126*(2), 297-310.

Liang, X., Liu, Z., & Wang, B. (2019). State-of-the-art of surface integrity induced by tool wear effects in machining process of titanium and nickel alloys: A review. *Measurement, 132*, 150-181.

Liu, E., An, W., Xu, Z., & Zhang, H. (2020). Experimental study of cutting-parameter and tool life reliability optimization in inconel 625 machining based on wear map approach. *Journal of Manufacturing Processes, 53*, 34-42.

Liu, M.-K., Tseng, Y.-H., & Tran, M.-Q. (2019). Tool wear monitoring and prediction based on sound signal. *The International Journal of Advanced Manufacturing Technology, 103*(9), 3361-3373.

Liu, R., Yang, B., Zio, E., & Chen, X. (2018). Artificial intelligence for fault diagnosis of rotating machinery: A review. *Mechanical Systems and Signal Processing, 108*, 33-47.

Liu, Y., Hu, X., & Jin, J. (2019). Remaining Useful Life Prediction of Cutting Tools based on Deep Adversarial Transfer Learning. Dans *Proceedings of the 2019 8th International Conference on Computing and Pattern Recognition* (pp. 434-439).

Maaten, L. v. d., & Hinton, G. (2008). Visualizing data using t-SNE. *Journal of machine learning research, 9*(11), 2579-2605.

MacQueen, J. (1967). Some methods for classification and analysis of multivariate observations. Dans *Proceedings of the fifth Berkeley symposium on mathematical statistics and probability* (Vol. 1, pp. 281-297). Oakland, CA, USA.

Mancisidor, R. A., Kampffmeyer, M., Aas, K., & Jenssen, R. (2021). Learning latent representations of bank customers with the Variational Autoencoder. *Expert Systems with Applications, 164*, 114020.

Marani, M., Zeinali, M., Kouam, J., Songmene, V., & Mechefske, C. K. (2020). Prediction of cutting tool wear during a turning process using artificial intelligence techniques. *The International Journal of Advanced Manufacturing Technology, 111*(1), 505-515.

Martínez-Arellano, G., Terrazas, G., & Ratchev, S. (2019). Tool wear classification using time series imaging and deep learning. *The International Journal of Advanced Manufacturing Technology, 104*(9), 3647-3662.

Meziani, S., Zarour, D., & Thomas, M. (2017). *Experimental study for early detection of bearing defects by vibration and acoustic emission* présentée à 23ème Congrès Français de Mécanique, Lille, France.

Michau, G., Palmé, T., & Fink, O. (2017). Deep feature learning network for fault detection and isolation. Dans *Annual Conference of the Prognostics and Health Management Society 2017.* (pp. 108-118). PHM Society.

Mirjavadi, S. S., Afshari, B. M., Barati, M. R., & Hamouda, A. (2019). Nonlinear free and forced vibrations of graphene nanoplatelet reinforced microbeams with geometrical imperfection. *Microsystem Technologies, 25*(8), 3137-3150.

Mirjavadi, S. S., Mohasel Afshari, B., Shafiei, N., Rabby, S., & Kazemi, M. (2018). Effect of temperature and porosity on the vibration behavior of two-dimensional functionally graded micro-scale Timoshenko beam. *Journal of Vibration and Control, 24*(18), 4211-4225.

Nath, C. (2020). Integrated Tool Condition Monitoring Systems and Their Applications: A Comprehensive Review. *Procedia Manufacturing, 48*, 852-863.

Ouafi, A. E., & Barka, N. (2014). An ANN Based Multi-Sensor Integration Approach for in-Process Monitoring of Product Quality in Turning Operations. *Journal of Automation and Control Engineering, 2*(3), 289-293.

Pang, J., Zhang, N., Xiao, Q., Qi, F., & Xue, X. (2021). A new intelligent and data-driven product quality control system of industrial valve manufacturing process in CPS. *Computer Communications, 175*, 25-34.

Papananias, M., McLeay, T. E., Mahfouf, M., & Kadirkamanathan, V. (2019). An Intelligent Metrology Informatics System based on Neural Networks for Multistage Manufacturing Processes. *Procedia CIRP, 82*, 444-449.

Park, H.-S., & Tran, N.-H. (2014). Development of a smart machining system using self-optimizing control. *The International Journal of Advanced Manufacturing Technology, 74*(9), 1365-1380.

Peng, Y., Dong, M., & Zuo, M. J. (2010). Current status of machine prognostics in condition-based maintenance: a review. *The International Journal of Advanced Manufacturing Technology, 50*(1), 297-313.

Proteau, A. (2016). *Prédiction de la complexité d'un produit usiné : proposition d'un modèle basé sur l'analyse du modèle 3D enrichi*. Montréal: École de technologie supérieure.

Proteau, A., Tahan, A., & Thomas, M. (2019a). Specific cutting energy: a physical measurement for representing tool wear. *The International Journal of Advanced Manufacturing Technology, 103*(1), 1-10.

Proteau, A., Tahan, A. S., & Thomas, M. (2019b). Toward the quality prognostic of an aircraft engine workpiece in Inconel Alloy 625: case study and proposed system architecture. Dans *Surveillance, Vishno and AVE conferences* (pp. 1-15).

Proteau, A., Zemouri, R., Tahan, A., & Thomas, M. (2020). Dimension reduction and 2D-visualization for early change of state detection in a machining process with a variational autoencoder approach. *The International Journal of Advanced Manufacturing Technology, 111*(11), 3597-3611.

Psarommatis, F., May, G., Dreyfus, P.-A., & Kiritsis, D. (2020). Zero defect manufacturing: state-of-the-art review, shortcomings and future directions in research. *International Journal of Production Research, 58*(1), 1-17.

Qiu, J. (2018). Modeling of cutting force coefficients in cylindrical turning process based on power measurement. *The International Journal of Advanced Manufacturing Technology, 99*(9-12), 2283-2293.

Rauch, M., Laguionie, R., Hascoet, J.-Y., & Suh, S.-H. (2012). An advanced STEP-NC controller for intelligent machining processes. *Robotics and Computer-Integrated Manufacturing, 28*(3), 375-384.

Reis, M., & Gins, G. (2017). Industrial Process Monitoring in the Big Data/Industry 4.0 Era: from Detection, to Diagnosis, to Prognosis. *Processes, 5*(3), 35.

Rezaeianjouybari, B., & Shang, Y. (2020). Deep learning for prognostics and health management: State of the art, challenges, and opportunities. *Measurement, 163*, 107929.

Ribeiro, M. T., Singh, S., & Guestrin, C. (2016). Why should i trust you?: Explaining the predictions of any classifier. Dans *Proceedings of the 22nd ACM SIGKDD International Conference on Knowledge Discovery and Data Mining* (pp. 1135-1144). ACM.

Saleem, M. Q., & Mumtaz, S. (2020). Face milling of Inconel 625 via wiper inserts: Evaluation of tool life and workpiece surface integrity. *Journal of Manufacturing Processes, 56*, 322-336.

San Martin, G., López Droguett, E., Meruane, V., & das Chagas Moura, M. (2019). Deep variational auto-encoders: A promising tool for dimensionality reduction and ball bearing elements fault diagnosis. *Structural Health Monitoring, 18*(4), 1092-1128.

Saxena, A., Celaya, J., Saha, B., Saha, S., & Goebel, K. (2010). Metrics for offline evaluation of prognostic performance. *International Journal of Prognostics and Health Management, 1*(1), 4-23.

Serin, G., Sener, B., Ozbayoglu, A. M., & Unver, H. O. (2020). Review of tool condition monitoring in machining and opportunities for deep learning. *The International Journal of Advanced Manufacturing Technology, 109*(3), 953-974.

Shahid, N., & Ghosh, A. (2019). TrajecNets: Online Failure Evolution Analysis in 2D Space. *International Journal of Prognostics and Health Management, 10*(Special Issue on Deep Learning and Emerging Analytics), 17.

Shen, N., Cao, Y., Li, J., Zhu, K., & Zhao, C. (2018). A practical energy consumption prediction method for CNC machine tools: cases of its implementation. *The International Journal of Advanced Manufacturing Technology, 99*(9-12), 2915-2927.

Silvestri, L., Forcina, A., Introna, V., Santolamazza, A., & Cesarotti, V. (2020). Maintenance transformation through Industry 4.0 technologies: A systematic literature review. *Computers in Industry, 123*, 103335.

Singh, S. K., Kumar, S., & Dwivedi, J. P. (2017). A novel soft computing method for engine RUL prediction. *Multimedia Tools and Applications, 78*(4), 4065-4087.

Srivastava, N., Hinton, G., Krizhevsky, A., Sutskever, I., & Salakhutdinov, R. (2014). Dropout: a simple way to prevent neural networks from overfitting. *The journal of machine learning research, 15*(1), 1929-1958.

Tahan, S.-A., & Levesque, S. (2009). Exploiting the process capability of profile tolerance according GD&T ASME-Y14.5M. Dans *2009 International Conference on Computers & Industrial Engineering* (pp. 1285-1290).

Takaya, Y. (2013). In-process and on-machine measurement of machining accuracy for process and product quality management: A review. *International Journal of Automation Technology, 8*(1), 4-19.

Terrazas, G., Martínez-Arellano, G., Benardos, P., & Ratchev, S. (2018). Online Tool Wear Classification during Dry Machining Using Real Time Cutting Force Measurements and a CNN Approach. *Journal of Manufacturing and Materials Processing, 2*(4), 72.

Thomas, M. (2011). *Fiabilité, maintenance prédictive et vibration des machines*. Montréal: Presses de l'Université du Québec.

Uekita, M., & Takaya, Y. (2017). Tool condition monitoring for form milling of large parts by combining spindle motor current and acoustic emission signals. *The International Journal of Advanced Manufacturing Technology, 89*(1), 65-75.

Ugaz, W., Sánchez, I., & Alonso, A. M. (2017). Adaptive EWMA control charts with time-varying smoothing parameter. *The International Journal of Advanced Manufacturing Technology, 93*(9-12), 3847-3858.

Verstraete, D., Droguett, E., & Modarres, M. (2020). A Deep Adversarial Approach Based on Multi-Sensor Fusion for Semi-Supervised Remaining Useful Life Prognostics. *Sensors, 20*(1), 176.

Vogl, G. W., Weiss, B. A., & Helu, M. (2016). A review of diagnostic and prognostic capabilities and best practices for manufacturing. *Journal of Intelligent Manufacturing, 30*(1), 79-95.

Voisin, A., Laloix, T., Iung, B., & Romagne, E. (2018). Predictive Maintenance and part quality control from joint product-process-machine requirements: application to a machine tool. *Procedia Manufacturing, 16*, 147-154.

Wang, B., Lei, Y., Yan, T., Li, N., & Guo, L. (2020). Recurrent convolutional neural network: A new framework for remaining useful life prediction of machinery. *Neurocomputing, 379*, 117-129.

Wang, D. (2011). Robust Data-Driven Modeling Approach for Real-Time Final Product Quality Prediction in Batch Process Operation. *IEEE Transactions on Industrial Informatics, 7*(2), 371-377.

Wang, K.-S. (2013). Towards zero-defect manufacturing (ZDM)—a data mining approach. *Advances in Manufacturing, 1*(1), 62-74.

Wang, L., Meng, Y., Ji, W., & Liu, X. (2019). Cutting energy consumption modelling for prismatic machining features. *The International Journal of Advanced Manufacturing Technology, 103*(5), 1657-1667.

Wang, S., Xiang, J., Zhong, Y., & Zhou, Y. (2017). Convolutional neural network-based hidden Markov models for rolling element bearing fault identification. *Knowledge-Based Systems, 144*, 65-76.

Waqar, T., & Demetgul, M. (2016). Thermal analysis MLP neural network based fault diagnosis on worm gears. *Measurement, 86*, 56-66.

Wuest, T., Irgens, C., & Thoben, K.-D. (2014). An approach to monitoring quality in manufacturing using supervised machine learning on product state data. *Journal of Intelligent Manufacturing, 25*(5), 1167-1180.

Xing-yu, Q., Peng, Z., Dong-dong, F., & Chengcheng, X. (2017). Autoencoder-based fault diagnosis for grinding system. Dans *2017 29th Chinese Control And Decision Conference (CCDC)* (pp. 3867-3872).

Xu, F., Yang, F., Fei, Z., Huang, Z., & Tsui, K.-L. (2021). Life prediction of lithium-ion batteries based on stacked denoising autoencoders. *Reliability Engineering & System Safety, 208*, 107396.

Yin, Q., Liu, Z., Wang, B., Song, Q., & Cai, Y. (2020). Recent progress of machinability and surface integrity for mechanical machining Inconel 718: a review. *The International Journal of Advanced Manufacturing Technology, 109*, 1-31.

Ying, X. (2019). An Overview of Overfitting and its Solutions. *Journal of Physics: Conference Series, 1168*(2), 022022.

Yu, J., Liang, S., Tang, D., & Liu, H. (2016). A weighted hidden Markov model approach for continuous-state tool wear monitoring and tool life prediction. *The International Journal of Advanced Manufacturing Technology, 91*(1), 201-211.

Yu, S., & Príncipe, J. C. (2019). Understanding autoencoders with information theoretic concepts. *Neural Networks, 117*, 104-123.

Yu, W., Kim, I. I. Y., & Mechefske, C. (2019). Remaining useful life estimation using a bidirectional recurrent neural network based autoencoder scheme. *Mechanical Systems and Signal Processing, 129*, 764-780.

Yu, W., Kim, I. Y., & Mechefske, C. (2021). Analysis of different RNN autoencoder variants for time series classification and machine prognostics. *Mechanical Systems and Signal Processing, 149*, 107322.

Zemouri, R., Al Masry, Z., Remadna, I., Terrissa, S. L., & Zerhouni, N. (2020). Hybrid architecture of deep convolutional variational auto-encoder for remaining useful life prediction. Dans *30th European Safety and Reliability Conference and 15th Probabilistic Safety Assessment and Management Conference* (pp. 7).

Zemouri, R., Lévesque, M., Amyot, N., Hudon, C., Kokoko, O., & Tahan, S. A. (2020). Deep Convolutional Variational Autoencoder as a 2D-Visualization Tool for Partial Discharge Source Classification in Hydrogenerators. *IEEE Access, 8*, 5438-5454.

Zhang, J. Z., & Chen, J. C. (2008). Tool condition monitoring in an end-milling operation based on the vibration signal collected through a microcontroller-based data acquisition system. *The International Journal of Advanced Manufacturing Technology, 39*(1), 118-128.

Zhang, S., Zhang, S., Wang, B., & Habetler, T. G. (2019). Machine Learning and Deep Learning Algorithms for Bearing Fault Diagnostics-A Comprehensive Review. *arXiv preprint arXiv:1901.08247*.

Zhang, W., Li, C., Peng, G., Chen, Y., & Zhang, Z. (2018). A deep convolutional neural network with new training methods for bearing fault diagnosis under noisy environment and different working load. *Mechanical Systems and Signal Processing, 100*, 439-453.

Zhang, X., Lu, X., Li, W., & Wang, S. (2021). Prediction of the remaining useful life of cutting tool using the Hurst exponent and CNN-LSTM. *The International Journal of Advanced Manufacturing Technology, 112*(7), 2277-2299.

Zhang, Y., Zhang, Y., He, K., Li, D., Xu, X., & Gong, Y. (2021). Intelligent feature recognition for STEP-NC-compliant manufacturing based on artificial bee colony algorithm and back propagation neural network. *Journal of Manufacturing Systems*.

Zhang, Y., Zhu, K., Duan, X., & Li, S. (2021). Tool wear estimation and life prognostics in milling: Model extension and generalization. *Mechanical Systems and Signal Processing, 155*, 107617.

Zhao, G., Cao, X., Xiao, W., Liu, Q., & Jun, M. B.-G. (2020). STEP-NC feature-oriented high-efficient CNC machining simulation. *The International Journal of Advanced Manufacturing Technology, 106*(5), 2363-2375.

Zhao, J., Li, L., Wang, Y., & Sutherland, J. W. (2019). Impact of surface machining complexity on energy consumption and efficiency in CNC milling. *The International Journal of Advanced Manufacturing Technology, 102*(9-12), 2891-2905.

Zhao, R., Yan, R., Chen, Z., Mao, K., Wang, P., & Gao, R. X. (2019). Deep learning and its applications to machine health monitoring. *Mechanical Systems and Signal Processing, 115*, 213-237.

Zheng, S., Ristovski, K., Farahat, A., & Gupta, C. (2017). Long Short-Term Memory Network for Remaining Useful Life estimation. Dans *2017 IEEE International Conference on Prognostics and Health Management (ICPHM)* (pp. 88-95).

Zhou, J.-T., Zhao, X., & Gao, J. (2019). Tool remaining useful life prediction method based on LSTM under variable working conditions. *The International Journal of Advanced Manufacturing Technology, 104*(9), 4715-4726.

Zhou, Y., & Xue, W. (2018). Review of tool condition monitoring methods in milling processes. *The International Journal of Advanced Manufacturing Technology, 96*(5), 2509-2523.

Zhu, K., Li, G., & Zhang, Y. (2020). Big Data Oriented Smart Tool Condition Monitoring System. *IEEE Transactions on Industrial Informatics, 16*(6), 4007-4016.

Zhu, Z., Peng, F., Tang, X., Yan, R., Li, Z., Chen, C., & Sun, H. (2019). Specific cutting energy index (SCEI)-based process signature for high-performance milling of hardened steel. *The International Journal of Advanced Manufacturing Technology, 103*(1), 1-13.

Zhuang, F., Qi, Z., Duan, K., Xi, D., Zhu, Y., Zhu, H., . . . He, Q. (2021). A Comprehensive Survey on Transfer Learning. *Proceedings of the IEEE, 109*(1), 43-76.